

# Department of Electrical and Computer Systems Engineering

## Technical Report MECSE-2-2005

MOCSS2004: Monash Optical Communication System Simulator  
for Optically Amplified DWDM Advanced Modulation Formats

L.N. Binh, A. Chua and G. Alagaratnam

**MONASH**  
UNIVERSITY

# **MOCSS2004: MONASH OPTICAL COMMUNICATION SYSTEM SIMULATOR FOR OPTICALLY AMPLIFIED DWDM ADVANCED MODULATION FORMATS**

**Le nguyen Binh, A. Chua and G. Alagaratnam**

**Department of Electrical and Computer Systems Engineering, Monash University, Clayton, Melbourne  
Victoria 3168 Australia e-mail: [le.nguyen.binh@eng.monash.edu.au](mailto:le.nguyen.binh@eng.monash.edu.au)**

## **SUMMARY**

*This report presents the further development of a comprehensive simulation package for modeling optically amplified dense WDM optical communication systems, particularly for long haul and ultra-high speed transmission. The Monash Optical Communication Systems Simulator MOCSS2004 (or OC2004 for short) package has been updated and proven to be an extensive engineering design tool for system engineers to simulate the transmission performance of ultra long-haul, high capacity and high-speed optical transmission systems. The software package is based on the MOCSS developed since 1995[1].*

*The ITU Grid conforming MUX/DEMUX modules have been added allowing accurate simulation of multi-carrier lightwave channels optical communications systems. The total channel transmission capacity reaching Tb/s can now be simulated with the MOCSS2004 package.*

*Furthermore, modules of new distributed feedback laser sources and modified EDFAs have been developed and integrated to enable system simulations of optically amplified light-wave channels operating in the L and C-Bands. Fiber Propagation Model based on the split-step Fourier (SSF) method with variable step-sizes add a new dimension for propagation of envelopes of light-wave channels over several kms of dispersion compensated fiber spans.*

*In addition, Gaussian profile pulses are developed to represent more realistic format of the external modulation. Thus a new module is developed and integrated allowing the transmission and studies of the effects of transmissions of different pulse formats. Finally, BER and Q-factor performance measures are implemented to evaluate various system configurations.*

*System simulations are performed for a single fiber transmission span consisting of 80km standard Single-Mode Fiber (SMF), an optical Pre-Amplifier, 16km Dispersion Compensated Fiber (DCF) and an optical Booster Amplifier. Different system combinations of line coding format (NRZ vs. RZ), pulse*

*format (Gaussian vs. square) and operating regions (C-Band vs. L-Band) are explored. Based on extensive simulations, most of the varying combinations allowed for error free transmission, corresponding to a Q-factor of greater than 8 or BER of  $10^{-16}$ . However, the best system combination is found to be propagation in the C-Band using a Gaussian pulse format and RZ line coding format with a Q-factor of 25. For completeness, results obtained from the OC2004 package are compared with Simulink models to confirm the outputs and accuracy of the program.*

*The 'ringing' effect, generated due to the windowing of the Matlab™ fftshift operator in the fiber propagation module is studied. An EDFA optimized for a flat gain spectrum over the L-Band may be implemented improve transmission in the L-band. Other improvements to the MOCSS2004 package can be to extend the transmission rate up to 40 Gb/s as well as to complete the receiver section, which may include modeling its physical limitations and other effects such as receiver noise.*

## TABLE OF CONTENTS

1	INTRODUCTION .....	7
1.1	Overview.....	7
1.2	A Summary of Developed Package and Simulated Results .....	8
2	Optically Amplified Optical Communications Systems.....	9
2.1	Overview.....	9
	Transmitter.....	10
	Laser Sources.....	10
	External Modulation .....	11
	Line Coding Format.....	12
	Pulse Format .....	12
	Optical Multiplexer and Demultiplexer.....	13
	The Optical Fibers .....	13
	Erbium Doped Optical Amplifier (EDFA).....	14
	Optical Receiver .....	15
	DWDM Sources and Propagation .....	15
	Distributed Feedback Laser Sources for L-Band Operation.....	15
	DWDM MUX/DEMUX Module.....	17
	EDFA for L-Band Operation.....	18
2.2	Split-Step Fourier Method for Fiber Propagation.....	20
	Optimization of SSF Method using Local Error Method .....	22
	Algorithm for Local Error Method .....	22
	‘Ringing’ Effect.....	23
3	Implementation of Gaussian pulse profile for different modulation formats .....	24
4	System performance measurement .....	27
5	System Simulations and Comparative Studies .....	33
5.1	Modeling of Fiber Span Using SMF, DCF and OA .....	34
5.2	Modeling of Fiber Span Using NZ-DSF.....	35
5.3	Effect of Channel Spacing.....	37
5.4	Measurement of Efficiency of Variable vs. Fixed Step Size Propagation.....	38
5.5	Accuracy of Q-factor and BER Estimation .....	39
5.6	Comparison of OC2004 and Simulink Models.....	41
6	Graphical Representation of OC2004 Simulator and Execution Procedures .....	47
6.1	Main Transmitter Module Window .....	48
6.2	Choice of Fiber: .....	54
6.3	Optical Fiber Module Results:.....	55
7	System Simulations and Comparative Studies .....	61
7.1	Different configurations.....	62
7.2	Experimental setup .....	62
7.3	Simulation Results and Discussion.....	63
	Gaussian pulse .....	64
	Square pulse.....	65
	Gaussian pulse, NRZ and RZ modulation format – NZ-DSF 80 km .....	66
8	Comparison of OC2004 and Experimental Results.....	68
8.1	Square pulse, NRZ modulation format - SMF 80 km and DCF 16km.....	68
8.2	Gaussian pulse, RZ modulation format - SMF 80 km and DCF 16km .....	71

8.3	Square pulse, NRZ modulation format – NZ DSF 80 km .....	72
8.4	Verification of Q-factor of the eye diagram .....	74
9	Concluding Remarks.....	76
10	References.....	77
11	APPENDIX.....	79
11.1	ITU GRID EXCEL FILES .....	79
11.2	TABLES OF SUMMARY OF RESULTS FOR SIMULATIONS ON OC2004.....	85

## TABLE OF FIGURES

Figure 1:	<i>General Optically Amplified Communications System [7]</i> .....	10
Figure 2:	<i>LiNbO<sub>3</sub> Modulator in Mach-Zender Configuration [1]</i> .....	11
Figure 3:	<i>NRZ and RZ Line Coding Formats</i> .....	12
Figure 4:	<i>Intersymbol Interference (ISI) as seen in eye diagram for RZ &amp; NRZ formats [10]</i> .....	12
Figure 5:	<i>Arrayed Waveguide Structure[8]</i> .....	13
Figure 6:	<i>Basic Operation and Construction of an EDFA [7]</i> .....	15
Figure 7:	<i>Eye Diagram Illustration.</i> .....	<b>Error! Bookmark not defined.</b>
Figure 8:	<i>Sample of a Wavelength Plan[9]</i> .....	17
Figure 9:	<i>OC2004 output for 16 channels multiplexed at (a) 200 GHz, (b) 100 GHz, (c) 50 GHz and (d) 25 GHz channel spacing in the C-band</i> .....	18
Figure 10:	<i>Gain and Absorption Spectra for EDFA after extension into L-Band operating region.</i> .....	19
Figure 11:	<i>Physical parameters of EDFA Operation at 1550nm pumped at 1480nm.</i> .....	20
Figure 12:	<i>Physical Parameters of EDFA operation at 1570nm pumped at 1480nm.</i> .....	20
Figure 13:	<i>Illustration of the Split-Step Fourier Method for Propagation [1].</i> .....	21
Figure 14:	<i>Eye Diagram of signals at transmitter without ‘ringing’ effect.</i> .....	24
Figure 15:	<i>Eye Diagram of signals after propagation with ‘ringing’ effect.</i> .....	24
Figure 16 –	<i>Gaussian pulse form represents a bit pattern on ‘1100’</i> .....	26
Figure 17 –	<i>Optical signal at output of external modulator showing a NRZ Square Pulse</i> .....	26
Figure 18 -	<i>Optical signal at output of external modulator showing a RZ Square Pulse</i> .....	27
Figure 19 -	<i>Optical signal at output of external modulator showing a NRZ Gaussian Pulse</i> .....	27
Figure 20 -	<i>Optical signal at output of external modulator showing a RZ Gaussian Pulse</i> .....	27
Figure 21 (a)	<i>Fluctuation of signals generated or arrived at the receiver (b) Gaussian Pdf of ‘1’ and ‘0’</i> ..	28
Figure 22	<i>AN example of BER versus Q factor</i> .....	31
Figure 23 –	<i>Sample eye diagram of a Square NRZ pulse</i> .....	32
Figure 24 –	<i>Sample PDF plotted for bit ‘0’</i> .....	32
Figure 25	<i>PDF of a Normal or Gaussian distribution of 2 standard deviations</i> .....	33
Figure 26:	<i>System Simulated for Performance Measurement</i> .....	34
Figure 27:	<i>Eye Diagram for NRZ, C-Band, Gaussian pulse input after 80km NZ-DSF Transmission</i> .....	35
Figure 28:	<i>Eye Diagram for NRZ, C-Band, Gaussian pulse input after 80km SMF + 16km DCF Optically Amplified Transmission</i> .....	36
Figure 29:	<i>Eye Diagram for RZ, C-Band, Gaussian pulse input after 80km NZ-DSF Transmission</i> .....	36
Figure 30:	<i>Eye Diagram for RZ, C-Band, Gaussian pulse input after 80km SMF + 16km DCF Optically Amplified Transmission</i> .....	36

Figure 31: Recovered signal with 3 Channels multiplexed at 200GHz spacing before fiber propagation. ....	37
Figure 32: Recovered signal with 3 channels multiplexed at 50GHz spacing before fiber propagation. ....	38
Figure 33: Recovered signal with 3 channels multiplexed at 12.5GHz spacing before fiber propagation. ....	38
Figure 34: Propagation Distance vs. Simulation Time for Variable Step-Size and Fixed Step-Size Propagation Methods for initial hstep = 500m. ....	39
Figure 35: Sample eye diagram to read Q-factor manually. ....	40
Figure 36: Simulink Model with NRZ input through 80km standard SMF and 16km DCF. ....	42
Figure 37: Electrical Eye Diagram of NRZ Simulink model at Receiver after 80km SMF and 16km DCF Transmission[2].....	42
Figure 38: Optical Eye Diagram of NRZ OC2004 model after 80km SMF and 16km DCF Transmission	43
Figure 39: Simulink Model with NRZ input through 80km NZ-DSF@1550nm.....	44
Figure 40: Eye Diagram of NRZ Simulink model at Receiver after 80km NZ-DSF@1550nm transmission[5].	44
Figure 41: Eye Diagram of NRZ OC2004 model after 80km NZ-DSF@1550nm transmission. ....	45
Figure 42: Simulink Model with DQPSK Transmitter and RZ input through 80km SSMF and 16km DCF. ..	45
Figure 43: Eye diagram for RZ Gaussian pulse input system with transmission over 80km SMF and 16km DCF detected by a single photo-detector. ....	46
Figure 44: Eye diagram output from OC2004 with RZ Gaussian input pulse after 80km SMF and 16km DCF transmission. ....	47
Figure 45: Main Transmitter Module for use to choose input bit sequence, modulator, line coding format, transmission rate, pulse format and laser source. ....	48
Figure 46: Output at External Modulator window. ....	49
Figure 47: Eye Diagram at Transmitter. ....	50
Figure 48: Transmitter Check-List Menu after WDM Transmission is chosen. ....	50
Figure 49: Frequency spectrum of first channel. ....	51
Figure 50: ITU Grid channel wavelength selection with different channel spacing. ....	51
Figure 51: ITU Grid conforming wavelengths for Multiplexing several channels. ....	52
Figure 52: Output waveform at Multiplexer. ....	53
Figure 53: Demultiplexed Signal, Demultiplexer Response and Filtered Signal Spectrum. ....	53
Figure 54 Window for choosing Fixed or Variable Step Size Fiber Propagation methods. ....	54
Figure 55: Main Fiber Module window after calculating Average Power Loss. ....	55
Figure 56: Optical Fiber Power Output plot. ....	56
Figure 57: Sample Eye Diagram after 80km standard SMF transmission. ....	56
Figure 58: Window for selecting amplifier length. ....	57
Figure 59: Optic Gain Transfer Characteristic of EDFA,.....	57
Figure 60: Wideband Noise-Power Transfer Characteristic of EDFA. ....	58
Figure 61: EDFA Properties and Output Window. ....	58
Figure 62: Main Fiber Module window showing Power Loss and Total Amplified after In-Line OA. ....	59
Figure 63: Designed Dispersion Compensating Fiber. ....	59
Figure 64: Main Fiber Module window after DCF transmission. ....	60
Figure 65: Eye Diagram after OAI and DCF. ....	60
Figure 66: BER and Q Estimator module window. ....	61
Figure 67 – schematic diagram showing setup of the transmission system used for the simulations.....	62
Figure 68 – Output signal after SSMF with a span of 80km.....	63
Figure 69 - Output signal after DCF with a span of 16km.....	63
Figure 70 – Gaussian: Optical Signal Power spectrum showing cross talk effects.....	65

Figure 71 – schematic diagram showing setup of the transmission system used for the simulations ..... 66

Figure 72 – NRZ, Gaussian at the end of 80km NZ-DSF transmission. ( a – signal power output, b – eye diagram)..... 67

Figure 73 - RZ, Gaussian at the end of 80km NZ-DSF transmission. (a) signal power output, (b) eye diagram ..... 67

Figure 74 – schematic diagram showing setup of the transmission system used for the simulations ..... 68

Figure 75 – NRZ Transmitter with a SMF(80km) and DCF (16km) ..... 69

Figure 76 - Eye Diagram before the SMF fiber (a – Simulink and b – OC2004) ..... 69

Figure 77 – Electrical and optical Eye Diagram after the SMF fiber (a)– Simulink and (b) OC2004..... 70

Figure 78 - Eye Diagram after the SMF and DCM (a) Simulink and( b) OC2004..... 70

Figure 79 – RZ -DQPSK Transmitter with 80Kms SSMF and 16 Kms DCF..... 71

Figure 80 Eye Diagram after the SMF and DCM. (a) DPQSK[8] and( b) OC2004 ..... 72

Figure 81 – Square pulse, NRZ format Transmitter with 80km DSF ..... 72

Figure 82 Eye Diagram at 10Gbps before the DSF (a) Simulink[4, 5] and ( b) OC2004. .... 73

Figure 83- Eye Diagram at 10Gbps after the DSF (a) Simulink and( b) OC2004..... 73

Figure 84 – Measurements for manually reading Q factor ..... 74

# 1 INTRODUCTION

## 1.1 Overview

Optical communications systems play an increasingly important role in the telecommunications global networks today due to the ever increasing demand for larger transmission capacity, higher speeds of transmission and long haul transmission. Whereas in the past optical communications is only used for transmitting voice channels, optical fiber networks now also carry high-speed internet and cable television signals. Deploying DWDM (Dense Wavelength Division Multiplexing) technology onto pre-existing optical fiber networks are a cost effective alternative to overhauling existing systems to increase bandwidth currently needed and also to provide for further demand in the future.

The bit rate per channels is also higher and higher reaching 10 Gb/s and then 40 Gb/s or faster. At the same time several optical channels are multiplexed together leading to an aggregate capacity reaching tens of Tb/s. The deployment of these muxed systems requires care planning and designed. Thus the availability of a comprehensive simulator is very critical for system engineering, both in professional practice and teaching environment.

This work presents a simulation package based on the MOCSS software, which models 10Gb/s DWDM optically amplified fiber transmission system. Development and testing of the OC2004 simulation package will attempt to identify the best system configuration for long haul optical transmission systems. Different configurations consist of varying pulse formats, modulation formats, laser sources, ITU Grid conforming wavelength spacing and optical fibers used. The availability of different components to be used in system configurations will enable system engineers to develop reliable optical communications systems.

This work aims to upgrade the development and testing of a comprehensive simulation package that accurately models different components in an optical communications system including: Laser Sources for C-Band (1530 – 1570nm) ; New Distributed Feedback laser source (DFB-III) for operation in the L-Band; Implementation of Gaussian pulse waveform for transmitter section; Novel line coding and pulse formats; ITU Grid conforming Multiplexer/Demultiplexer Modules; Refining the ITU Grid conforming wavelengths available down to the super-dense range of 12.5GHz and 7GHz including extensions for wavelength propagation in the L-Band; Different types of advanced optical fibers for transmission and dispersion compensating; Efficient fiber propagation methods ; Optimization of Split-Step Fourier Method for fiber

propagation module and enabling the options of choosing fixed and variable step size for propagation and study of ‘ringing’ effect due to the fiber propagation module.; Optical fiber in-line amplifiers for operation in the C-Band and modification of Erbium Doped Fiber Amplifier (EDFA) gain and absorption spectrum to enable L-Band operation; Optical receiver modules for system performance measurement ; System performance evaluation after propagation through a fiber span to obtain measures of the Q-factor and bit error rate (BER); Development and testing of comprehensive simulation package including: lasers for L-Band and C-Band operation, different modulation and pulse formats, ITU grid conforming MUX/DEMUX modules, dispersion managed fibers, efficient fiber propagation methods, optical amplifier for L-Band and C-Band operation, Q-factor and BER measurement for ultra-high speed optical communication systems; Setting the ITU Grid conforming MUX/DEMUX modules for the OC2004 package to run in MATLAB 6.5 and Matlab 6.5; Completing the DWDM OC2004 package with additional features that can be run in MATLAB version 6.5.

Since the original MOCSS package has been written for MATLAB 6.1, debugging and updating the program are conducted[1]; different system configurations are explored to evaluate their performances and to determine the best overall configuration for optimum performance; The results obtained from the MATLAB simulations are then to be compared and analysed together with the published experimental results; general integration with other simulators[2-5] developed in SIMULINK and C+; These modules are essential for examining the difference due to propagation in the C-Band and L-Band, effects of closer channel spacing, performance of different line coding and pulse formats, as well as the use of different optical fibers including variations in results due to different fiber propagation models.

Evaluation of the results obtained from the simulations enables the best system configuration to be determined for optimum performance over a high-speed optical fiber transmission span.

## 1.2 A Summary of Developed Package and Simulated Results

Modules that have been developed and tested for the OC2004 simulation package are described in Table 1.

Module	Functions
Laser Source	DFB-II for C-Band and DFB-III for L-Band
Line Coding Format	NRZ) and RZ
Pulse Format	Gaussian and Square pulse
MUX/DEMUX	ITU Grid conforming wavelengths for C-Band and L-Band with 200GHz, 100GHz, 50GHz, 25GHz, 12.5GHz and 7GHz channel spacings
Propagation Method	Fixed Step-Size and Variable Step-Size Propagation
Optical Fibers	Standard SMF, NZ-DSF at 1550nm and 1310nm
Optical Amplifier	EDFA for C-Band and L-Band
Performance Measure	Q-factor and BER Estimation

**Table 1:** *Summary of Developed OC2004 Modules.*

System simulations are employed to model a single transmission span which consists of 80 km Standard Single-Mode Fiber (SSMF), EDFA booster amplifier, 16 km Dispersion Compensating Fiber (DCF) and an EDFA in-line amplifier. BER and Q-factor estimations are obtained at the end of each span and used for comparison of system performances. Various system combinations are tested extensively. It can be concluded that the propagation in the C-Band provides consistently better performances than that performed in the L-Band. This can be improved by implementing an EDFA with a flat gain spectrum over the L-Band [6].

The best system configuration, which allowed for error free transmission with a Q-factor estimation of approximately 25, utilizes RZ line coding format, a Gaussian pulse waveform and C-Band operation. This result agrees with expectations which assume that the Gaussian pulse waveform is more resilient towards noise and dispersion as compared to the square pulse.

Evaluating the fixed step-size versus variable step-size propagation methods, the Q-factor and BER estimations obtained at the end of each fiber transmission span are consistent. The main difference noticed is the decreased simulation time when using the variable step-size propagation as it incorporates the local error method for optimization of the Split-Step Fourier fiber propagation method. This method allows for variable step-size selection in simulations whilst controlling the local error to achieve more efficient simulation time without compromising on accuracy.

## **2 Optically Amplified Optical Communications Systems**

### **2.1 Overview**

An optical transmission system consists of various components that have their own individual roles in ensuring efficient and reliable data communication throughout the communications network. Figure 1 shows a general setup for an optical communications system.

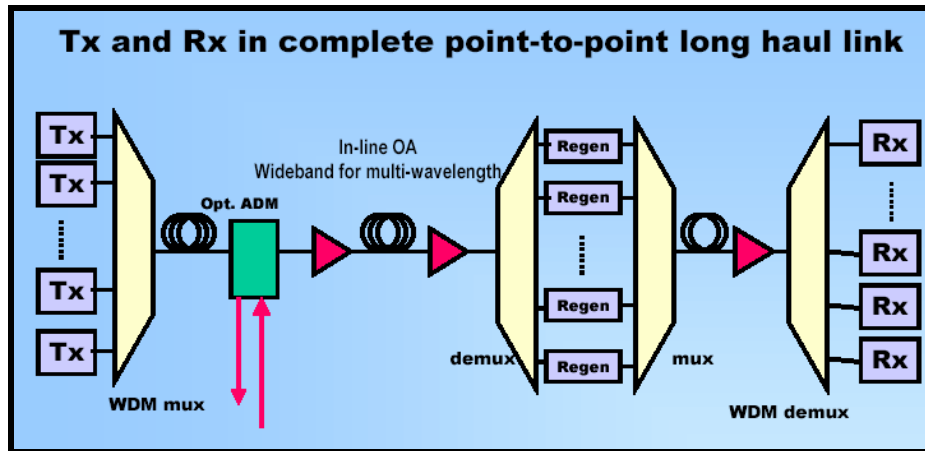


Figure 1: General Optically Amplified Communications System [7]

The following sections attempt to briefly explain the various components used in the simulations related to this work from the transmitter end to the receiver end of the simulated optical communications system.

### Transmitter

In brief description, the fundamental understanding of the optical transmitters used in the simulation package, the three main sections are the laser source, modulation, line coding formats and pulse formats.

### Laser Sources

There are many laser sources that can be used in optical transmitters such as distributed feedback (DFB) lasers, Fabry-Perot (FP) lasers and so on. The OC2004 software package aims to simulate a high speed optical communications system. DFB lasers are selected due to its single-frequency generation. They are uniquely suitable for high speed transmission with a narrow single longitudinal mode linewidth emission. These lasers are ideal for multiplexing higher number of channels closer together. This is commonly known as Dense Wavelength Division Multiplexing (DWDM) optical communications systems. Furthermore, the laser is tunable, which allows users selection of the lasing mode at the carrier wavelength [1]. These characteristics make the DFB laser a much better choice compared to the Fabry-Perot laser which is more suitable to “coarse” wavelength division multiplexing and system speeds which are limited to several hundred Gb/s[8].

Bragg diffraction allows coupling of waves backwards and forwards in the DFB laser optical cavity. This phenomenon occurs for only wavelengths closest to the Bragg wavelength,  $\lambda_B$ . For tunable DFB lasers, wavelength selectivity depends on both grating period and the refractive index of the laser’s semiconductor material. Hence, some methods of tuning lasers may include changing the temperature or passing a current through the material. However, these methods make only small changes and limit the tunable range to several

nanometers only [8]. Other methods of operating a truly tunable laser over a wider range of wavelengths include dividing the active medium of the semiconductor material into two sections and injecting varying amounts of bias current or biasing three independent sections of the DFB namely the active, phase-control and Bragg grating sections as mentioned in [9].

### External Modulation

Modulating a signal onto the output of a laser source can be done via direct modulation or external modulation. However, for high speed operation, direct modulation causes frequency chirp. This is a phenomenon that causes the signal carrier frequency to vary with time, thus causing pulse broadening or dispersion of the signal. As direct modulation varies the modulation current of the laser, this causes changes in the refractive index of the semiconductor material which causes the chirp effect. External modulation avoids this problem since the laser is operated with a constant bias current and modulation is carried out using an external modulating signal and is used for systems at speeds of 10 Gb/s and above [1].

The modulator used in system simulations is an electro-optic lithium niobate ( $\text{LiNbO}_3$ ) modulator in a Mach-Zehnder interferometer (MZIM) configuration. Figure 2 illustrates this modulator.

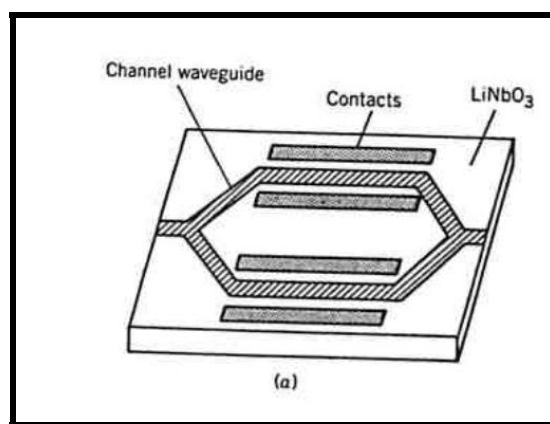


**Figure 2:** *LiNbO<sub>3</sub> Modulator in Mach-Zehnder Configuration [1].*

The lightwaves in the two arms experience identical phase shifts and interfere constructively when there is no external voltages applied to the electrodes on either side of the arms. However, when a voltage is applied to induce a  $\pi$  phase difference in the signals of both arms, the combined signals at the output interfere destructively. This phase shift results from the change in refractive index of the  $\text{LiNbO}_3$  material due to the externally applied voltage. Thus, a '1' signal is detected at the output when the signals interfere constructively and a '0' signal is detected for destructive interference.

## Line Coding Format

Although there are other line coding formats available, the formats examined in this work report are the Non-NRZ and RZ format. Figure 3 shows the different transitions used to represent a string of bits for both these formats.

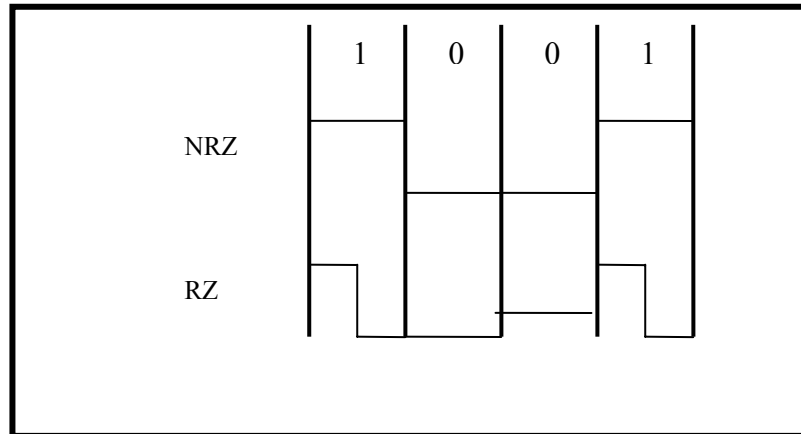


**Figure 3:** NRZ and RZ Line Coding Formats

For NRZ format, the signal level is held low for a '0' bit and high for a '1' bit. For a '1' bit in RZ format, the first half of the bit period will be held high and low for the following second half bit period. For a RZ format '0', the signal will be held low for the whole bit period.

For NRZ, the maximum bandwidth is half of the data transmission rate, while RZ has a bandwidth equal to that of its transmission rate. Although RZ requires higher bandwidth, it has an advantage over NRZ in that it does not degrade as rapidly under transmission and that it is not as susceptible to intersymbol interference (ISI), which is the corruption of isolated '0' bits by their neighbouring '1' bits [10] as shown in Figure 4.

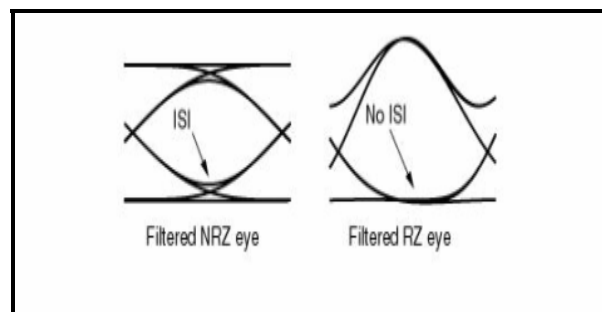


**Figure 4:** Intersymbol Interference (ISI) as seen in eye diagram for RZ & NRZ formats [10].

## Pulse Format

The two different pulse formats used in the simulations are square pulse waveform and the Gaussian pulse waveform. A square pulse's rise time (and fall time) is used to describe the pulse shape. The rise time is

defined as the time taken to rise from 10% to 90% of the final level once the input is turned on instantaneously [8]. For an optical Gaussian pulse, it is usually defined by its full-width-half-maximum (FWHM), which is the 3dB point.

### Optical Multiplexer and Demultiplexer

Arrayed Waveguide Gratings (AWG) can be used as both a multiplexer and a demultiplexer, depending on the direction of propagation. Figure 5 shows an illustration of the AWG.

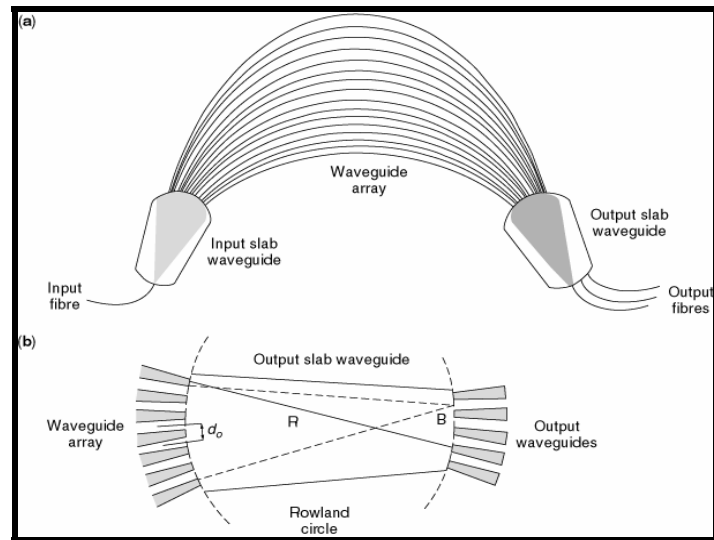


**Figure 5:** *Arrayed Waveguide Structure*[8].

As the multi-wavelength signals enters the first input slab waveguide (free propagation region), it is coupled to the waveguide array. In each waveguide, the multi-wavelength signal experiences a different phase shift due to the different waveguide lengths. Hence, when the signals exit in the second free propagation region, the different channels focus onto different output waveguides [4, 11].

The optical MUX/DEMUX is of interest in this work as this particular simulation module has been developed for DWDM systems conformed to the International Telecommunications Union (ITU) grid. Furthermore, various channel spacing is investigated to study the effect on system performance, including down to the ‘superdense’ region of 12.5GHz and 7GHz.

### The Optical Fibers

Standard single mode fibers (SSMF) are the most commonly used fibers and are thus used in the simulations of one span of fiber propagation. SMF has a small core diameter, less than 10  $\mu\text{m}$ . The lightwave guiding effect in optical fibers is weakly guiding phenomena with the polarization of the electromagnetic waves are

linear and hence the LP guided mode. This is due to the minute relative refractive index difference between the core and the cladding region of the fiber. The core refractive index must be larger than the cladding refractive index for effective operation as an optical waveguide.

The material and waveguide dispersion of an optical fiber contribute to its total dispersion spectrum. The dispersion spectrum is of interest to system engineers as it specifies the amount of pulse broadening that can be expected over a particular transmission distance. Material dispersion arises from slight variations in the refractive index of the silica fibers as a function of wavelength [10] which causes the pulse traveling through the fiber to disperse. In an ideal case, all light signals would be confined to the core, but this is not so in practice. Waveguide dispersion occurs as light in the cladding region encounters a lower refractive index and thus travels the faster than light in the core region.

The use of Non-Zero Dispersion Shifted Fibers (NZ-DSF) is also provided in OC2004 simulator. In practice, these fibers have their dispersion spectrum shifted to a very low (non-zero) value at the operating wavelength to gain minimum dispersion, and also to avoid the four-wave mixing (FWM) effect. FWM accumulates at close to zero dispersion because different channels travel at the same relative positions along the length of the fiber and interfere to produce noise at wavelengths close to another signal wavelength. Dispersion Compensating Fibers (DCF) are also used routinely to compensate for dispersion effects over long transmission distances. Only short lengths of DCFs are used for long spans of transmission as they are designed to have large finite values of dispersion at the operating frequency of choice.

### **Erbium Doped Optical Amplifier (EDFA)**

Erbium Doped Fiber Amplifiers (EDFA) have been used in the system simulations because they have the advantage of providing high gain, low noise, wide bandwidth and are polarization dependent [7]. The basic operation of an EDFA is shown in Figure 6.

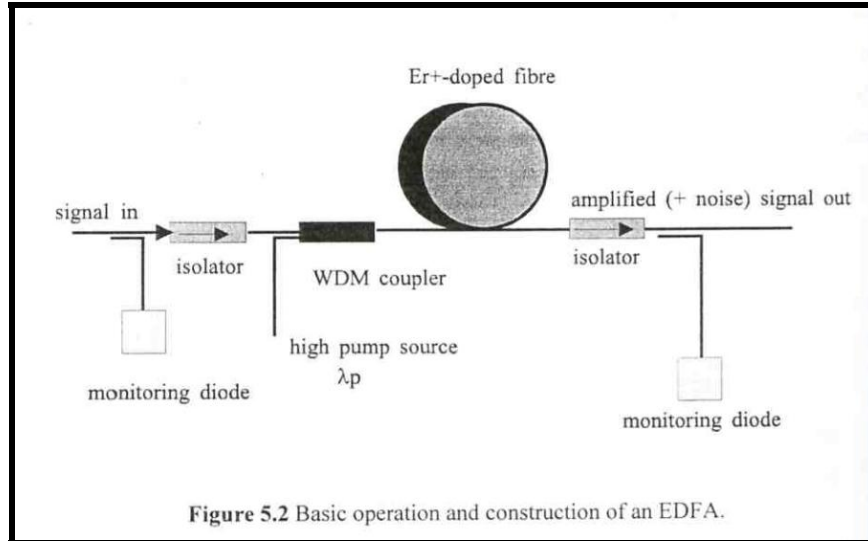


Figure 6: Basic Operation and Construction of an EDFA [7].

The Er:doped fiber is connected to a laser pump source using a coupler which allows the pump and signal powers to propagate together in the amplifying fiber. The pump lasers usually operate at either 980nm or at 1480nm to produce gains in the signal power output over the whole C-band spectrum.

### Optical Receiver

Although this simulation package does not simulate a complete optical receiver as such, there are modules included to inspect the system performance at the end of transmission. The performance measures used are the Q-factor and BER. The voltage eye level (decision level) is sampled to obtain the means for a ‘1’ and ‘0’ signal ( $\mu_1$  and  $\mu_0$ ) as well as for their respective standard deviations ( $\sigma_1$  and  $\sigma_0$ ), assuming a Gaussian distribution for the noise fluctuations. The Q-factor is then determined and the BER is related to the Q-factor by

$$Q = \frac{\mu_1 - \mu_0}{\sigma_1 + \sigma_0} \quad (1)$$

$$BER = 0.5 \operatorname{erfc} \left( \frac{Q}{\sqrt{2}} \right) \quad (2)$$

### DWDM Sources and Propagation

#### Distributed Feedback Laser Sources for L-Band Operation

A new laser source is implemented in the OC2004 simulation package to facilitate simulations of an optical communication system operating in the L-Band. This new laser (DFB-III) is modeled to be essentially the

same as the pre-existing DFB-II laser in the original MOCSS package. However, it is distinguished from the DFB-II laser as it operates in the L-Band region of 1570 – 1620 nm. The following variables are used to design the DFB-III laser as discussed in [7, 9].

- **Trise,  $\tau_r$  : Rise Time:** A short rise time is required for high speed communications to minimize dispersion effects on the pulse transmitted. However, this may lead to a higher overshoot.
- **Gamma,  $\Gamma$ : Optical Confinement Factor:** This factor is a ratio of the fractional optical power confined to the core region to total power. Maximizing  $\Gamma$  has the effect of less time delay of the output pulse once the laser is turned on and lower overshoot. A large  $\Gamma$  can compensate for the overshoot caused by a short rise time.
- **Alpha,  $\alpha$  : Line width Enhancement/Chirp Factor:** In order to minimize the effect of frequency chirp when using direct modulation, a small  $\alpha$  value is desirable. However, the use of external modulation ensures that there is very little frequency chirp effect.
- **Mune,  $\eta$  : Total Differential Quantum Efficiency:** This is a measure of the proportion of photons generated with respect to injected electrons. The value of  $\eta$  needs to be maximized so as to increase the laser source's total power output although there are limitations to this in practice.
- **Tphot,  $\tau_p$  : Photon Lifetime:** The laser's physical cavity structure is related to this variable in which a small value of  $\tau_p$  corresponds to a short laser cavity. Minimizing  $\tau_p$  will increase the laser power output, decrease the effect of frequency chirp and minimize the laser turn-on delay but this may cause an increase in overshoot of the signal.
- **Tcarr,  $\tau_n$  : Carrier Lifetime:** This is relates to the loss of electrons due to spontaneous emission and non-radiative recombination.  $\tau_n$  should be reduced to minimize the overshoot effect.
- **Epsil,  $\varepsilon$  : Gain Compression Factor:** Minimizing  $\varepsilon$  leads to less oscillatory and overshoot effects.
- **Nnull,  $N_0$  : Carrier Density at Transparency:** When the injected carrier density exceeds this value, population inversion occurs and the active region will exhibit optical gain.
- **Anull,  $A_0$  : Gain Coefficient:** Input signals in the active region of the semiconductor material will be amplified by this factor when population inversion occurs.
- **I<sub>th</sub> : Threshold Current:** Current in the laser must be pumped above this level for laser operation.

## DWDM MUX/DEMUX Module

ITU Grid conforming DWDM MUX/DEMUX modules are developed to allow system engineers to develop Terabits per second optical communications systems. The effect of packing more and more channels onto a single transmission fiber can be investigated by further refining the channel spacing available according to the ITU Grid as currently used in industry. Channel spacing of 200GHz, 100GHz, 50GHz, 25GHz and 7GHz can be implemented for system operation in both the C- and L-bands. A sample wavelength plan which conforms to ITU grid specifications is

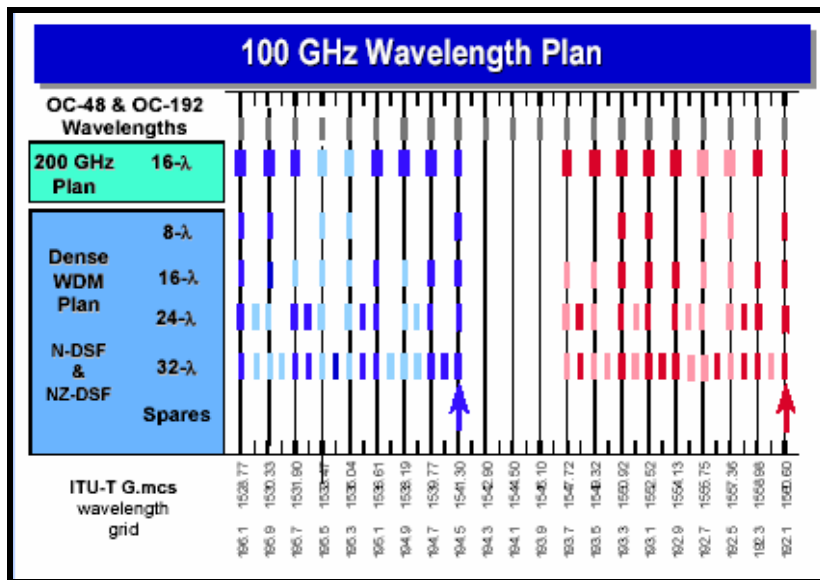
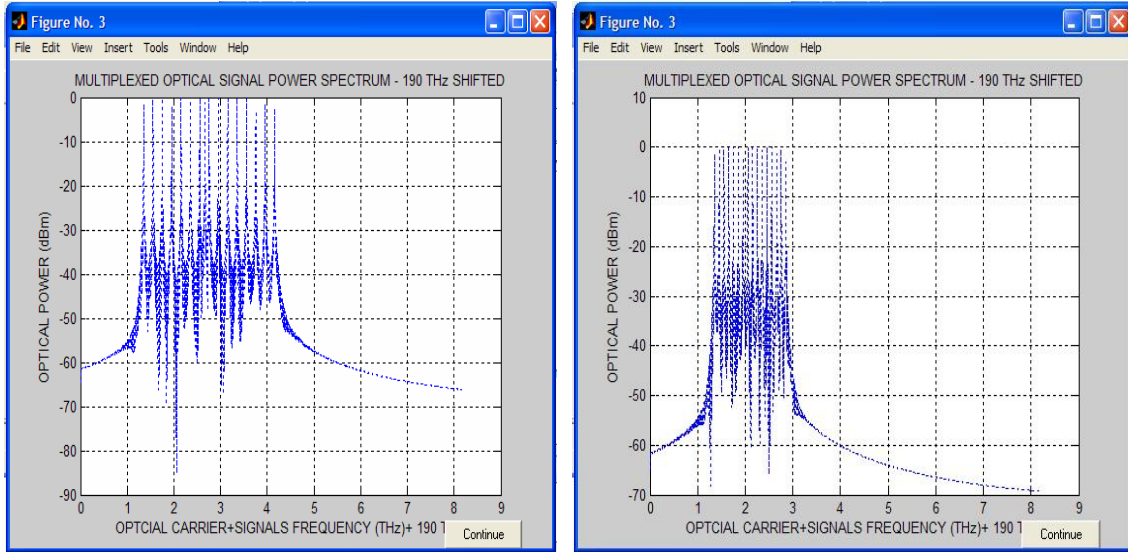


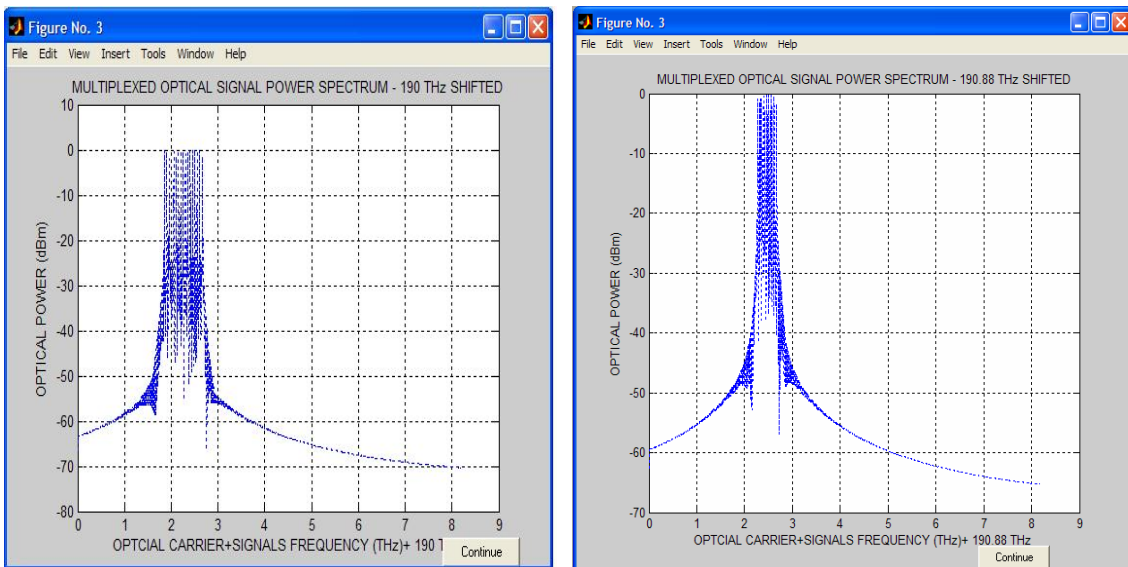
Figure 7: Sample of a Wavelength Plan[9]

The following are examples of output from the DWDM MUX module from the OC2004 simulations showing the optical power spectrum of 16 channels multiplexed together with 200 GHz, 100 GHz, 50 GHz and 25 GHz spacing.



(a)

(b)



(c)

(d)

**Figure 8:** OC2004 output for 16 channels multiplexed at (a) 200 GHz, (b) 100 GHz, (c) 50 GHz and (d) 25 GHz channel spacing in the C-band

### EDFA for L-Band Operation

Since one of the objectives of this work is to observe the performance of optical communications systems operating in both the C-Band and the L-Band, it is necessary to extend the operation of the existing EDFA model used in the MOCSS simulation package to the L-Band. This is achieved by modifying the gain and absorption spectra of the EDFA as shown in Figure 9.

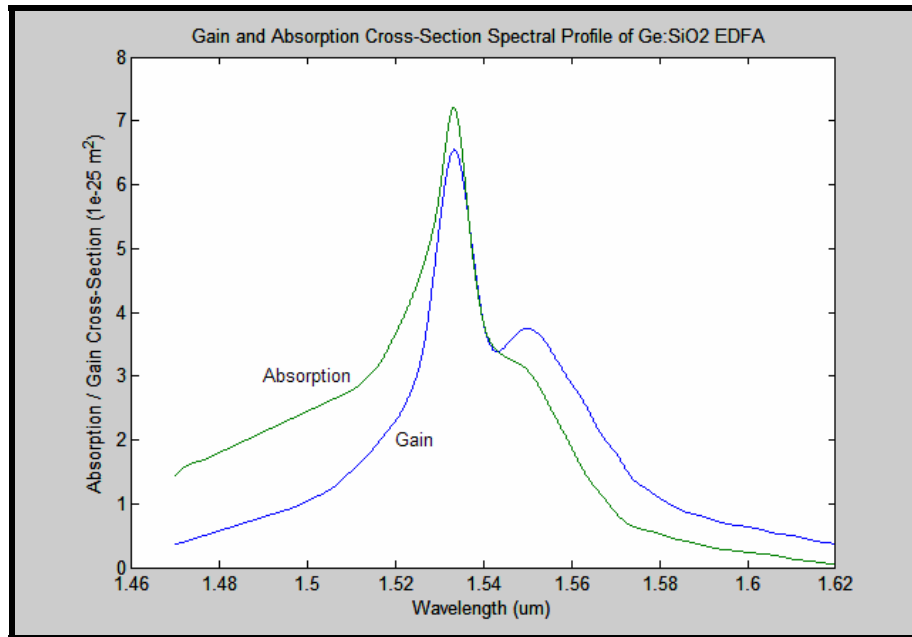


Figure 9: Gain and Absorption Spectra for EDFA after extension into L-Band operating region.

The operation of L-Band EDFAs is of interest as they can be used in parallel with C-Band EDFAs to effectively double system capacity [12] by enabling transmission in both C-Band and L-Band operating windows simultaneously. However, at this stage we are only investigating transmission in each operating region separately. The EDFA properties operating at 1550nm and 1570nm are shown in Figure 10 and **Figure 11** respectively .

EDF OPTICAL AMPLIFIER: PROPERTIES AND OUTPUT

Fiber Parameters		
Signal Wavelength (um) >>	1.55	< Gain vs PumpPower >
Pump Wavelength (um) >>	1.48	< Gain vs Length >
Er-doped Core Radius (um) >>	2.2	< Gain Saturation >
Noise Bandwidth (GHz) >>	5218.3852	< Gain and Absorption >
Signal Absorption Coeff (dB/m) >>	4.3	< ASE Power Spectra >
Pump Absorption Coeff (dB/m) >>	2.5	< Noise Figure >
Signal Absorp X-section (sq m) >>	3.096e-025	<< Back
Pump Absorp X-section (sq m) >>	1.8e-025	Implement >>
Metastable Lifetime (msec) >>	10	
Input and Optimum Output		
Gain (dB) >>	13.6421	
Amplifier Length (m) >>	2.2248	
Input Signal Power (dBm) >>	-25.5923	
Input Pump Power (mW) >>	10	
Pump Threshold (mW) >>	1.83	
Maximum Gain (dB) >>	14.7515	

Figure 10: Physical parameters of EDFA Operation at 1550nm pumped at 1480nm.

EDF OPTICAL AMPLIFIER: PROPERTIES AND OUTPUT		
Fiber Parameters		
Signal Wavelength (um) >>	1.57	< Gain vs PumpPower >
Pump Wavelength (um) >>	1.48	< Gain vs Length >
Er-doped Core Radius (um) >>	2.2	< Gain Saturation >
Noise Bandwidth (GHz) >>	5089.1964	< Gain and Absorption >
Signal Absorption Coeff (dB/m) >>	1.2	< ASE Power Spectra >
Pump Absorption Coeff (dB/m) >>	2.5	< Noise Figure >
Signal Absorp X-section (sq m) >>	8.64e-026	<< Back
Pump Absorp X-section (sq m) >>	1.8e-025	Implement >>
Metastable Lifetime (msec) >>	10	
Input and Optimum Output		
Gain (dB) >>	14.3322	
Amplifier Length (m) >>	4.0524	
Input Signal Power (dBm) >>	-26.8363	
Input Pump Power (mW) >>	10	
Pump Threshold (mW) >>	1.83	
Maximum Gain (dB) >>	16.2551	

Figure 11: Physical Parameters of EDFA operation at 1570nm pumped at 1480nm.

## 2.2 Split-Step Fourier Method for Fiber Propagation

This section briefly explains the well known Split Step Fourier Method (SSF) [9] for modeling the pulse propagation through a single mode optical fiber. More extensive derivations and the explanation of algorithms used are explained in Section 6 of Ref. [1]. For a pulse waveform traveling in a nonlinear dispersive waveguide medium is represented using the nonlinear Schrodinger equation (NSE). Linear effects included in the model include Group Velocity Dispersion (GVD) and fiber attenuation while nonlinear effects modeled include Self Phase Modulation (SPM) and cross phase modulation (XPM). The NSE is given as

$$\frac{\partial A_k}{\partial z} + \frac{\alpha}{2} A_k + \frac{i}{2} \beta_2 \frac{\partial^2 A_k}{\partial T^2} - \frac{1}{6} \beta_3 \frac{\partial^3 A_k}{\partial T^3} = i \gamma_k \left( |A_k|^2 + \sum_{j=1, j \neq k}^N 2 |A_j|^2 \right) A_k \quad (3)$$

where the pulse envelope  $A_k(z,t)$  is propagating in an optical fiber that has nonlinear dispersive properties in channel  $k$ . Fiber attenuation is represented by  $\alpha$ , while  $\beta_2$  and  $\beta_3$  represent second and third order GVD factors. Nonlinear effects are accounted for by  $\gamma$  and the remaining two factors on the right hand side of the equation represent SPM and XPM effects.

As the effects of propagation in an optical fiber can be separated into linear dispersive ( $\hat{D}$ ) and nonlinear ( $\hat{N}$ ) parts, the instantaneous result for the pulse envelope at time  $t$  and propagation distance  $z$  can be obtained by rearranging (3) to obtain

$$\frac{\partial A}{\partial z} = (\hat{D} + \hat{N})A \quad (4)$$

given that

$$\hat{D} = -\frac{\alpha}{2} - \frac{i}{2}\beta_2 \frac{\partial^2}{\partial T^2} + \frac{1}{6}\beta_3 \frac{\partial^3}{\partial T^3} \quad (5)$$

$$\hat{N} = i\gamma_k \left( |A_k|^2 + \sum_{j=1, j \neq k}^N 2|A_j|^2 \right) \quad (6)$$

These two effects can be assumed to act independently. By dividing the whole length of fiber into steps of size  $h$  and using the previous assumption, pulse propagation through one segment of optical fiber of size  $h$  can be thought of as: firstly propagating through segment of size  $h/2$  of purely linear dispersive medium, accumulating all lumped nonlinear effects due to whole segment  $h$  and then finally propagating through another purely linear dispersive medium of size  $h/2$ . This split-step method of approximating the solution to the NSE can be illustrated as shown in Figure 12.

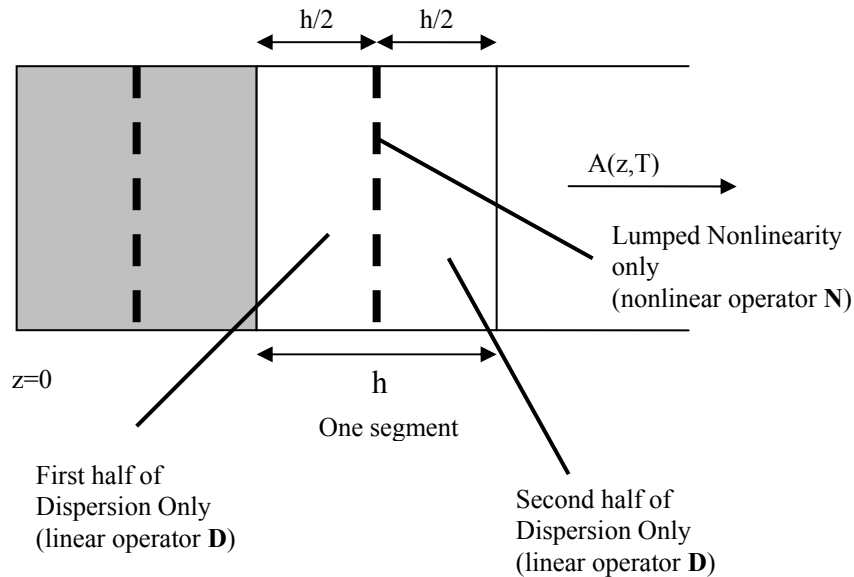


**Figure 12:** Illustration of the Split-Step Fourier Method for Propagation [1].

Mathematically, this method of pulse propagation can be represented as:

$$A(z+h, T) = \exp\left(\frac{h}{2}\hat{D}\right) \exp\left(\int_z^{z+h} \hat{N}(z') dz'\right) \exp\left(\frac{h}{2}\hat{D}\right) A(z, T) \quad (7)$$

where  $\exp(h\hat{D})$  is evaluated using the Fast Fourier Transform (FFT).

### Optimization of SSF Method using Local Error Method

The drawback of using the SSF method is that it requires computations using two FFT per step size which are quite time consuming. Adding to that, it should be acknowledged that the step size used is usually held constant in system simulations as in the case of the original propagation method used in the MOCSS program.

In [13], several step-size selection schemes have been investigated which have found that in most cases, the constant step size method is the least efficient of all methods. In the abovementioned paper, a local error method for step-size selection is introduced. The local error is a measure of the error incurred in propagating through a single step  $h$ . This method is adopted to incorporate a variable step-size selection method in order to achieve more efficient propagation by decreasing the simulation time, while controlling the relative local error.

#### Algorithm for Local Error Method

Step 1: Define the pulse envelope  $u$  (identical  $A$  as used in derivation of split step method theory as above) at distance  $z$  and the relative goal local error,  $\delta_G$ . In the simulations, this is specified as 0.01 (1%). The step size  $h$  is initialized as 500m to match with that used in the fixed step size propagation module.

Step 2: Compute the coarse solution,  $u_c$  at  $(z+2h)$  using step size  $2h$ .

$$u(z+h) \approx \exp\left(h\hat{D}\right) \exp\left\{2h\hat{N}\left[u(z+h, t)\right]\right\} \exp\left(h\hat{D}\right) \quad (8)$$

Step 3: Compute fine solution,  $u_f$  at  $(z+2h)$  using step size of  $h$  for 2 steps.

$$u(z_1, t) = u(z+h, t) \approx \exp\left(\frac{h}{2}\hat{D}\right) \exp\left\{h\hat{N}\left[u\left(z+\frac{h}{2}, t\right)\right]\right\} \exp\left(\frac{h}{2}\hat{D}\right) \quad (9)$$

$$u(z+2h, t) = u(z_1+h, t) \approx \exp\left(\frac{h}{2}\hat{D}\right) \exp\left\{h\hat{N}\left[u\left(z_1+\frac{h}{2}, t\right)\right]\right\} \exp\left(\frac{h}{2}\hat{D}\right) \quad (10)$$

Step 4: Find local relative error given by

$$\delta = \frac{\|u_f - u_c\|}{\|u_f\|} \quad (11)$$

where the norm  $\|u\|$  is defined as

$$\|u\| = \left( \int |u(t)|^2 dt \right)^{1/2} \quad (12)$$

Step 5: Conditions to choosing the step size are as follows

$\delta > 2 \delta_G :$	Solution discarded and step size halved
$\delta_G < \delta < 2 \delta_G :$	Step size divided by a factor of $2^{1/3}$ for next step
$\delta < 1/2 \delta_G :$	Step size multiplied by a factor of $2^{1/3}$ for next step

These conditions are used for most of the propagation unless the remainder of the propagation distance is  $< 2h$ , in which case the next and final step size is set to equal the remainder of propagation distance. This condition is chosen to avoid infinite loops in the simulation which may use very small and improbable step sizes for propagation.

Step 6: Proceed to the next step of propagation with new step size. The fine solution can be used acceptably as the input into the next propagation step.

### ‘Ringing’ Effect

A problem encountered in the pulse propagation simulations is a ‘ringing’ effect causing unwanted oscillations in the pulse waveform due to numerical computations. This problem arises due to the use of an *fftshift* function in MATLAB. Implementing the differential operator  $\partial/\partial T$  requires the operator to be replaced using  $j2\pi f$  [4], where  $f$  utilizes the *fftshift* function. The purpose of this function is to shift the zero-frequency component of a discrete Fourier transform to the center of the spectrum [14].

A possible explanation of the cause of this ‘ringing’ effect is that the discontinuities on both sides of the spectrum are forced to overlap after the *fftshift*, thus causing the unwanted oscillations. Although there have been several attempts at solving this problem, none have achieved the desired outcome. The following figures illustrate the signals before the propagation module (without oscillations) and after a short propagation distance (with ‘ringing’ effect) in eye diagram form.

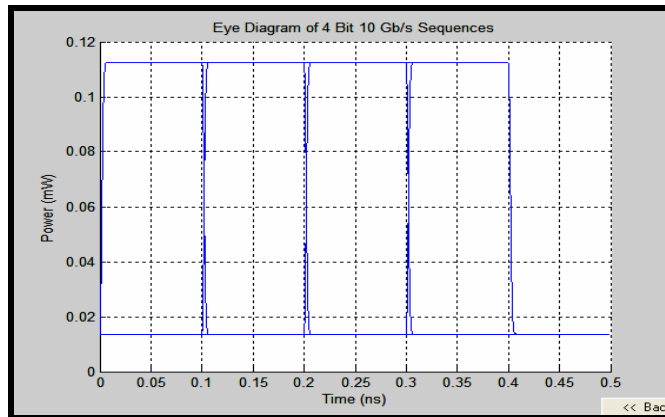


Figure 13: Eye Diagram of signals at transmitter without ‘ringing’ effect.

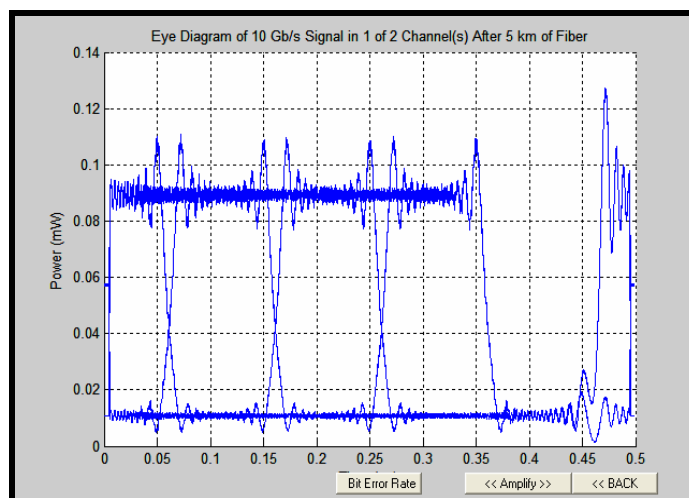


Figure 14: Eye Diagram of signals after propagation with ‘ringing’ effect.

### 3 Implementation of Gaussian pulse profile for different modulation formats

Data transmission forms in one of the crucial factors of the optical communication systems. One of the aims is to implement different modulation and pulse formats into the OC2004 package. This is implemented in order to observe if different modulations formats or different pulse formats significantly influence the system performance. OC2004 package already contains square pulse format for RZ and NRZ modulations. Further two pulse profile, the Gaussian and a raised cosine types are considered.

The time domain representation of a raised cosine pulse profile is given as [15]:

$$R_p(t) = \frac{\sin\left(\frac{\pi t}{T}\right) \cos\left(\frac{\beta \pi t}{T}\right)}{\frac{\pi}{T} \left[1 - \left(\frac{4\beta^2 t^2}{T^2}\right)\right]} \quad (13)$$

where  $\beta$  is roll off factor or the Bandwidth expansion factor.  $0 < \beta < 1$ ,  $\beta = 0$  for a square pulse,  $T$  is the bit period.

Unable to shift the raised cosine by required bit period caused certain problems in implementing the NRZ format. This without further ado considerations are given to implementing Gaussian Pulse format. The Gaussian pulse form is considered as it more accurately models the data waveforms generated in practical optical communications systems[16]. Furthermore Gaussian pulse accurately reflects the practical optical data generators. The Gaussian pulse profile is defined by [15].

$$I_p = e^{-\frac{t^2}{\tau_r^2}} \quad (14)$$

where  $\tau_r$  determines the pulse rise time and fall time. The gradual rise and fall time of the Gaussian pulse reflects the non-instantaneous rise/fall of modern electrical/optical equipment and can be altered at any time by changing the values in the associated .m-file.

The input signal is electrically encoded. The optical source is a single longitudinal mode semiconductor laser which inject laser current  $I(t)$  is a digital pulse waveform that can be defined as[1]

$$I(t) = I_{bias} + \sum_{k=-\infty}^{\infty} A_k I_p(t - kT) \quad (15)$$

where,  $A_k$  is the input data sequence, i.e.  $A_k$  is equal to either 1 or 0 for each  $k$ .  $k$  is bit number.

$$\left\{ \begin{array}{ll} 0 & t < 0 \\ I_p(t) = I_m \left( e^{-\left(\frac{t-T/4}{\tau_r}\right)^2} \right) & 0 \leq t \leq T/2 \\ 0 & T/2 \leq t \leq T \end{array} \right. \quad (16)$$

where,  $I_m$  is the peak modulation current,  $T$  is the bit period and  $\tau_r$  determines the pulse rise time and fall time.

The data pulses become the means through which the laser is modulated to generate data stream[16]. The equation defined above is for the RZ modulation format. implementation of RZ is straight forward, however implementing NRZ is slightly challenging, where different conditions had to be specified in order to consider situations such as ‘11’ where the pulse would not be RZ format. This effect can be overcome by setting a number of conditions where (k-1) bit and (k+1) bit is considered before plotting the k<sup>th</sup> bit. For example to plot ‘1 1 0’ waveform, when plotting the first ‘1’ bit, it must be considered that the following bit is also a ‘1’ this the waveform does not RZ like a RZ modulation would do. So the waveform follows the Gaussian form for first half of the bit period and it stays high for the following one bit period, the next bit is checked. Given that the next bit is a ‘0’ the waveform then Gaussian formula and returns to the ‘0’ level. This is shown in figure below.

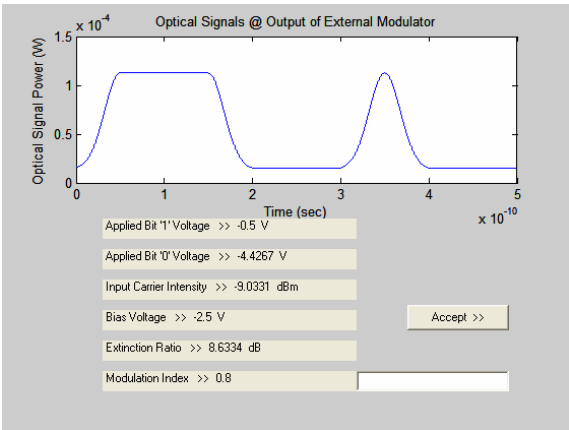


Figure 15 – Gaussian pulse form represents a bit pattern on ‘1100’

Shown below is the RZ and NRZ modulation formats for Square and Gaussian pulse formats.

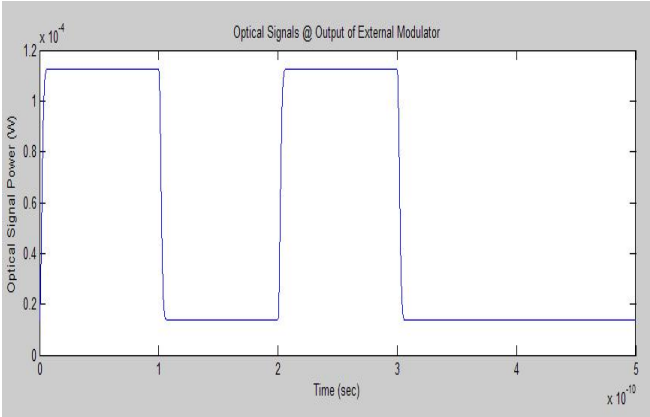


Figure 16 –Optical signal at output of external modulator showing a NRZ Square Pulse

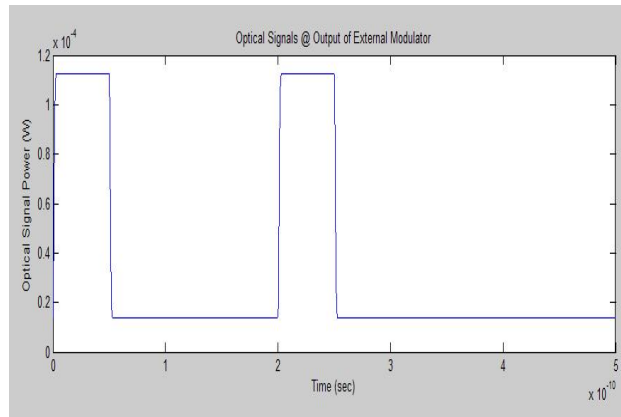


Figure 17 - Optical signal at output of external modulator showing a RZ Square Pulse

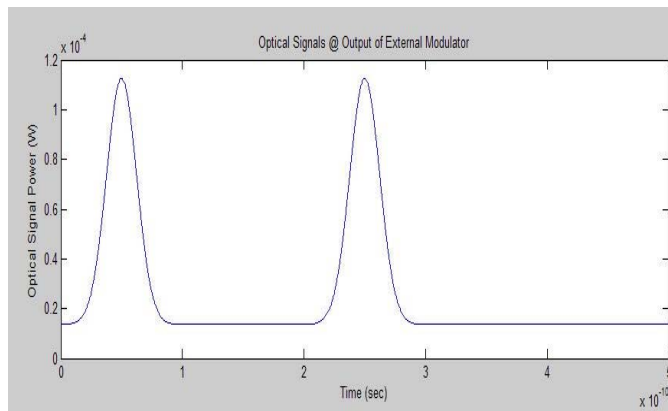


Figure 18 - Optical signal at output of external modulator showing a NRZ Gaussian Pulse

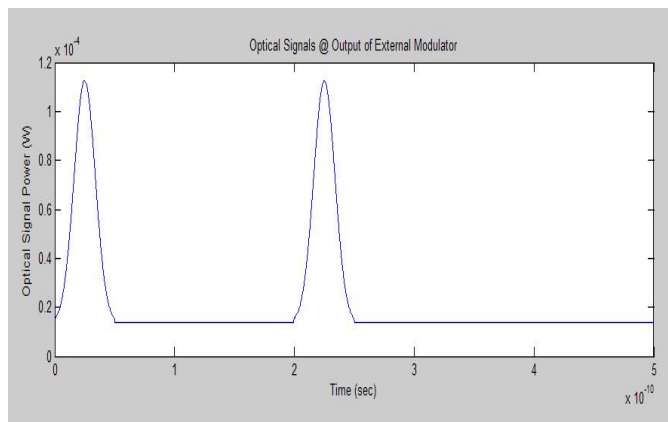


Figure 19 - Optical signal at output of external modulator showing a RZ Gaussian Pulse

#### 4 System performance measurement

In a digital communication system, the system performance measurement or the measure of system accuracy is the BER which is defined as the probability of incorrect identification of a bit by the decision circuit of the

receiver[17]. In another word the BER is the number of incorrect bits received as a proportion of the number of correct bits. It is usually expressed as a single number such as  $10^{-6}$  which is equivalent to an average of 1 error per million bits transmitted. BER of around  $10^{-12}$  is considered to be the minimum acceptable range for error free operation [18].

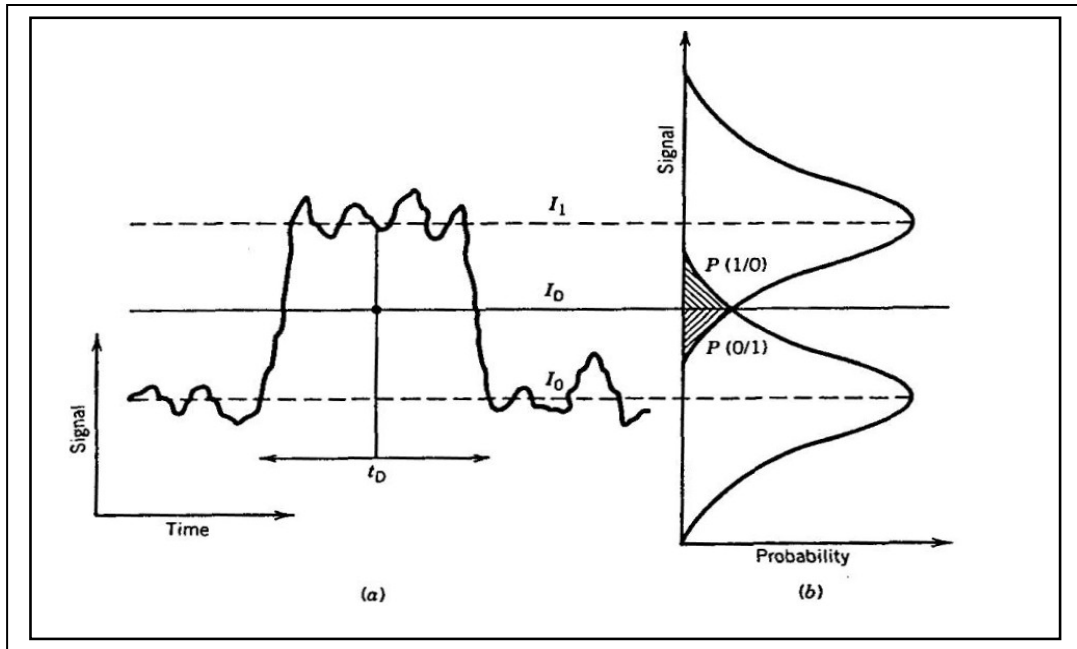


Figure 20 (a) Fluctuation of signals generated or arrived at the receiver (b) Gaussian Pdf of “1” and “0”

Figure 20 [9] shows a sketch of fluctuating signal received by the decision circuit that samples the data at the decision point  $t_D$ . The sampling value  $I$  fluctuates around the average value  $I_1$  and  $I_0$  from one bit to another depending on the value bit corresponds to, either ‘1’ or ‘0’ in the bit stream.  $I_D$  is the threshold value that is used to decide if the sampled value is a ‘1’ or ‘0’. The decision circuit compares the signal value  $I$  with the threshold value and decides it as bit ‘1’ if  $I > I_D$  and decides it as a bit ‘0’ if  $I < I_D$ . Due the noise present, it is likely for errors to occur, and an error occurs when  $I > I_D$  for a bit ‘1’ and  $I < I_D$  for a bit ‘0’. Thus the BER or the total probability of error can be defined as [17]

$$BER = p(1) P(0/1) + p(0) P(1/0) \quad (17)$$

Where  $p(1)$  is the probability of receiving '1' and  $p(0)$  is the probability of receiving '0' and  $p(1/0)$  is deciding '1' when '0' is transmitted and  $p(0/1)$  is deciding '0' when '1' is transmitted. In a binary bit stream obtaining '1's and '0's are equally likely thus

$$p(1)=p(0) = 1/2 \quad (18)$$

The BER equation can then be written as

$$BER = \frac{1}{2}[P(0/1)+P(1/0)] \quad (19)$$

Figure 20 it can be seen that  $P(0/1)$  and  $P(1/0)$  depend on the probability density function  $p(I)$  of the sampled value  $I$ . Noises of optical receivers consist of the thermal noises and quantum shot noises[17]. Thus the functional form of  $p(I)$  depends on statistics of the thermal noise ( $i_T$ ) and the shot-noise contribution ( $i_s$ ). Thermal noise is described by Gaussian statistics with zero mean and variance of  $\sigma_T^2$  and a common approximation treats  $i_s$  as a Gaussian random variable for  $p-i-n$  and APD receivers with different variances ( $\sigma_s^2$ ) [11]. Thus  $I$  can also be described by a Gaussian probability density function since the sum of two Gaussian random variables is also a Gaussian random variable. The variance of sampled value  $I$  is given by

the sum of the variance of thermal noise and shot-noise contribution ( $\sigma = \sigma_T^2 + \sigma_s^2$ ). It must be noted that the average and variance are different for '1' and '0' bits. If  $\sigma_I^2$  and  $\sigma_0^2$  are the corresponding variances for  $I_1$  and  $I_0$  then the conditional probability can be written as

$$P(0/1) = \frac{1}{\sigma_1 \sqrt{2\pi}} \int_{-\infty}^{I_D} \exp\left(-\frac{(I-I_1)^2}{2\sigma_1^2}\right) dI \quad (20)$$

$$P(1/0) = \frac{1}{\sigma_0 \sqrt{2\pi}} \int_{I_D}^{\infty} \exp\left(-\frac{(I-I_0)^2}{2\sigma_0^2}\right) dI = \frac{1}{2} \operatorname{erfc}\left(\frac{I_D - I_0}{\sigma_0 \sqrt{2}}\right) \quad (21)$$

An *erfc* (a complementary error function) is given by

$$\operatorname{erfc}(x) = \frac{2}{\sqrt{\pi}} \int_x^{\infty} \exp(-y^2) dy \quad (22)$$

and this can be used to re-write the above equations as

$$P(0/1) = \frac{1}{2} \operatorname{erfc}\left(\frac{I_1 - I_D}{\sigma_1 \sqrt{2}}\right) \quad (23)$$

$$P(1/0) = \frac{1}{2} \operatorname{erfc}\left(\frac{I_D - I_0}{\sigma_0 \sqrt{2}}\right) \quad (24)$$

MATLAB has its own built in *erfc* function which is used for the simulations. (23) and (24) can be substituted into (19) leading to

$$\operatorname{BER} = \frac{1}{4} \left[ \operatorname{erfc}\left(\frac{I_1 - I_D}{\sigma_1 \sqrt{2}}\right) + \operatorname{erfc}\left(\frac{I_D - I_0}{\sigma_0 \sqrt{2}}\right) \right] \quad (25)$$

From the above equation it can be seen that BER is dependent on the decision threshold  $I_D$  and in practice can be optimized in order to achieve a minimum BER. BER is minimum when  $I_D$  is chosen such that

$$\frac{(I_D - I_0)}{\sigma_0} = \frac{(I_1 - I_D)}{\sigma_1} \equiv Q \quad (26)$$

An explicit expression for  $I_D$  is given by

$$I_D = \frac{\sigma_0 I_1 - \sigma_1 I_0}{\sigma_0 - \sigma_1} \quad (27)$$

The  $Q$  factor can be obtained by combining equations (15) and (16) together,

$$Q = \frac{I_1 - I_0}{\sigma_1 + \sigma_0} \quad (28)$$

The optimized BER can then be written in terms of  $Q$  factor by substituting (28) into (25).

$$BER = \frac{1}{2} \operatorname{erfc}\left(\frac{Q}{\sqrt{2}}\right) \approx \frac{\exp(-Q^2/2)}{Q\sqrt{2\pi}} \quad (29)$$

The asymptotic expansion of  $\operatorname{erfc}\left(\frac{Q}{\sqrt{2}}\right)$  can be used to obtain the approximate form of BER and is reasonably accurate for  $Q$  factor values greater than 3.

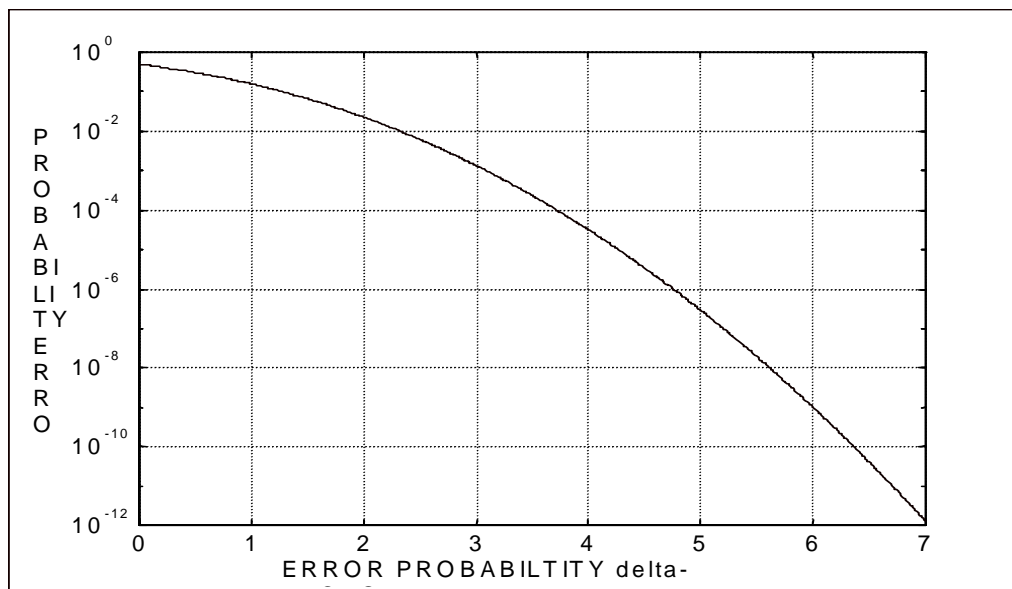


*Figure 21 AN example of BER versus Q factor*

The variation of BER with  $Q$  factor is shown in **Figure 21** [9]. It can be seen that BER decreases as  $Q$  increases and for a  $Q > 7$ , BER becomes lower than  $10^{-12}$ . For  $Q$  values greater than 8, the systems can be considered as error free. The receiver sensitivity corresponds to the average optical power when  $BER \approx 10^{-9}$  for which  $Q \approx 6$ .

Sample of a square pulse NRZ eye diagram is shown in **Figure 22**.

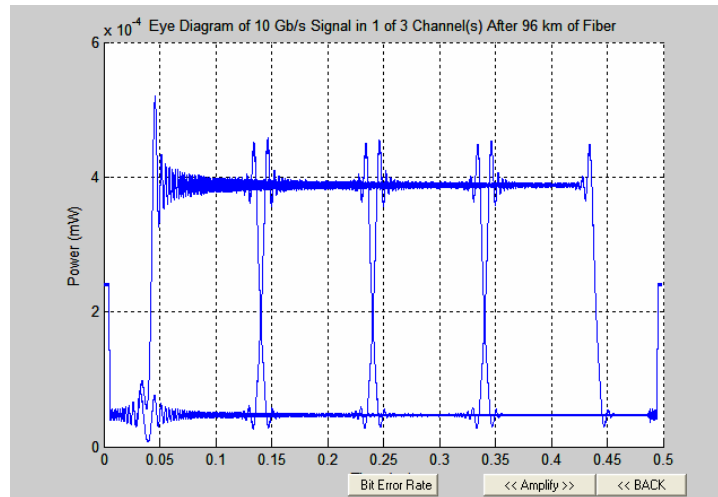


Figure 22 – Sample eye diagram of a Square NRZ pulse

In order to find the BER or the Q factor it is important to find the probability density function for bits ‘1’ and ‘0’ so that the mean and standard deviations of function can be used to find the BER and Q factor. By plotting a PDF function it can be seen if the function is a Gaussian PDF. And due to the ringing effect present in the eye diagram, it is a problem to obtain a Gaussian PDF. Thus when selecting the range for the eye diagram, it is made sure that the inconsistency caused by the ringing effect is ignored from the PDF. The PDF for bits ‘1’s and ‘0’s are plotted to verify that they can be approximated to a Gaussian distribution. An example of one of the PDF plotted using MATLAB is shown in **Figure 23**

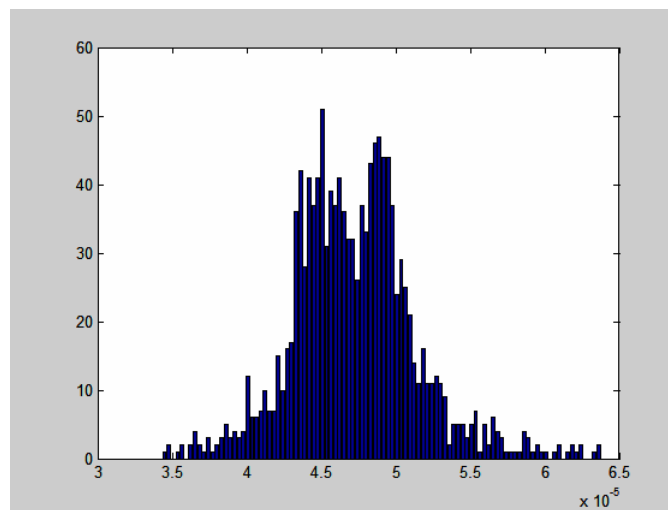


Figure 23 – Sample PDF plotted for bit ‘0’

Once it is approximated to be a Gaussian distribution, then  $\sigma_0$  and  $\sigma_1$  are found by finding the standard deviation of PDF. The red arrow in figure below shows where the standard deviation  $\sigma_0$  and  $\sigma_1$  lies within the PDF of '1' or '0'.

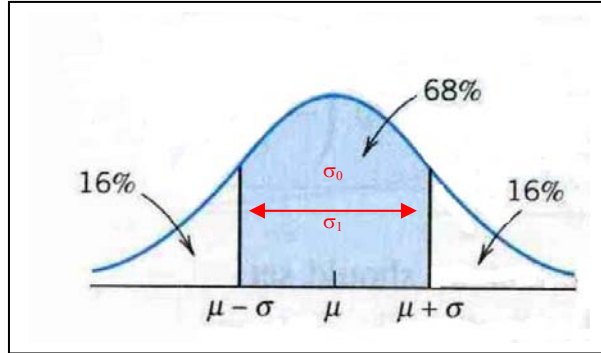


Figure 24 PDF of a Normal or Gaussian distribution of 2 standard deviations

**Figure 24** [19] shows the probability density function of a Gaussian distribution with a mean of  $\mu$  and standard deviation of ' $\sigma$ '. Around 2/3 of all values to be observed will lie between  $\mu \pm \sigma$ . Thus  $\sigma_0$  and  $\sigma_1$  are found by calculating  $2\sigma$  of the PDF.  $I_1$  and  $I_0$  are found by finding the mean  $\mu_0$  and  $\mu_1$ . Once these values are found it can be substituted into the Q factor in order to obtain a Q value.

$$Q = \frac{I_1 - I_0}{\sigma_1 + \sigma_0} \quad (30)$$

BER is then calculated using the relationship between Q factor and BER as mentioned earlier.

$$BER = \frac{1}{2} \operatorname{erfc}\left(\frac{Q}{\sqrt{2}}\right) \approx \frac{\exp(-Q^2/2)}{Q\sqrt{2\pi}} \quad (31)$$

Performance measurement is implemented for both Gaussian and square pulse form and both the RZ and NRZ modulation formats.

## 5 System Simulations and Comparative Studies

A single fiber transmission span is simulated to obtain a measure of its performance over 80 km SSMF with a dispersion compensation (DCF) module which consists of two optical amplifiers with 16km DCF located in between the amplifiers. It is acceptable to simulate results for one fiber span to predict an optical communications link's performance over several hundred kilometers as these spans can be cascaded from one

end of the transmission link to another. Figure 25 illustrates the fiber span which is simulated on the OC2004 software.

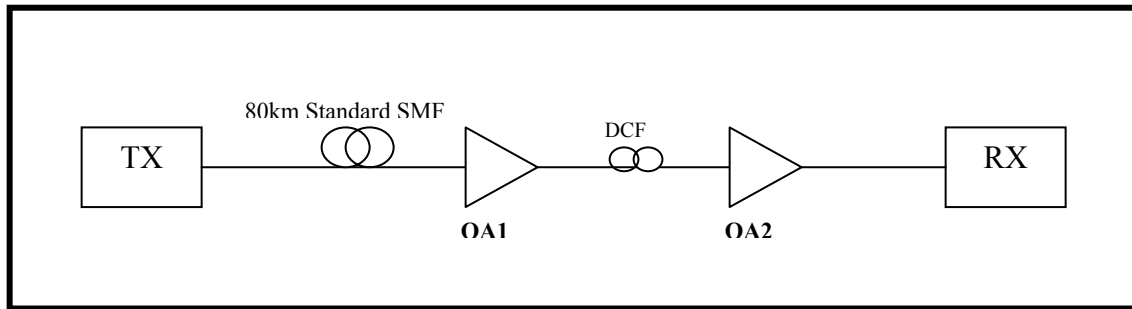


Figure 25: System Simulated for Performance Measurement

### 5.1 Modeling of Fiber Span Using SMF, DCF and OA

The obvious configuration that provides the best performance amongst the various combinations tested is using a Gaussian pulse format propagating in the C-Band using RZ line coding format as seen in Table 2. Propagation in the C-Band performs consistently better than that in the L-Band. This outcome can be improved upon if the EDFA length, pump power and pumping scheme could be optimized for a flat gain spectrum over the L-Band [6].

Whilst most of the results show error free transmission ( $Q\text{-factor} > 8$ ), the combination that shows the worst overall performance is the square pulse waveform operating in the L-Band. However, the very low  $Q\text{-factor}$  value obtained (approximately  $Q\text{-factor} = 2$ ) for the RZ modulation format is unexpected. This can partly be attributed to the ‘ringing’ effect as the square pulse waveform does not seem as resilient towards these oscillations as compared to the Gaussian pulse waveform.

Line Coding Format	Operating Region	Pulse Waveform	Q-factor before OA2	Q-factor after OA2
NRZ	C-Band	Square	10.4	10.8
		Gaussian	18.5	19.0
	L-Band	Square	7.3	7.4
		Gaussian	11.7	12.4
RZ	C-Band	Square	7.6	8.0
		Gaussian	20.6	25.0
	L-Band	Square	2.2	2.1
		Gaussian	10.8	12.6

**Table 2:** Summary of  $Q\text{-factor}$  results after single fiber span propagation of 80km SMF and DCF module. Comparing the  $Q\text{-factors}$  estimated before and after the second optical amplifier (OA2), a higher  $Q\text{-factor}$  is obtained for nearly all of the system configurations after the second optical amplifier. This result is as

expected since the DCF can compensate for the majority of the pulse broadening effects before OA2 amplifying the signal.

### 5.2 Modeling of Fiber Span Using NZ-DSF

This section studies the differences in system performance between an optically amplified system using 80km SSMF and 16km DCF with another system transmitting 80 km using Non-Zero Dispersion Shifted Fiber (NZ-DSF). The NZ-DSF is chosen to have minimum dispersion at the 1550nm wavelength. Two C-band system configurations are chosen for this comparison namely the RZ and NRZ Gaussian input transmitting through 80km fiber. The eye diagrams and their corresponding Q-factor estimations are shown in Figure 26 to Figure 29.

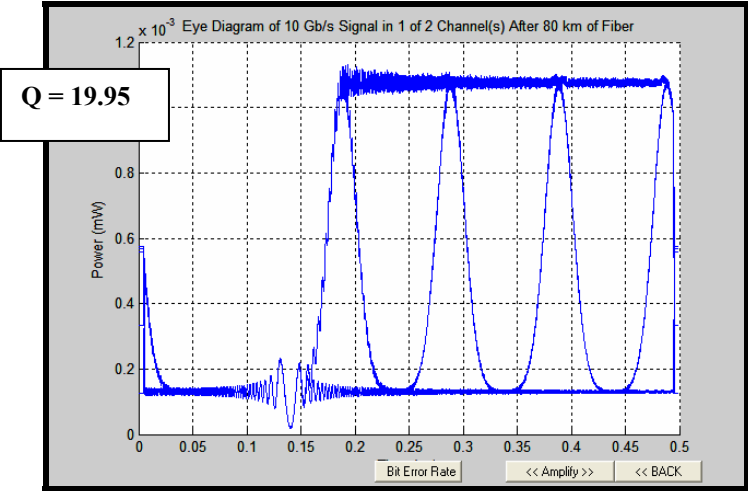
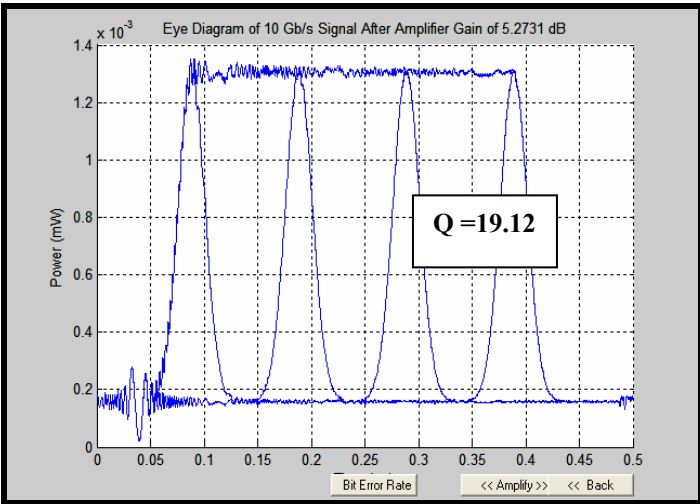
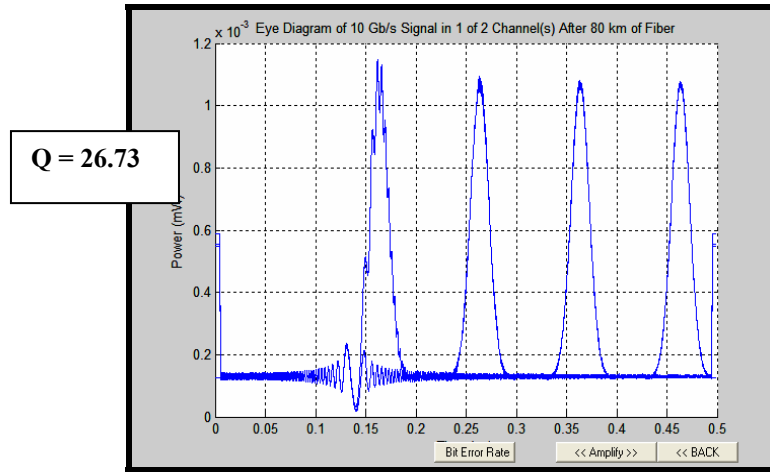


Figure 26: Eye Diagram for NRZ, C-Band, Gaussian pulse input after 80km NZ-DSF Transmission



**Figure 27:** Eye Diagram for NRZ, C-Band, Gaussian pulse input after 80km SMF + 16km DCF Optically Amplified Transmission



**Figure 28:** Eye Diagram for RZ, C-Band, Gaussian pulse input after 80km NZ-DSF Transmission

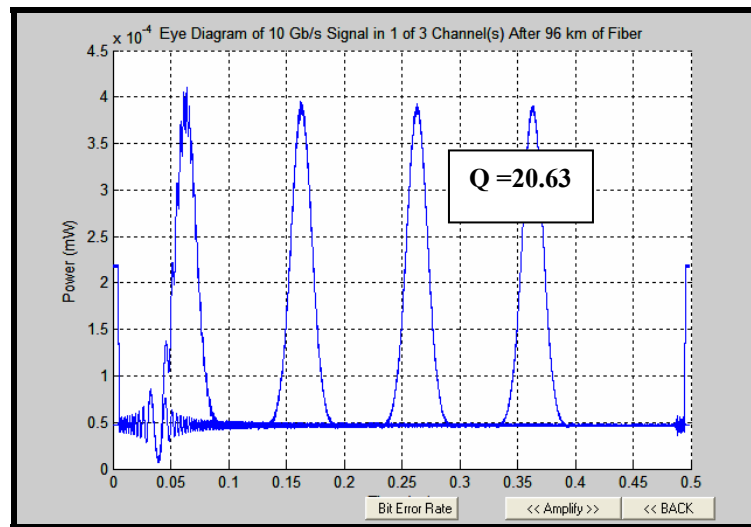


**Figure 29:** Eye Diagram for RZ, C-Band, Gaussian pulse input after 80km SMF + 16km DCF Optically Amplified Transmission

Comparing the two system configuration results, it can be concluded that using 80 km NZ-DSF transmission allows for improvements in the Q-factor derived from the eye diagrams as compared to that using 80 km SSMF + 16 km DCF and optical amplifiers. For the RZ configuration, the improvement in the Q-factor by 6.1 is much larger compared to the NRZ configuration with an improvement of 0.83. The main difference in the eye diagrams show that the NRZ configuration has more signal distortion, whereas there is minimum waveform distortion in the RZ case. This leads us to conclude that the very small changes in the RZ

configuration will impact greatly on the change in Q-factor estimated for the system thus leading to the large difference in Q-factor improvement.

However, the above results leads to confirmation that the NZ-DSF system shows improved performance as compared with the SSMF system due to its minimum dispersion tuned within the system operating C-Band.

### 5.3 Effect of Channel Spacing

In order to monitor the effect of channel spacing on the signal waveform, the demultiplexed output before fiber propagation are compared. Overall, most the signals could be recovered down to 50GHz channel spacing, although with some acceptable level of distortion as seen in Figure 16 and 17. However, for channel spacing smaller than this, there is significant distortion of the transmitted waveform due to inter-channel crosstalk. The crosstalk effect leads to a decreased level of system performance as the signal power from one channel is transferred to a neighbouring channel, causing corruption of the signal waveform which can be observed in Figure 30. Figure 30 to Figure 32 illustrate the demuxed channels for channel spacing of 200, 50 and 12.5 GHz respectively.

Referring to the output of the *Demultiplexer* module, it can be observed that at larger channel spacings such as 200GHz and 100GHz spacing, there is adequate suppression of the signal in adjacent channels when individual channel waveforms are recovered. In the extreme case, with 12.5GHz and 7GHz channel spacing, the filtered signal spectrum show that all the multiplexed signals interact and there is negligible suppression of adjacent channels. This is evidenced by the extremely distorted recovered signal waveforms.

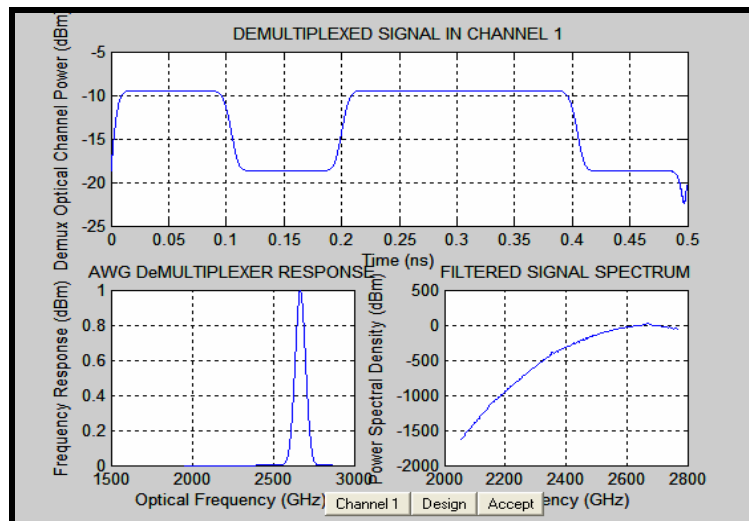


Figure 30: Recovered signal with 3 Channels multiplexed at 200GHz spacing before fiber propagation.

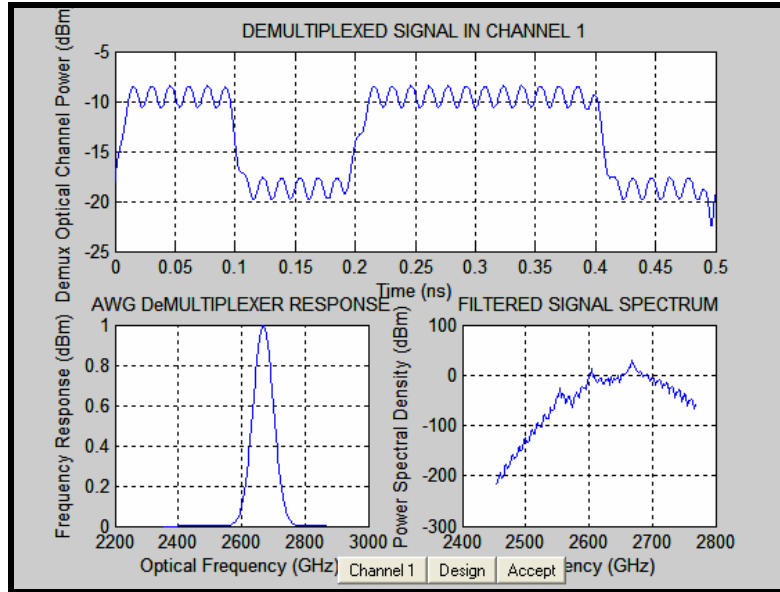


Figure 31: Recovered signal with 3 channels multiplexed at 50GHz spacing before fiber propagation.

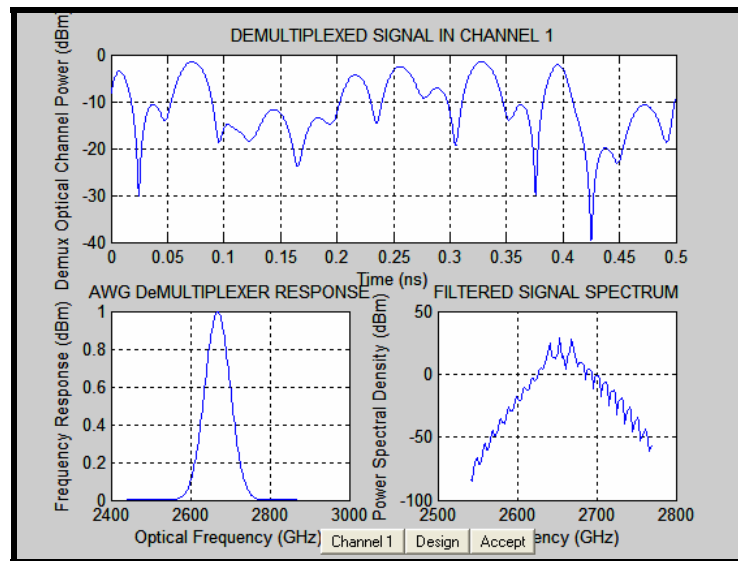


Figure 32: Recovered signal with 3 channels multiplexed at 12.5GHz spacing before fiber propagation.

To improve performance of the overall system to obtain the smallest channel spacing for the purpose of increasing channel capacity, a recommendation for further improvement would be to redesign the passband of the MUX/DEMUX module.

#### 5.4 Measurement of Efficiency of Variable vs. Fixed Step Size Propagation

Contrasting the Q-factor output obtained for the simulations using both variable and fixed step size propagation methods, it is observed that there is no significant difference. However, efficiency of the fiber propagation module can be said to have improved when using the variable step size method as it decreases the

overall simulation time greatly. Figure 24 below shows a plot of measure simulation time versus propagation distance.

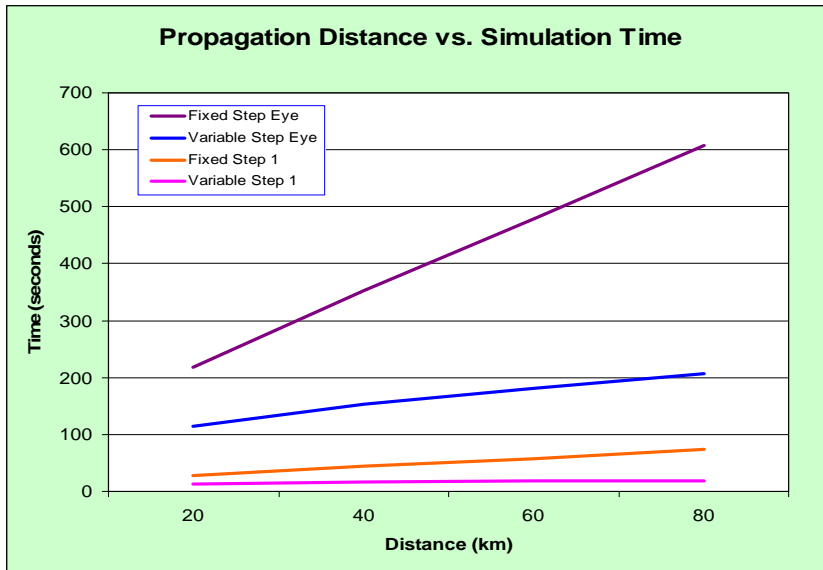


**Figure 33:** Propagation Distance vs. Simulation Time for Variable Step-Size and Fixed Step-Size Propagation Methods for initial hstep = 500m.

Figure 33 shows that there is improvement in simulation time especially for the processing of eye diagrams. Whilst the simulation time for 20km propagation using the fixed step-size method is roughly double that of the variable step-size method, at 80km propagation, the simulation time difference is approximately tripled. Note that Fixed Step 1 and Variable Step 1 both measure the time taken to calculate the Average Power Loss for the propagation distance as stated in the x-axis.

### 5.5 Accuracy of Q-factor and BER Estimation

In order to check the accuracy of the Q-factor and BER estimation module in OC2004, four general system formats with their eye diagrams after one span of propagation are extracted to calculate the Q-factor by hand.

Manual calculation of the Q-factor is done using:

$$Q = \frac{\mu_1 - \mu_0}{\sigma_1 + \sigma_0} \tag{32}$$

where

$$\begin{aligned} \sigma_1 &= 0.68(\delta_1) \\ \sigma_0 &= 0.68(\delta_0) \end{aligned} \tag{33(a) (b)}$$

The noise levels around the ‘1’ and ‘0’ mean values  $\mu_1$  and  $\mu_0$ , are assumed to be of a Gaussian distribution. Thus as shown in equation 15, only 68% (corresponding to 2 standard deviations of a Gaussian distribution) of the range of ‘1’ and ‘0’ values ( $\delta_1$  and  $\delta_0$ ) in the sampled area are considered when obtaining the standard deviation values. Notice that extreme points attributed to the ‘ringing’ effect are ignored in order to obtain acceptable values for the  $Q$ -factor manually. This is acceptable due to the fact that this method enables more accurate results that reflect the true performance of the system to be measured.

Uncertainties are obtained for the manually calculated  $Q$ -factor values by

$$\frac{\Delta Q}{Q} = \frac{2\Delta\mu}{\mu_1 - \mu_0} + 0.68 \left( \frac{2\Delta\delta}{\delta_1 + \delta_0} \right) \quad (34)$$

given  $\Delta\delta$  and  $\Delta\mu$  are 0.05 cm each, as this is the smallest value that can be read.

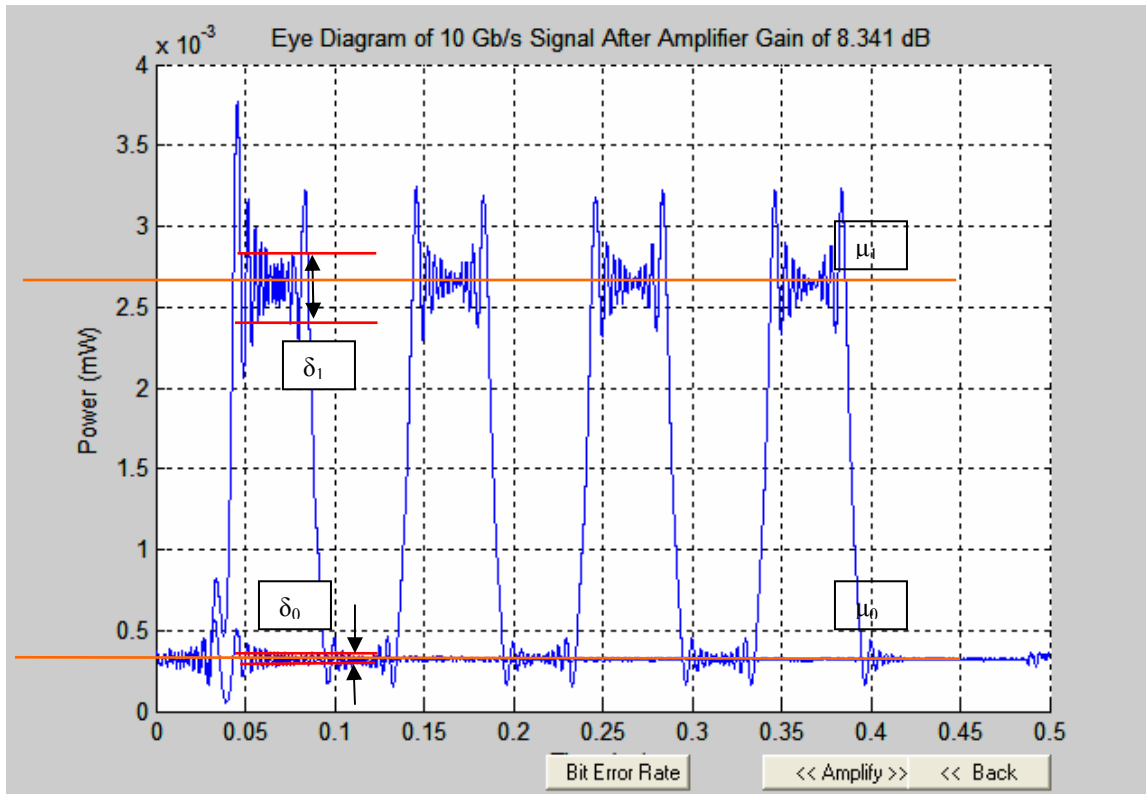


Figure 34: Sample eye diagram to read  $Q$ -factor manually.

System	Measurements (cm)		Q calculations
NRZ square	$\mu_1 = 6.05$	$\delta_1 = 0.5$	$Q = \frac{6.05 - 0.7}{0.68(0.5 + 0.3)} = 9.83$
	$\mu_0 = 0.7$	$\delta_0 = 0.3$	
RZ square	$\mu_1 = 5.65$	$\delta_1 = 0.85$	$Q = \frac{5.65 - 0.65}{0.68(0.5 + 0.1)} = 7.74$
	$\mu_0 = 0.65$	$\delta_0 = 0.1$	

NRZ Gaussian	$\mu_1 = 7.35$	$\delta_1 = 0.3$	$Q = \frac{7.35 - 0.9}{0.68(0.3 + 0.15)} = 21.1$
	$\mu_0 = 0.9$	$\delta_0 = 0.15$	
RZ Gaussian	$\mu_1 = 7.35$	$\delta_1 = 0.25$	$Q = \frac{7.35 - 0.85}{0.68(0.25 + 0.1)} = 27.3$
	$\mu_0 = 0.85$	$\delta_0 = 0.1$	

**Table 3:** Measurements obtained manually from eye diagrams.

The following system formats tabulated in Table 4 in operating in the C-Band are selected for comparison between the manually (M) obtained values as compared to the OC2004 simulation (S) values:

<i>System</i>	$Q_S$	$Q_M$	$\Delta Q_M$	$\Delta Q_M (\%)$	$Q_M \pm \Delta Q_M$
NRZ square	10.8	9.83	1.02	10.4	$9.83 \pm 1.02$
RZ square	8.0	7.74	0.71	9.17	$7.74 \pm 0.71$
NRZ Gaussian	19.0	21.1	3.52	16.68	$21.1 \pm 3.52$
RZ Gaussian	25.0	27.3	5.72	20.95	$27.3 \pm 5.72$

**Table 4:** Uncertainty calculations for manually obtained Q-factor values and comparison with Q-factor values from OC2004 simulations.

Table 4 shows that the simulation results for the Q-factor fall within the acceptable range when compared to the manually obtained values. It is also observed that the uncertainty values for  $Q_M$  are much larger for Gaussian pulse input system configurations. This is due to the fact that there is very small distortion in the Gaussian pulse waveform after amplification and compensation. Thus, when measurements are obtained from the eye diagrams, very small changes can greatly affect the manually obtained Q-factor values.

It would also be appropriate to note here that the BER and Q-factor estimation model as is in the OC2004 package at the moment is configured to read for the 80km SSMF + OA1 + 16km DCF + OA2 system. Other system configurations require manual adjustment of the sampling code in order to obtain the correct estimations for the Q-factor and BER from the eye diagrams.

## 5.6 Comparison of OC2004 and Simulink Models

In order to obtain a measure of the accuracy of the OC2004 results, the output from three Simulink models are compared with the OC2004 output. The system combination consist of a square pulse waveform with NRZ line coding format operating in the C-Band transmitting through 80 km SSMF and 16km DCF. The Simulink model is shown in Figure 35.

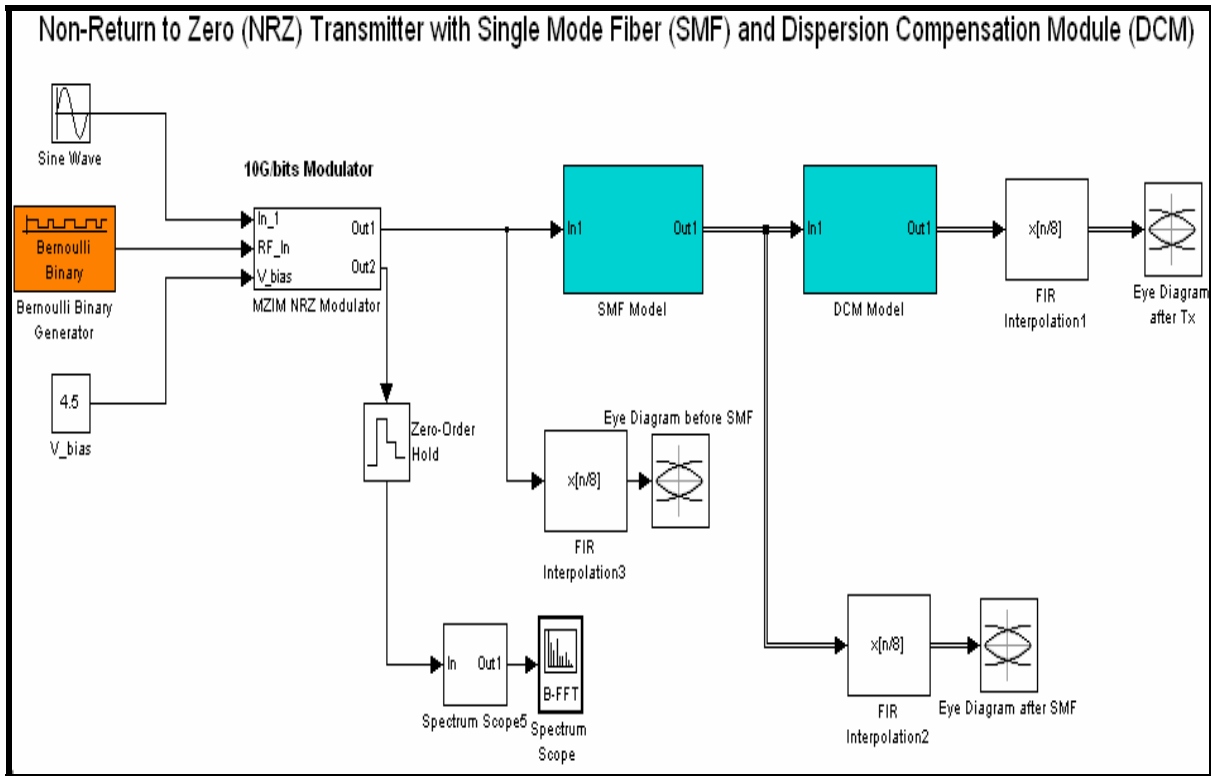


Figure 35: Simulink Model with NRZ input through 80km standard SMF and 16km DCF.

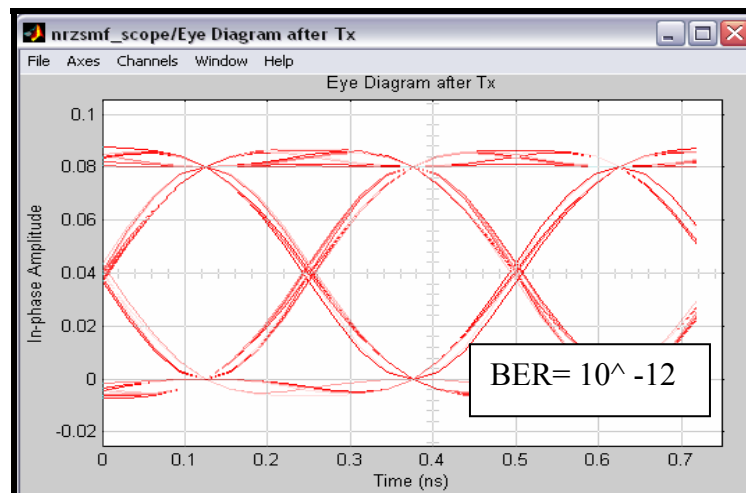
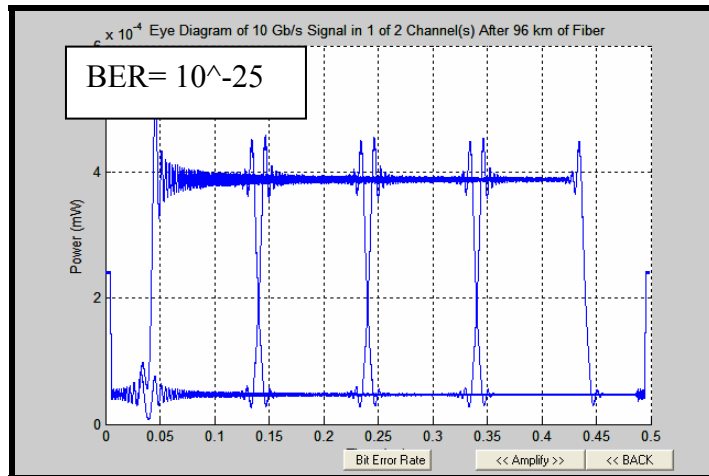


Figure 36: Electrical Eye Diagram of NRZ Simulink model at Receiver after 80km SMF and 16km DCF Transmission[2]



**Figure 37:** *Optical Eye Diagram of NRZ OC2004 model after 80km SMF and 16km DCF Transmission*

For the same NRZ simulated system, the OC2004 results show an estimated BER of  $10^{-12}$  for the Simulink model as compared to  $10^{-25}$  for the OC2004 model. This discrepancy can be attributed to the fact that the OC2004 model only simulates for a 4-bit input sequence at the eye diagram but the Simulink model simulates an 8-bit sequence.

The second Simulink model as seen in Figure 38 simulates an NRZ system that propagates through 80km Non-Zero Dispersion Shifted Fiber (NZ-DSF@1550nm). A BER of  $10^{-12}$  is obtained whilst a similar system when modeled in the OC2004 package gives a BER of  $10^{-24}$ . The corresponding eye diagrams can be seen in Figure 38 and Figure 39. This discrepancy can also be explained by the difference in eye diagram modeling.

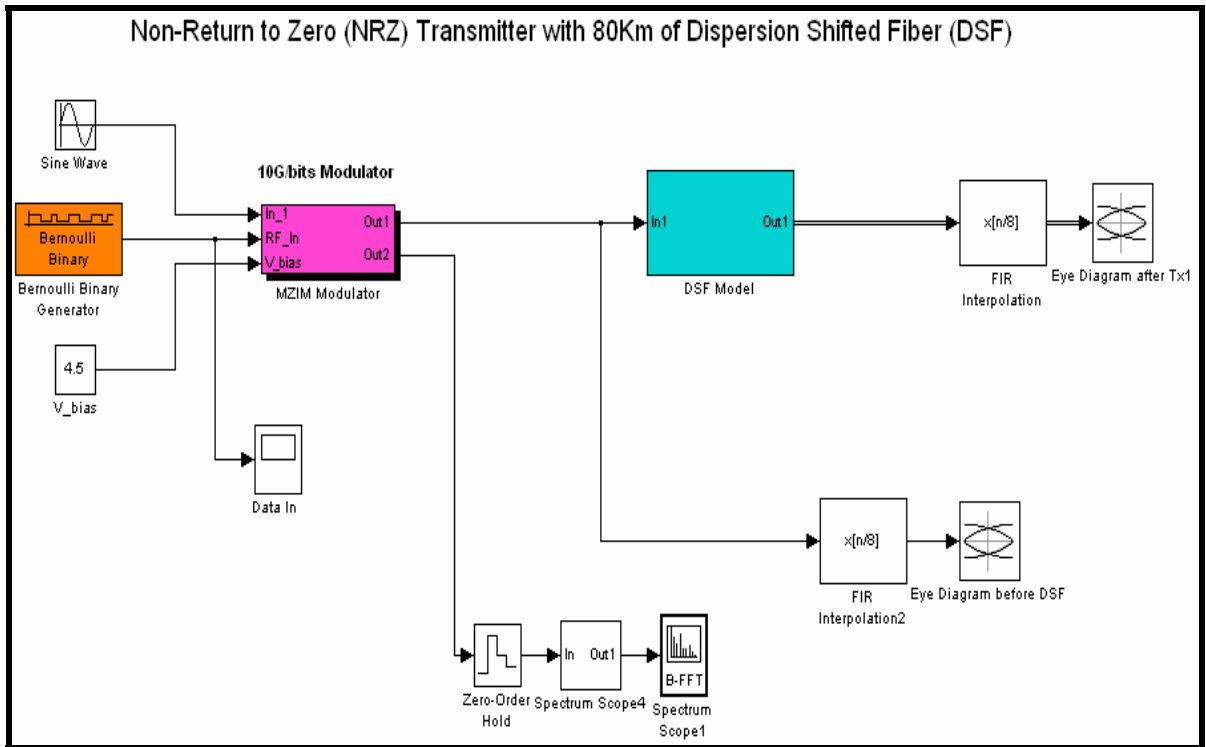


Figure 38: Simulink Model with NRZ input through 80km NZ-DSF@1550nm

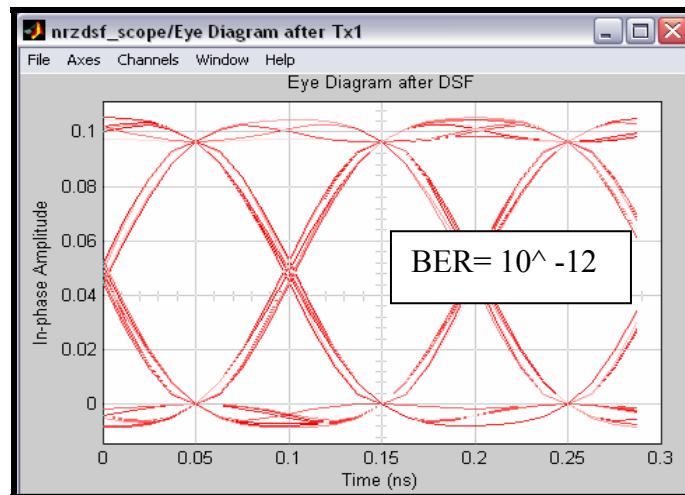
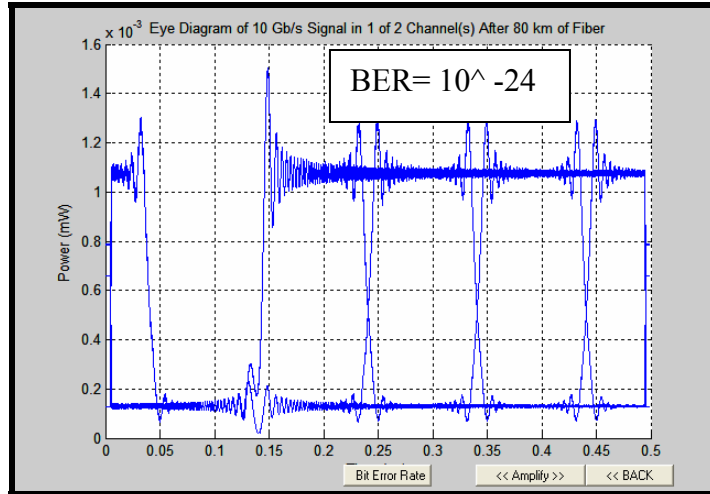


Figure 39: Eye Diagram of NRZ Simulink model at Receiver after 80km NZ-DSF@1550nm transmission[5].



**Figure 40:** Eye Diagram of NRZ OC2004 model after 80km NZ-DSF@1550nm transmission.

The final Simulink model utilizes a Differential Quadrature Phase Shift Keying (DQPSK) modulator with output that is half the bandwidth of the transmitter used in OC2004. By using two Mach-Zehnder Modulators (MZMs) and a phase modulator, this enables the DQPSK transmitter to effectively double the transmission rate. The Simulink transmitter module as shown in Figure 41 transmits an RZ Gaussian pulse in the C-band which propagates through 80km SSMF and 16km DCF.

### RZ-DQPSK Transmitter

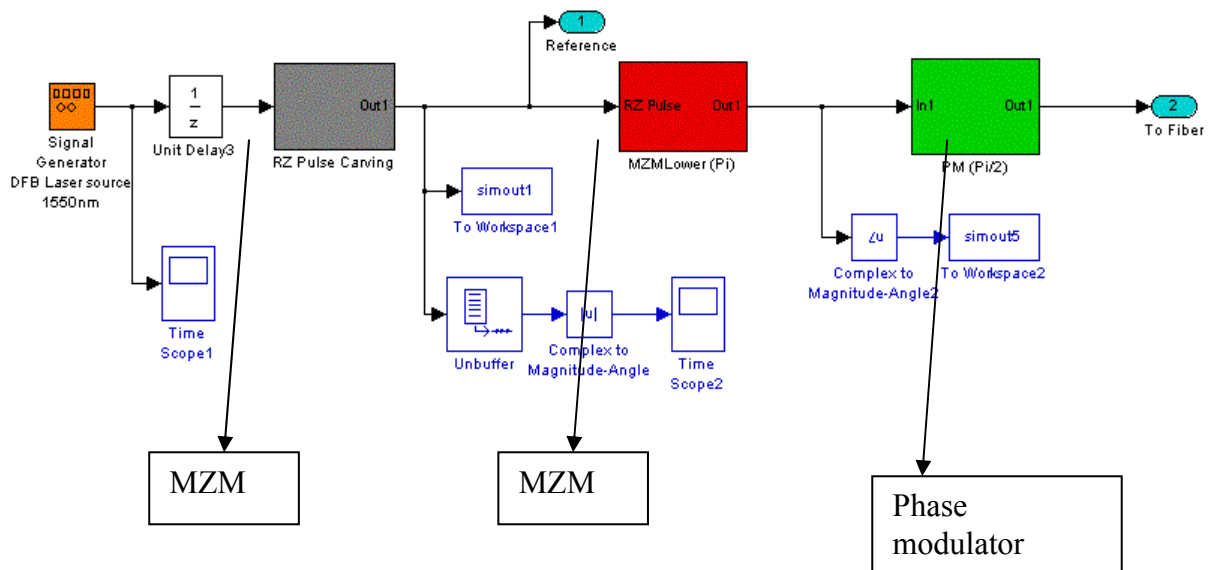
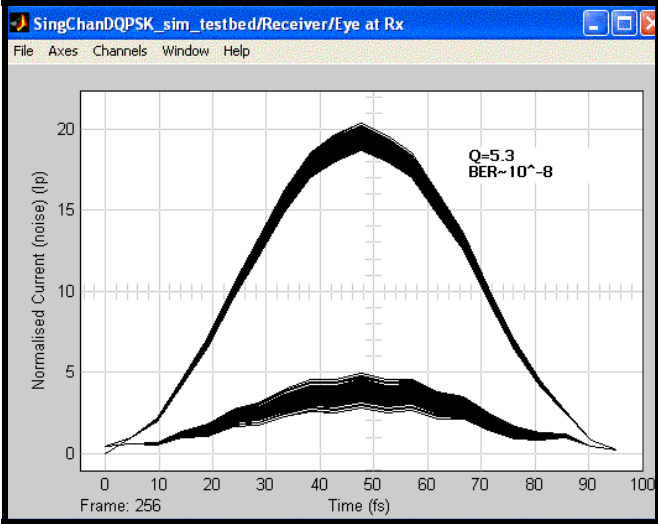


Figure 41: Simulink Model with DQPSK Transmitter and RZ input through 80km SSMF and 16km DCF.

This DQPSK Simulink model provides an output eye diagram which overlays the output for a 256-bit combination. The overall performance is measured to have a Q-factor of 5.3 and a BER value of  $10^{-8}$  from the eye diagram in Figure 42.



**Figure 42:** Eye diagram for RZ Gaussian pulse input system with transmission over 80km SMF and 16km DCF detected by a single photo-detector.

Comparing results from OC2004 with RZ Gaussian pulse input and transmission over 80km SSMF and 16km DCF, we obtain  $Q = 20.6$  as seen from Figure 43. This notable difference in the Q factor obtained can be explained by the fact that the OC2004 eye diagram is generated for a 4-bit input sequence only. Furthermore, as the DQPSK Simulink model provides half the bandwidth as compared to the OC2004 model, the transmission distance in our model needs to be halved for more suitable comparison since dispersion is proportional to the length and bandwidth of transmission.

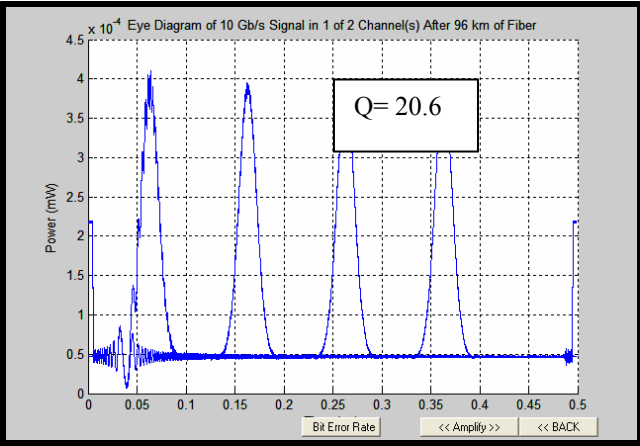


**Figure 43:** *Eye diagram output from OC2004 with RZ Gaussian input pulse after 80km SMF and 16km DCF transmission.*

As the OC2004 model simulates only 4-bit input sequences in each eye, the BER and Q-factor estimation can be regarded as best case scenarios when compared to Simulink model outputs which may present slightly worse case scenarios.

Contrasting the Simulink models with the OC2004 model, it can be concluded that a recommendation for future development would be to extend the capability of the eye diagram plotting module to at least 64 bits as this would facilitate more direct comparisons of results with other models such as the Simulink models. Overlapping all traces for each of the bits onto a single eye trace can also be considered. Readers should note that in practice, simulations should be run for at least 64 – 128 bits.

## **6 Graphical Representation of OC2004 Simulator and Execution Procedures**

This section aims to provide a brief manual to guide users in the use of the OC2004 software package. As should be noted, this package has been designed to work in MATLAB 6.5 and performance in all other versions of MATLAB is not guaranteed. Readers who do not need to follow the execution procedures can skip this section and proceed to Section 7.

The example below is for 80km SSMF + OA1 + 16km DCF + OA2 configuration.

1. Load all of OC2004 files into a folder.
2. Set this folder as the Current Directory in MATLAB.
3. To start this package, type 'start1' in the Command Window.
4. Follow Prompt: "Click to Begin" or "Click to Exit".

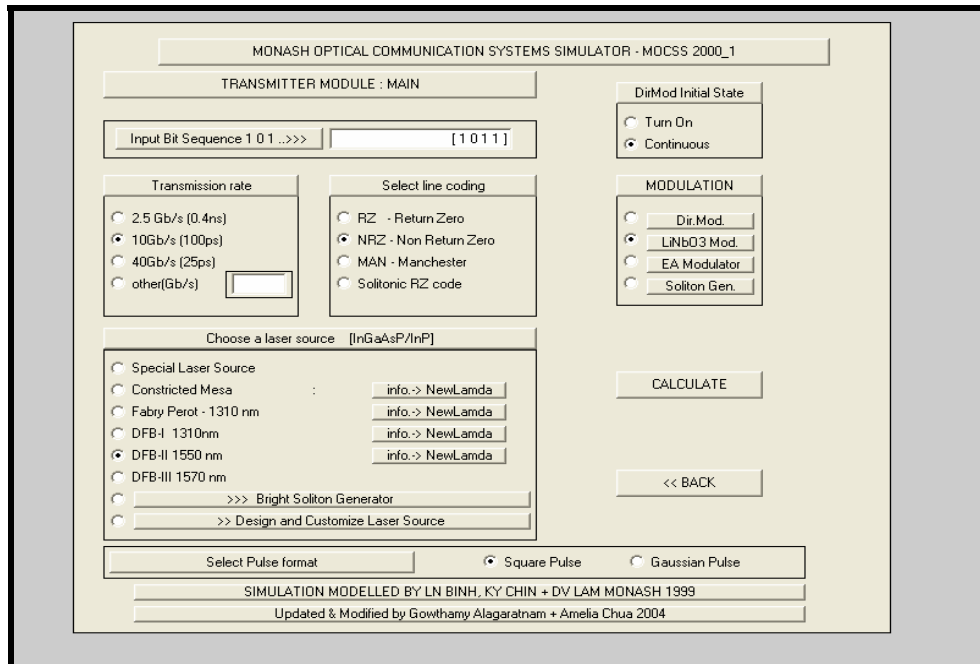


**Figure 44:** Main Transmitter Module for use to choose input bit sequence, modulator, line coding format, transmission rate, pulse format and laser source.

## 6.1 Main Transmitter Module Window

- Input Bit Sequence : Up to 4 bits
  - Transmission Rate: 10Gb/s
  - Modulator: LiNbO<sub>3</sub> for external modulation
  - DirMod Initial State: Always set as ‘Continuous’ to initialize external modulation
  - Select Line Coding: NRZ or RZ
  - Laser Source: DFB-II@1550nm for C-Band operation or DFB-III@1570nm for L-Band operation
  - Pulse Format: Square Pulse or Gaussian Pulse format
5. Press Calculate. This will call up the output at External Modulator window. Click Accept.

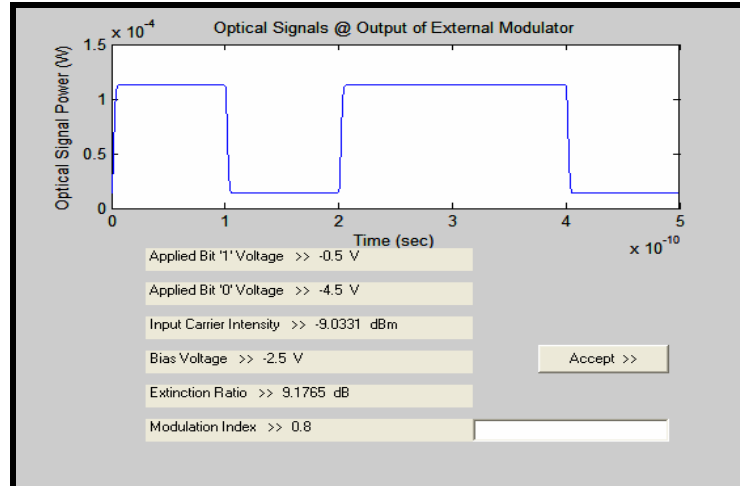
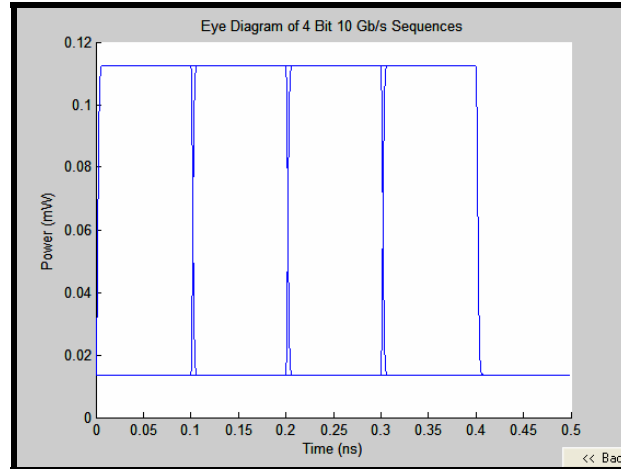


Figure 45: Output at External Modulator window.

6. This calls up the Main Transmitter Window again. Click on the 'Transmitter Plot' button to view various plots of interest.
7. The plots available for viewing are such as:
  - Modulator Applied Voltage
  - Power Output, Spectrum and Noise Spectral
  - Photon and Carrier Density, Phase and Frequency Chirp
  - Eye Diagram (at transmitter)
  - Sample Eye Diagrams
  - Laser Source Line-Width Spectral Plot

Note that the Eye Diagram *must* be viewed at this section in order to view further eye diagrams in the progressive modules.



**Figure 46:** *Eye Diagram at Transmitter.*

8. Click on ‘WDM Transm>>’ for Wavelength Division Multiplexing.
9. The Transmitter Check-List Menu will appear as in Figure 47.

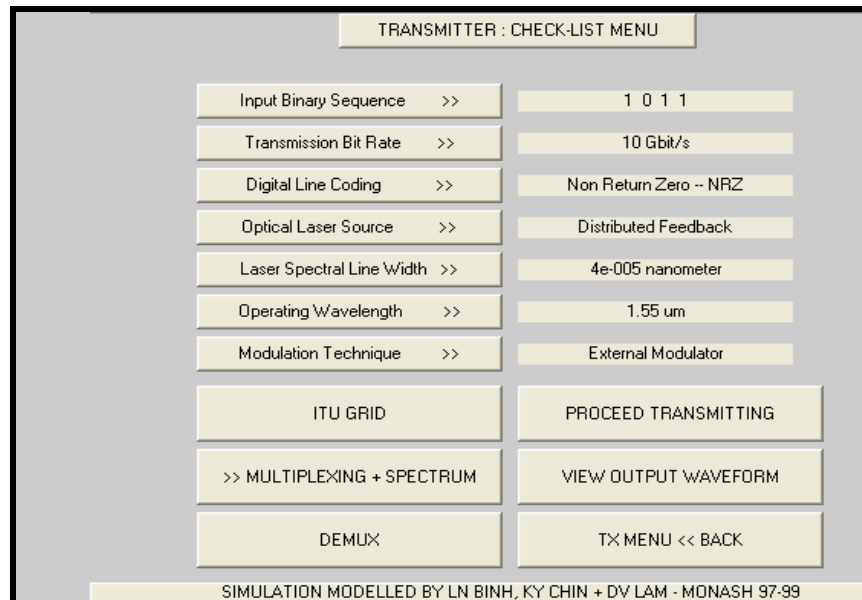


**Figure 47:** *Transmitter Check-List Menu after WDM Transmission is chosen.*

10. Choosing ‘>> Multiplexing + Spectrum’ before adding any channels will show the frequency spectrum of the first channel.

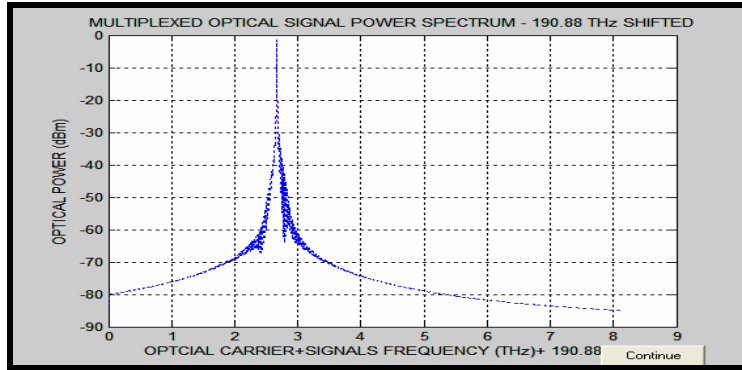


Figure 48: Frequency spectrum of first channel.

11. The 'ITU Grid' button will show the wavelength channels available for WDM Transmission with different channel spacings at both the C and L-Bands.

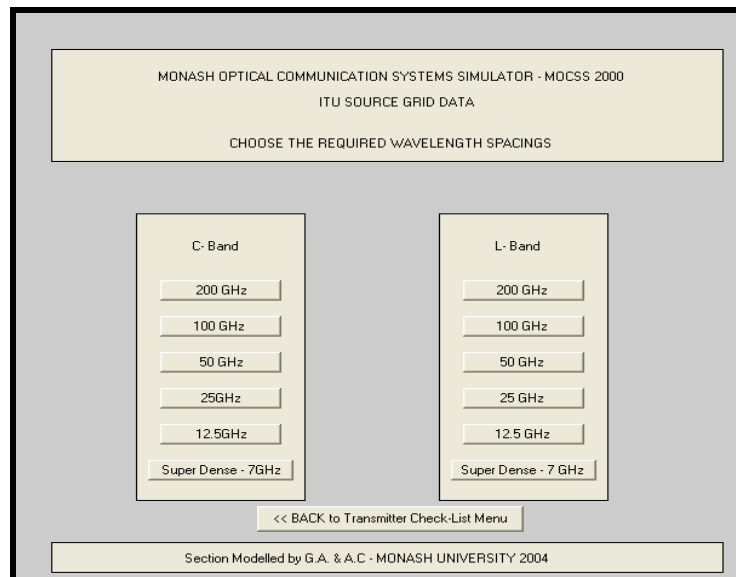
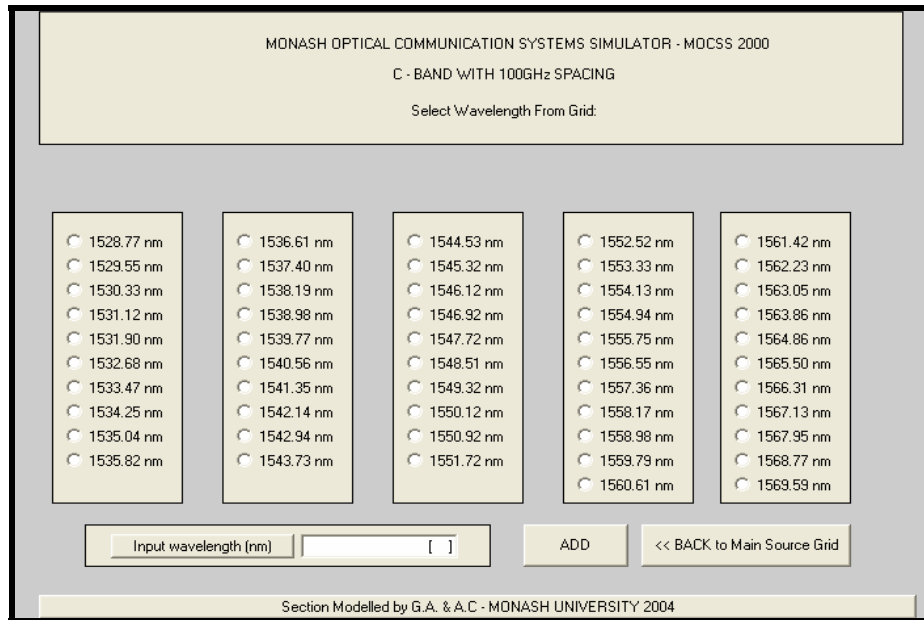


Figure 49: ITU Grid channel wavelength selection with different channel spacing.



**Figure 50:** *ITU Grid conforming wavelengths for Multiplexing several channels.*

12. Select desired wavelength for the next channel and press ‘Add’. Alternatively, users can add their own input wavelength.
13. This will show the ‘Output at External Modulator’ window again. Click ‘Accept’. This returns users to the Main Transmitter Module window. Click on ‘WDM Transm>>’ again to return to Transmitter Check-List Menu.
14. To view the two multiplexed channel frequency spectrum, click ‘>> Multiplexing + Spectrum’.
15. Otherwise the user can click on ‘View Output Waveform’ to see the signal output at the Multiplexer Module as in Figure 49. The demultiplexed waveforms can also be viewed with the ‘Demux’ button (Figure 50).

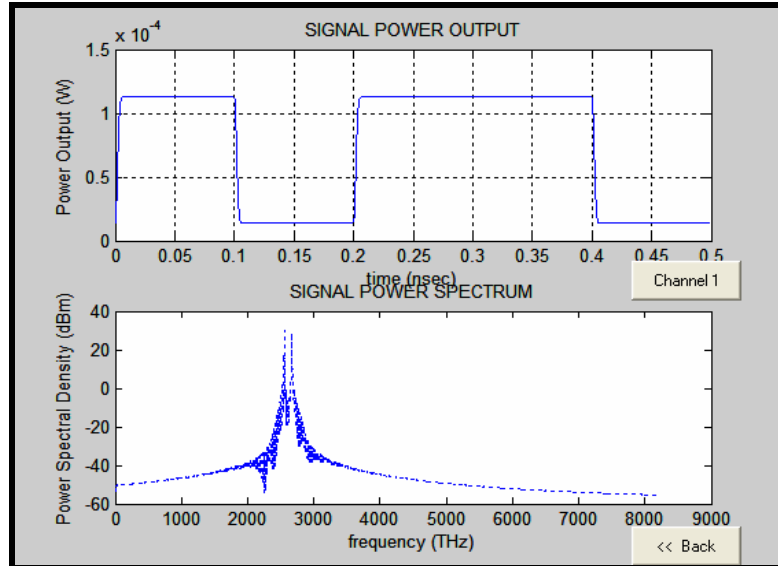


Figure 51: Output waveform at Multiplexer

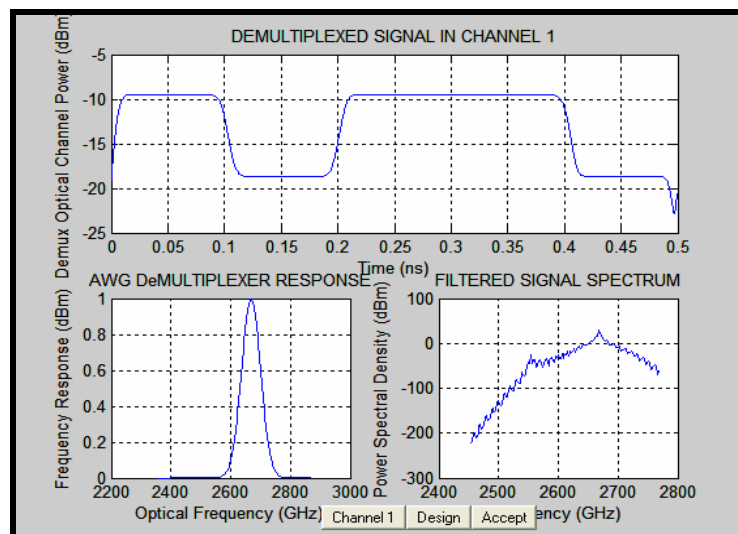
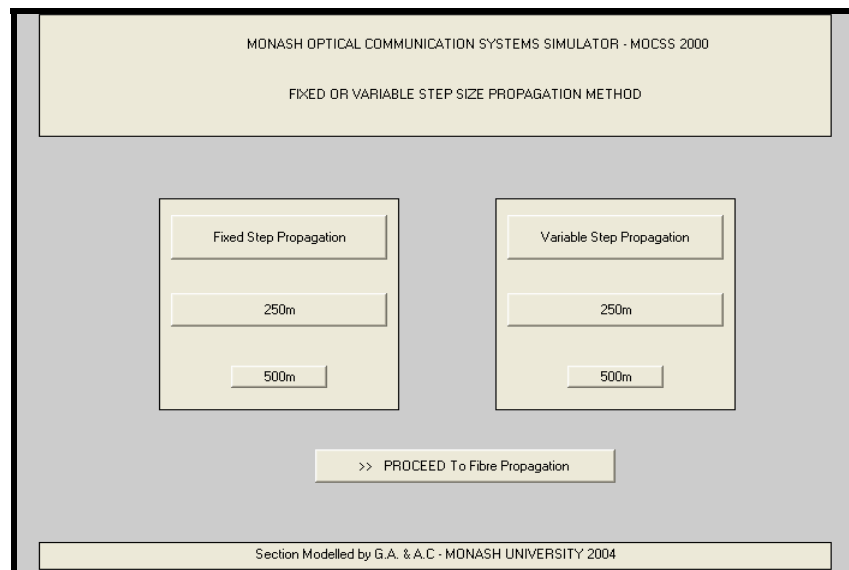


Figure 52: Demultiplexed Signal, Demultiplexer Response and Filtered Signal Spectrum

16. Users can add more channels as per steps 11 – 13.
17. To enter Fiber Propagation Module, click on “Proceed Transmitting”. An alternative to entering this Module is to enter ‘start2’ in the MATLAB command window if intending to use previously selected system configuration.
18. Select ‘Fixed Step Propagation’ or ‘Variable Step Propagation’. This will call up the corresponding step-size for propagation.

19. User to choose step-size. Recommended input is 500m. Click '>> Proceed to Fiber Propagation' once step-size is chosen.



**Figure 53** Window for choosing Fixed or Variable Step Size Fiber Propagation methods.

20. The Main Optical Fiber Module window is as shown in Figure 53. The user will enter propagation distance in km and choose the type of fiber to be used before clicking on 'Transmit'.

## 6.2 Choice of Fiber:

- Standard SMF: Dispersion of 17 ps/nm.km at 1550nm
- DSF@ 1310nm (Non-zero minimal dispersion at 1310nm)
- DSF@1550nm (Non-zero minimal dispersion at 1550nm)

21. After transmission over selected distance, the Average Power Loss in dB is calculated and displayed on the Fiber Module Main window.

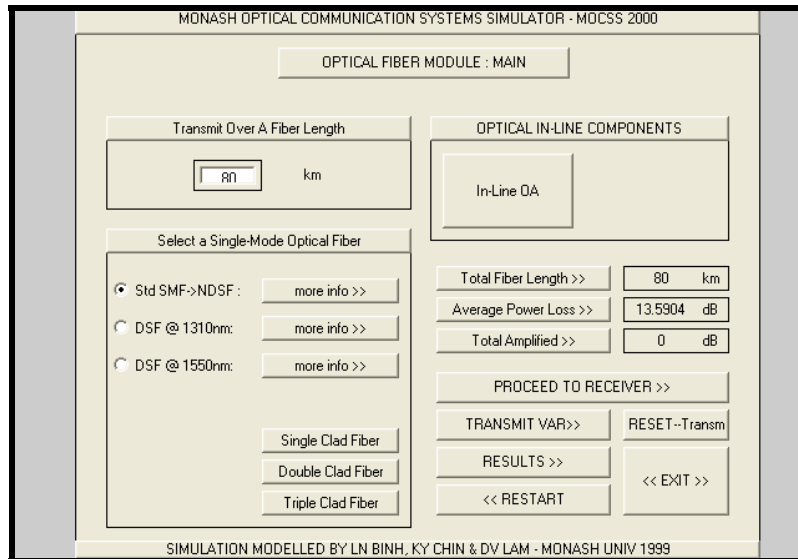


**Figure 54:** Main Fiber Module window after calculating Average Power Loss.

22. Click on ‘Results>>’ to view output after transmission (in this case over 80km standard SMF).

### 6.3 Optical Fiber Module Results:

- Optical Fiber Power Output
- Optical Fiber Transfer Function
- Optical Fiber Impulse Response
- Material, Waveguide and Total Dispersion plot of Fiber
- Eye Diagram
- Optical Fiber Refractive Index Profile
- Optical Waveguide Factor

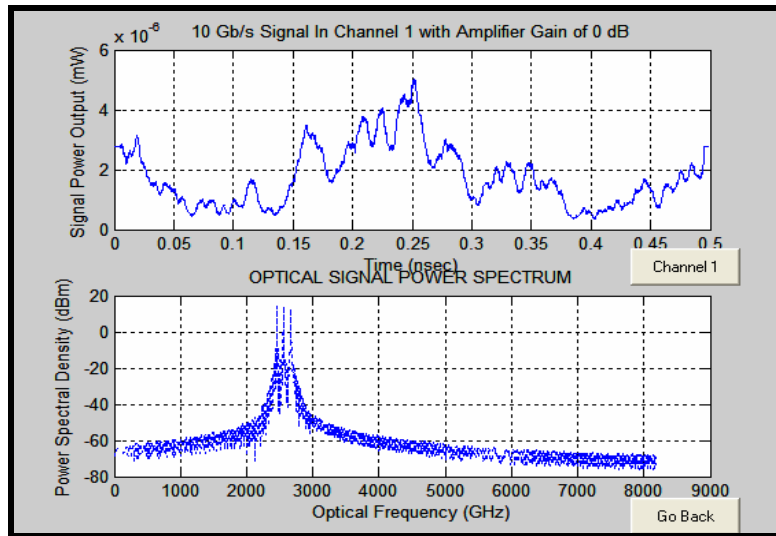


**Figure 55:** *Optical Fiber Power Output plot.*

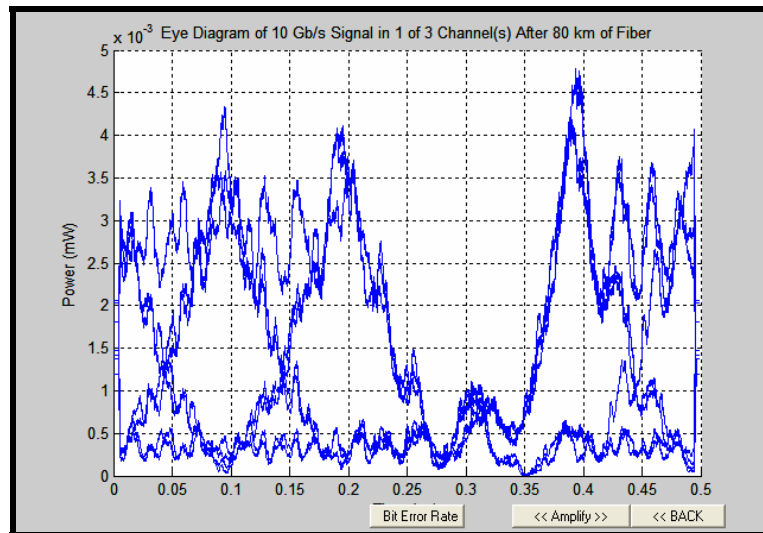


**Figure 56:** *Sample Eye Diagram after 80km standard SMF transmission*

23. Click 'Back' and 'Return to Main Menu' to return to Main Optical Fiber Module window.
24. Next, insert 'In-Line OA' by clicking on the button. Enter length of amplifier to match or slightly exceed Average Power Loss as calculated in step 21, then click 'Maximum Gain' to rescale the graphs.
25. If the selection is satisfactory click on 'Balance Loss', else a new length can be entered and 'Maximum Gain' is selected to rescale the graph again. (Note: if any errors are encountered when clicking 'Balance Loss' this means the length chosen is too short. Select longer amplifier length.)

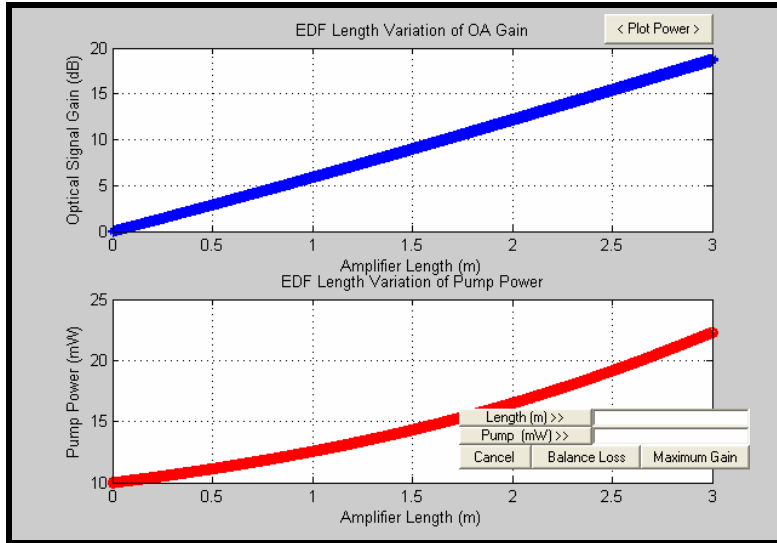


**Figure 57:** Window for selecting amplifier length.

26. Windows detailing response of the EDFA will appear as shown in Figure 58 and Figure 59. Click ‘Next’.

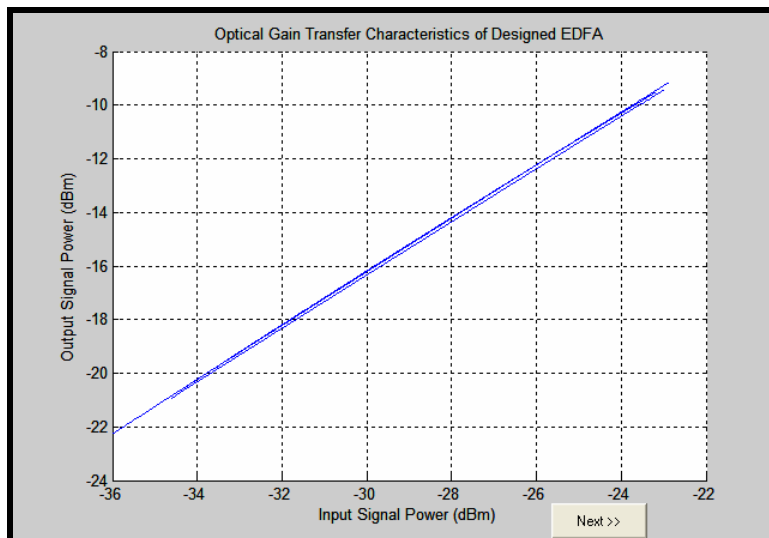


**Figure 58:** Optic Gain Transfer Characteristic of EDFA,

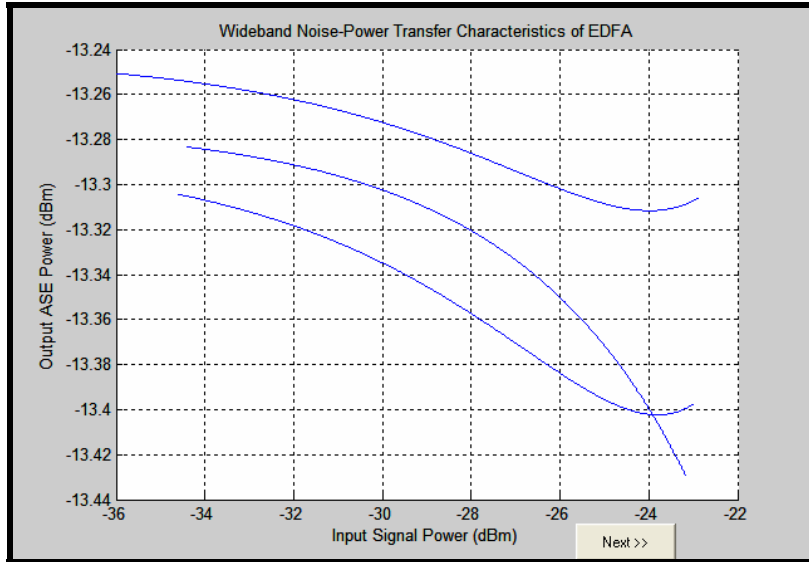


Figure 59: Wideband Noise-Power Transfer Characteristic of EDFA.

27. This will bring up the EDFA Properties window as shown in Figure 59. Various plots as described in this figure can be accessed. If satisfactory, click “Implement”.

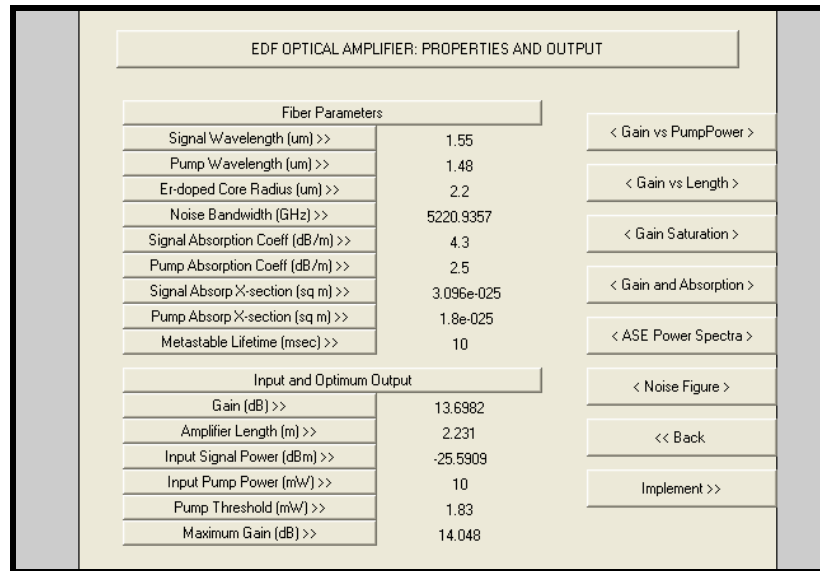
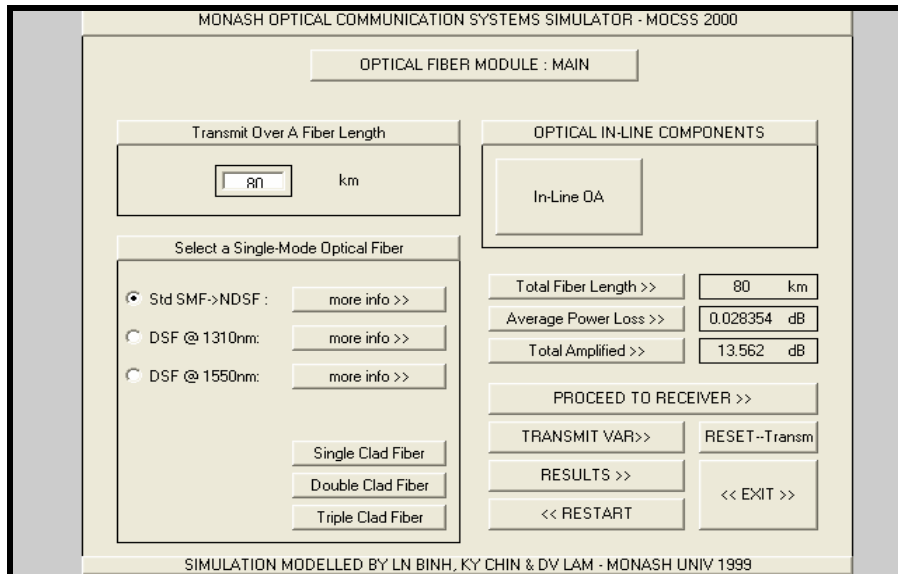


Figure 60: EDFA Properties and Output Window.

28. The main module window will show the Average Power Loss and Total Power Amplified after the implementation of the In-Line OA.



**Figure 61:** Main Fiber Module window showing Power Loss and Total Amplified after In-Line OA.

29. To add Dispersion Compensating Fiber, click on ‘Single Clad Fiber’ on the main fiber module window. Select fiber type and enter wavelength of channel to be compensated (e.g. 1550nm) and Dispersion value (e.g. -85ps/nm.km). Then click on ‘Maximize Radius’.

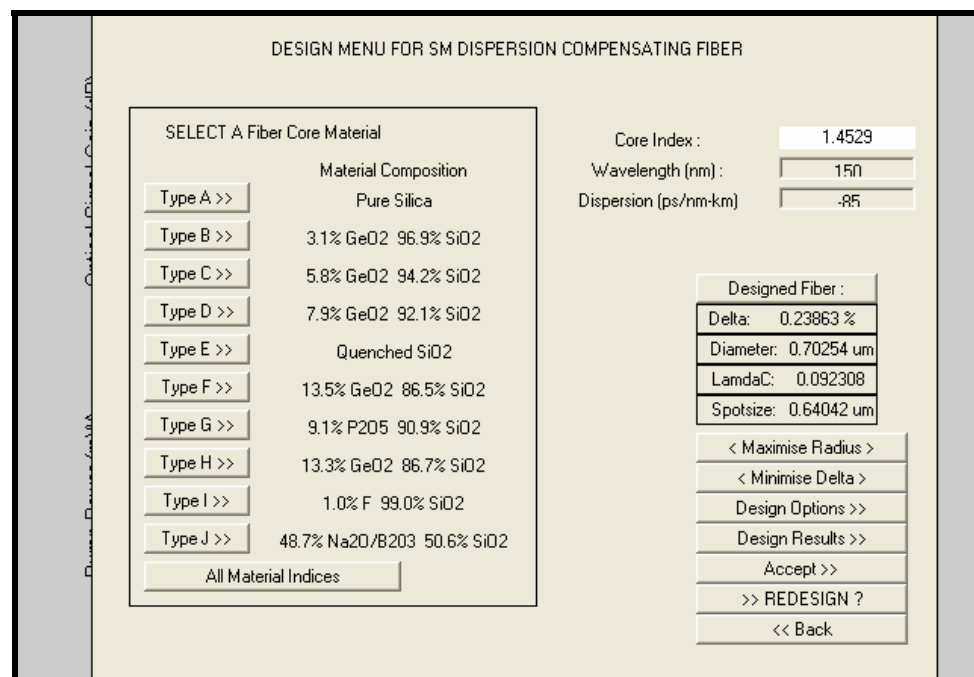


**Figure 62:** Designed Dispersion Compensating Fiber.

30. Once the desired design is achieved, click ‘Accept’. This returns to the main window.

31. Click on ‘Compensating’ and enter length of DCF. (Rule of thumb: For every 5km SMF, 1km of DCF is needed). Therefore for 80km standard SMF, enter 16km for DCF length then click ‘Transmit’.
32. The main window will show Total Length of transmission (km) and Average Power Loss (dB).

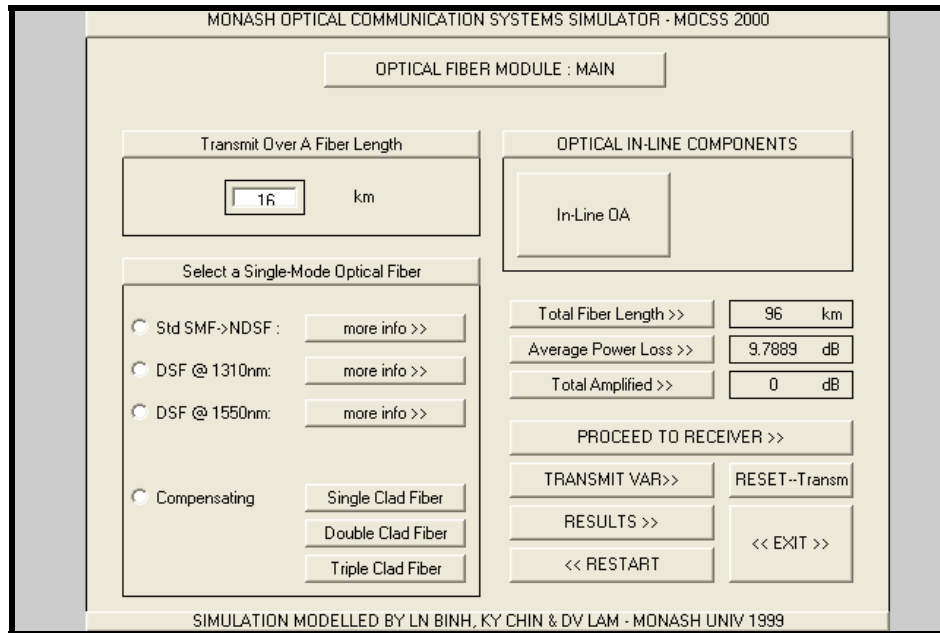


Figure 63: Main Fiber Module window after DCF transmission.

33. View the Output Power Plot and Eye Diagram using ‘Results’. At this stage, the user can now make use of the BER and Q-factor estimator module in the Eye Diagram.

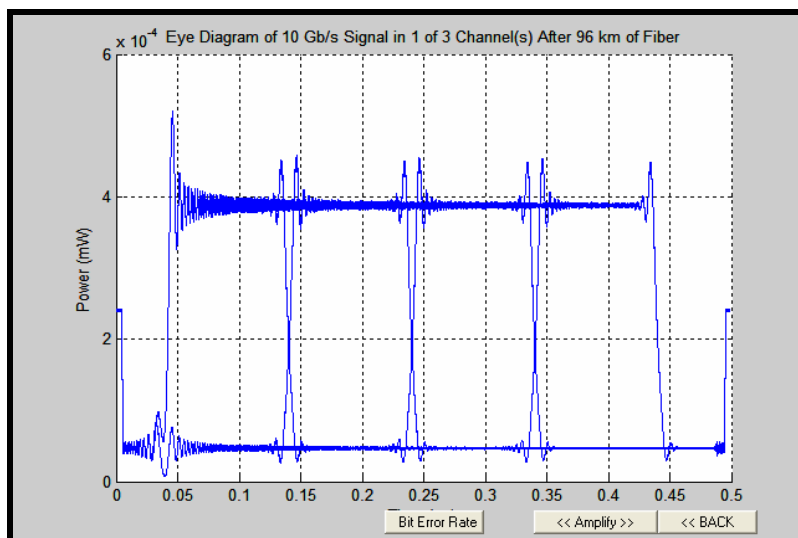
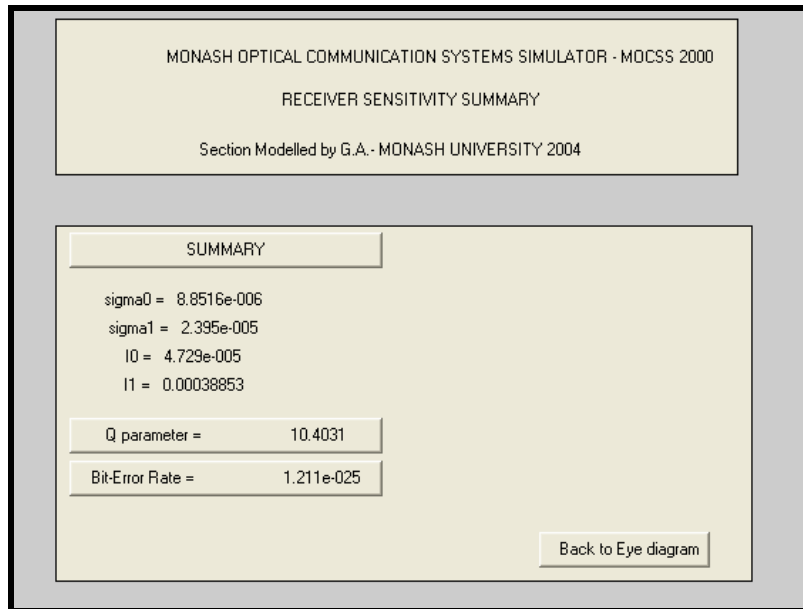


Figure 64: Eye Diagram after OAI and DCF.



*Figure 65: BER and Q Estimator module window.*

34. To add the second OA, click '<<Amplify>>' on the Eye Diagram.
35. Enter amplifier length as corresponds to the signal gain that will cancel out the Average Power Loss after the DCF, press 'Maximum Gain' to rescale the graphs and then 'Maximum Gain'.
36. Click 'Next' on the two EDFA transfer characteristics windows that will appear to obtain the eye diagram after the second OA is implemented.
37. The BER and Q can also be obtained from the eye diagram. End of simulation of transmission over one span.

Users should note that the BER and Q-factor estimator samples the points in the 2<sup>nd</sup> eye of the eye diagram. Therefore for other lengths of fiber other than 80km SMF + 16km DCF, the values obtained may not be correct as the eye diagram shifts according to the length of fiber propagation.

## 7 System Simulations and Comparative Studies

In this section the testings and case-study simulations for long-haul DWDM high-speed system are described. All the different possible combinations are tested in order find the system configuration with the best performance. The results obtained from the MATLAB simulations are then compared and analysed with published experimental results. Performance evaluation is through measures of eye diagrams and the Q-factor and BER.

## 7.1 Different configurations

The configurations presented in this section are:

- Pulse formats: Square pulse vs. Gaussian pulse
- Modulation Formats: RZ vs. NRZ
- Propagation methods: Fixed Step vs. Variable Step Propagation
- Step Size: 500m vs 250m
- Operating window frequency range: L-band vs. C-band
- Channel Spacing: 200GHz, 100GHz, 50GHz, 25GHz, 12.5GHz and 7GHz.
- *Different Fibers: standard SMF, DSF @1330nm and DSF @1550nm.*

## 7.2 Experimental setup

The schematic diagram of the setup of the 10 Gb/sec transmission systems that is used in the simulation is shown in the figure below.

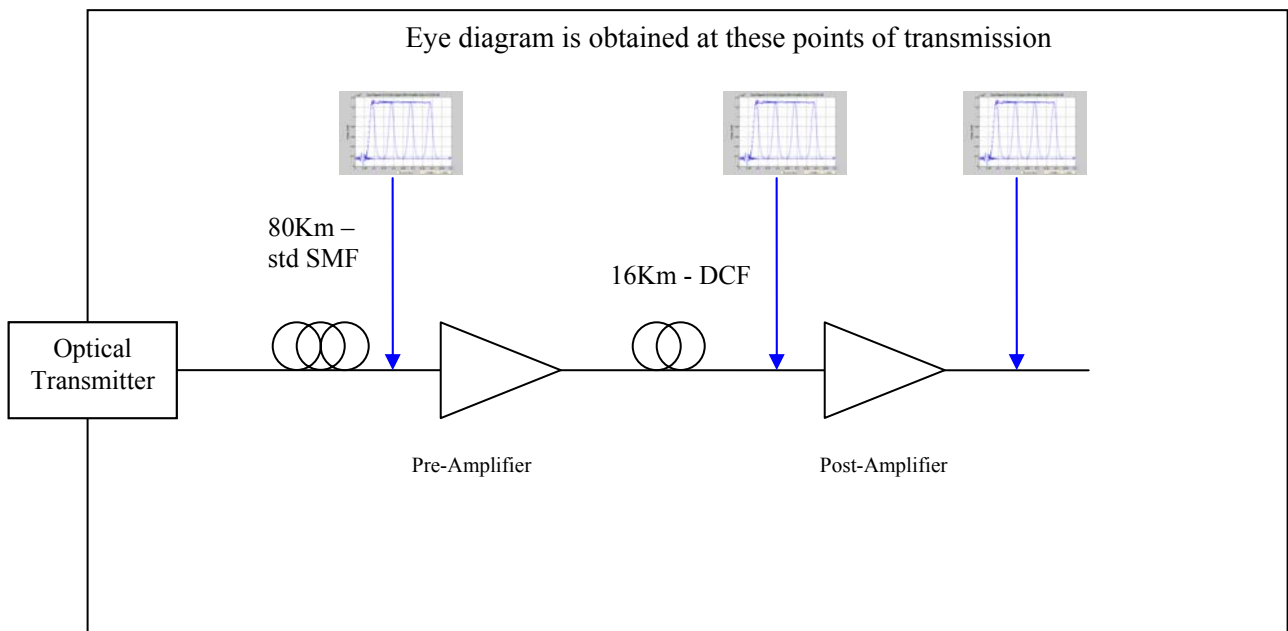


Figure 66 – schematic diagram showing setup of the transmission system used for the simulations

It consists of an optical transmitter module that has three channels chosen according the ITU grid and transmitted at the specified wavelengths. Each channel is generated at 10 Gb/s with a LiNbO<sub>3</sub> external

modulator. The SSMF span is 80km, which is an ideal dispersion limited distance for 10 Gbits/s with a required DCF module of 16 km @ -850 ps/nm at 1550nm.

### 7.3 Simulation Results and Discussion

From the simulation results it is observed that a stable pulse shape can be obtained after the compensation for power loss and dispersion. With this stable pulse the system can be potentially be transmitted for very long distances. *Figure 67* and *Figure 68* display the output pulse form after SSMF and after the DCF respectively.

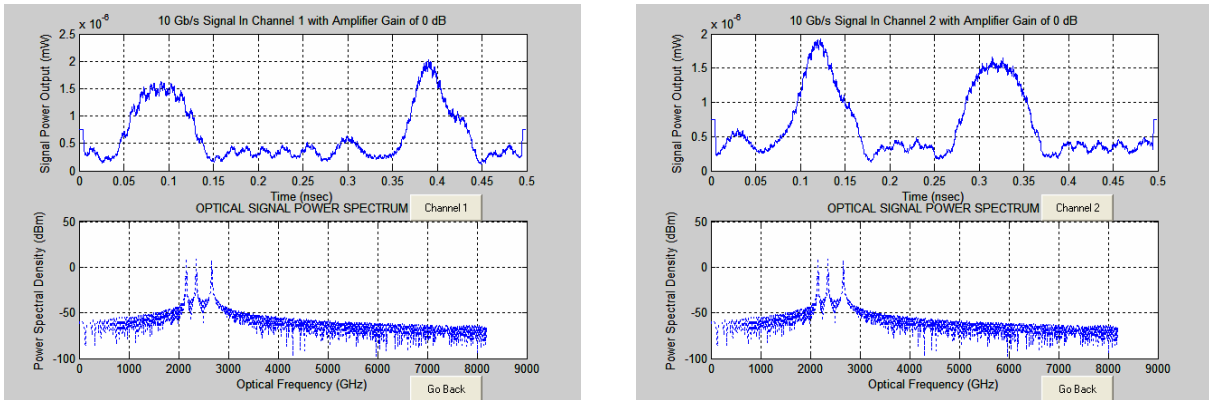


*Figure 67 – Output signal after SSMF with a span of 80km*

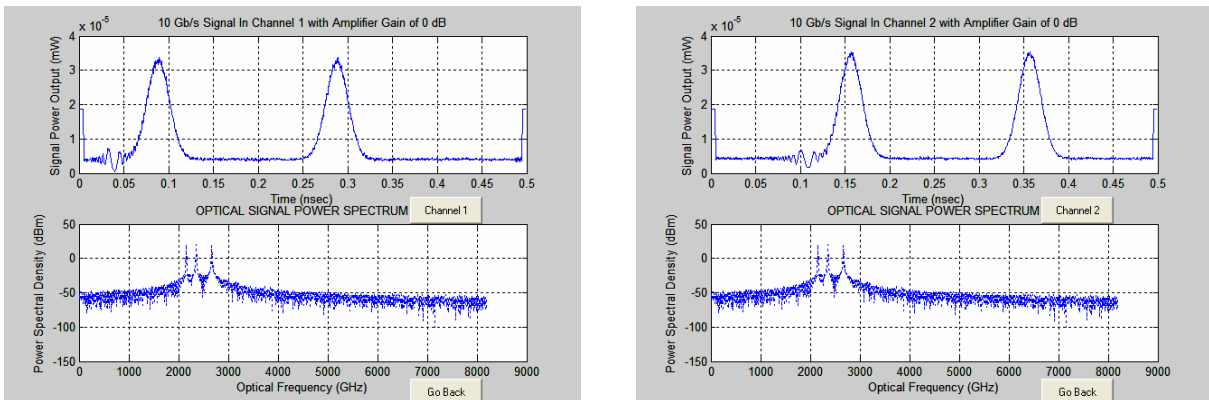


*Figure 68 - Output signal after DCF with a span of 16km*

Overall, stable pulse sequences are observed after the compensation and a post amplifier is used to boost the signal to its original level. The DCF is designed to equalize the dispersion caused by the single mode fiber at an operating wavelength. Final testing and simulations are performed for all the different wavelength channels and configurations stated in previous sections and the findings from the final testing of the simulation package is summarized in *Table 5*.

From the results obtained one of the main things observed is that the Q factor or the BER for different wavelength spacing did not vary as expected. There is only a very slight difference between the BER obtained when the wavelength spacing is altered. However, the effect of different channel spacing is observed in the signal power output spectrum. Since the Q factor and BER did not vary much for different spacing, only the results for 200GHz for the rest of the configurations is tabulated below. Detailed results for all configurations are given in Appendix 11.2.

Q factor after 80km SMF + OA + 16km DCF (200 GHz spacing)					
		Gaussian Pulse		Square Pulse	
		RZ	NRZ	RZ	NRZ
C-Band	Fixed propagation	20.630	18.496	7.577	10.402
	Variable propagation	20.630	18.499	7.577	10.405
L-Band	Fixed propagation	10.765	11.763	2.165	7.297
	Variable propagation	10.763	11.762	2.165	7.296

*Table 5 Q factor after 80km SMF + OA + 16km DCF (200GHz spacing)*

Q factor after 80km SMF + OA + 16km DCF + OA (200 GHz spacing)					
		Gaussian Pulse		Square Pulse	
		RZ	NRZ	RZ	NRZ
C-Band	Fixed propagation	25.619	19.087	8.046	10.856
	Variable propagation	25.524	19.117	8.062	10.867
L-Band	Fixed propagation	12.631	12.456	2.125	7.440
	Variable propagation	12.627	12.450	2.124	7.429

*Table 6 Q factor after 80km SMF + OA + 16km DCF + OA (200GHz spacing)*

### Gaussian pulse

It is found that the highest Q factor value obtained is for the C-band operating wavelengths comparing the L-band wavelengths. C-band operations had after DCF the Q factors of 18.496 for NRZ and 20.630 for RZ and following post amplifier their values of 19.087 for NRZ and 25.619 for RZ in the C-band 200 GHz spacing. With the same spacing, the L-band operations have values of 11.763 for NRZ before DCF and 12.456 after the compensation. Similarly the RZ eye exhibits a Q of 10.765 after DCF and 12.631 after EDFA. Thus we could state that for a Gaussian pulse form, C-band operation delivers improved BER as compared to the L-band operation.

The RZ format offers better Q value s compared to that of the NRZ format in the C-band operation. s a Q factor value of an average of 20.63 after the DCF and a value of 25.619 after the second amplifier for RZ format in the C-band wavelength. NRZ eye, on the other hand offers a Q factor of 18.496 after compensation and 19.087 after the post-amplifier. Thus the RZ modulation format is more resilient compared to the NRZ format for the Gaussian profile in the C-band operation.

In the L-band however, RZ modulation format gives an average after DCF value of 10.76 and 12.26 after being amplified. Comparing this with the NRZ format in the L-band wavelength gives an average Q factor of 11.76 after compensation and 12.45 following the amplification. This shows that NRZ format is better when operating L-band with a Gaussian pulse format. The mismatch of the dispersion compensation due to the dispersion slope plays a major part in this system performance.

Comparing the results obtained for fixed and variable propagation steps, no major changes are observed. The Q factor for the variable propagation step deviates slightly and noticeably than the fixed step propagation. For example fixed propagation for NRZ, C-band, 200 GHz spacing after DCF had a Q value of 18.496 where the variable propagation for the same factors gives a Q value of 18.499.

Results are also observed as the channel spacing varies from 200, 100, 50, 25, 12.5 and 7 GHz. Though there is not any significant degradation of the eye diagram, the difference is observed in the signal power output spectrum. Cross talk effects are found on the optical signal power spectrum at the fiber module for spacing less than 25GHz. Optical signal power spectrum for a 12.5GHz spacing NRZ Gaussian pulse as shown in **Figure 69**. The best system configuration is observed for Gaussian pulse with RZ modulation, operating at the centre of the C-band.

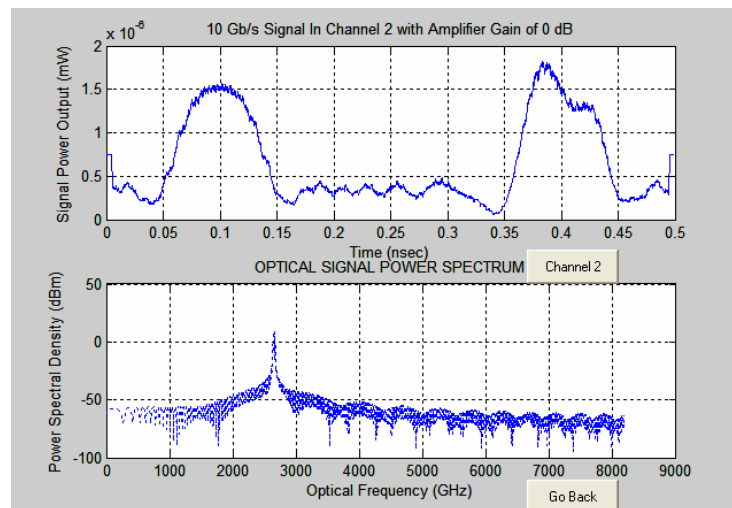


Figure 69 – Gaussian: Optical Signal Power spectrum showing cross talk effects

### Square pulse

Overall the Q-factor values obtained for square pulse are relatively lower than the Gaussian pulse which emphasizes that Gaussian pulse is more suitable to this simulation package than square pulse format.

Once again C-band operation gave rise to a better system configuration. The best configuration obtained from the square pulse format is NRZ operating and C-band wavelengths with average Q-factor of 10.402 after compensation and a value of 10.856 following post amplification. The RZ format, C-band configuration is the second best performance with average Q factor values of 7.577 after DCF and 8.046 (error-free) after being amplified.

L-band wavelengths with NRZ are significantly better compared to the RZ configuration. L-band, RZ configuration gives the least value of Q factor of around 2.15 (complete closeness of the eye), thus the configuration with the most errors.

### Gaussian pulse, NRZ and RZ modulation format – NZ-DSF 80 km

One other experimental set up is used to gauge the effect of using a NZ-DSF instead of SSMF. The schematic diagram of the setup of the 10 Gb/s transmission systems that is used in the simulation is shown in *Figure 70*.

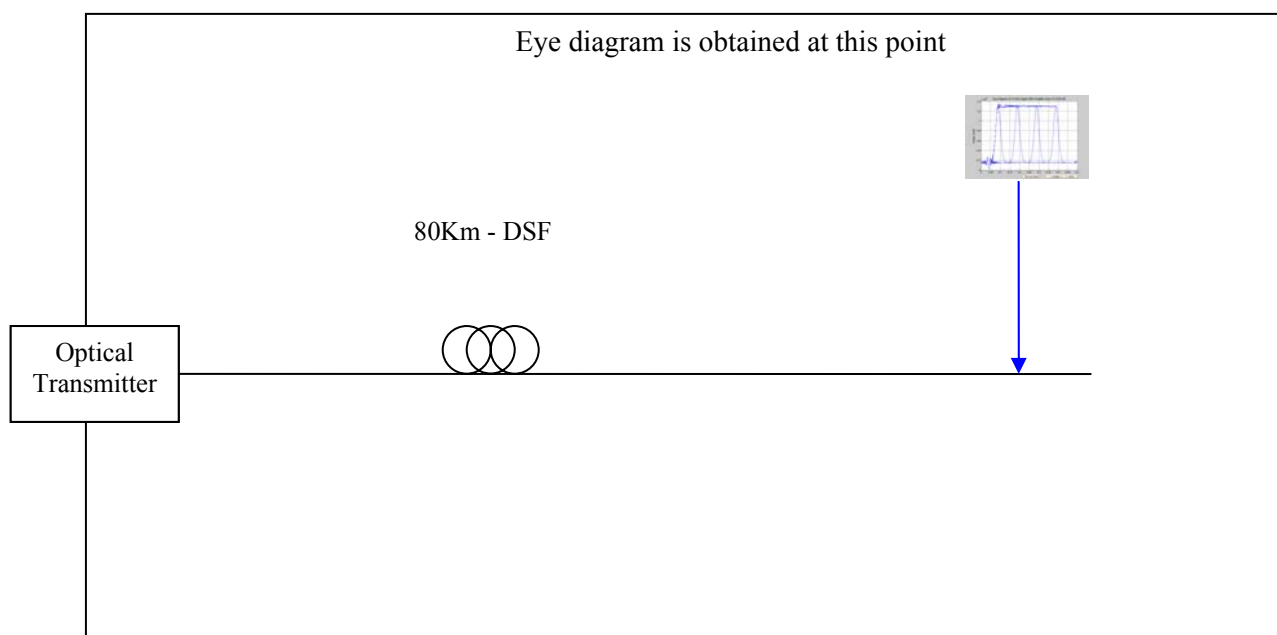


*Figure 70 – schematic diagram showing setup of the transmission system used for the simulations*

It consists of an optical transmitter module that has two channels chosen according the ITU grid and transmitted at the specified wavelengths. The NZ-DSF (Non-zero Dispersion Shifted Fiber) span is 80km

operating at 1550 nm. An eye diagram is obtained at the end of the NZ-DSF. There is no OA used in this configuration.

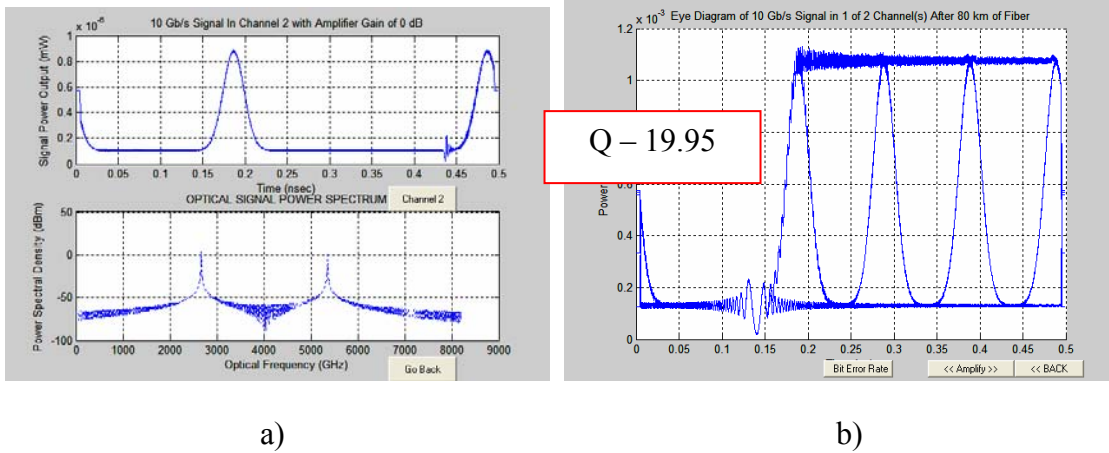


Figure 71 – NRZ, Gaussian at the end of 80km NZ-DSF transmission. ( a – signal power output, b – eye diagram)

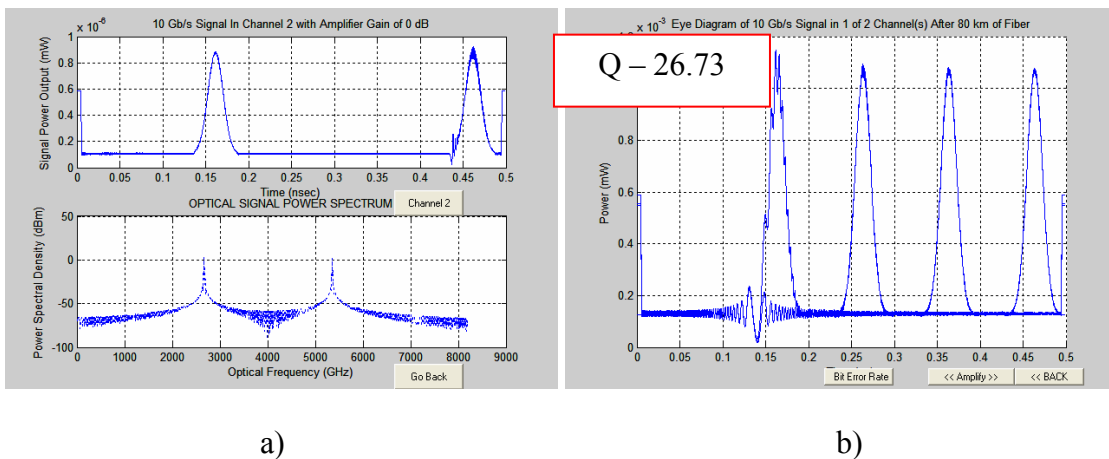


Figure 72 - RZ, Gaussian at the end of 80km NZ-DSF transmission. (a) signal power output, (b) eye diagram

A NZ-DSF fiber is designed to obtain minimum dispersion at the desired wavelength, thus minimising negative effects on optical transmission. The signal power output figure for both RZ and NRZ indicate the original pulse shape has been recovered well when transmitting with NZ-DSF, even without any amplification. Also when compared the eye diagram and the respective Q-factor, it is observed that they are higher than the Q-factor obtained for the SSMF 80km and 16km DCF with amplification.

## 8 Comparison of OC2004 and Experimental Results

In order to verify the simulated results, it is compared to an experiment reported at OFC'95[20] which used a DCF to transmit 125km of SMF of 20 Gb/s without a repeater. This is similar to the experimental set up used for the OC2004 simulations, except a 10 Gb/s system with 80km SSMF span is used. The experiment tested proves that the 20 Gb/s NRZ signal repeaterless can be transmitted over a distance of 125km of SSMF by the use of DCF. The OC2004 simulation results showed that the recovered signal is stable similar to what is verified by the experiment by K Fukuchi et al. This further verifies that the OC2004 simulator for the SMF and DCF combination is used effectively for evaluation of the system performance.

### 8.1 Square pulse, NRZ modulation format - SMF 80 km and DCF 16km

The schematic diagram of the setup of the 10 Gb/s transmission systems that is used in this simulation is shown in *Figure 73*.

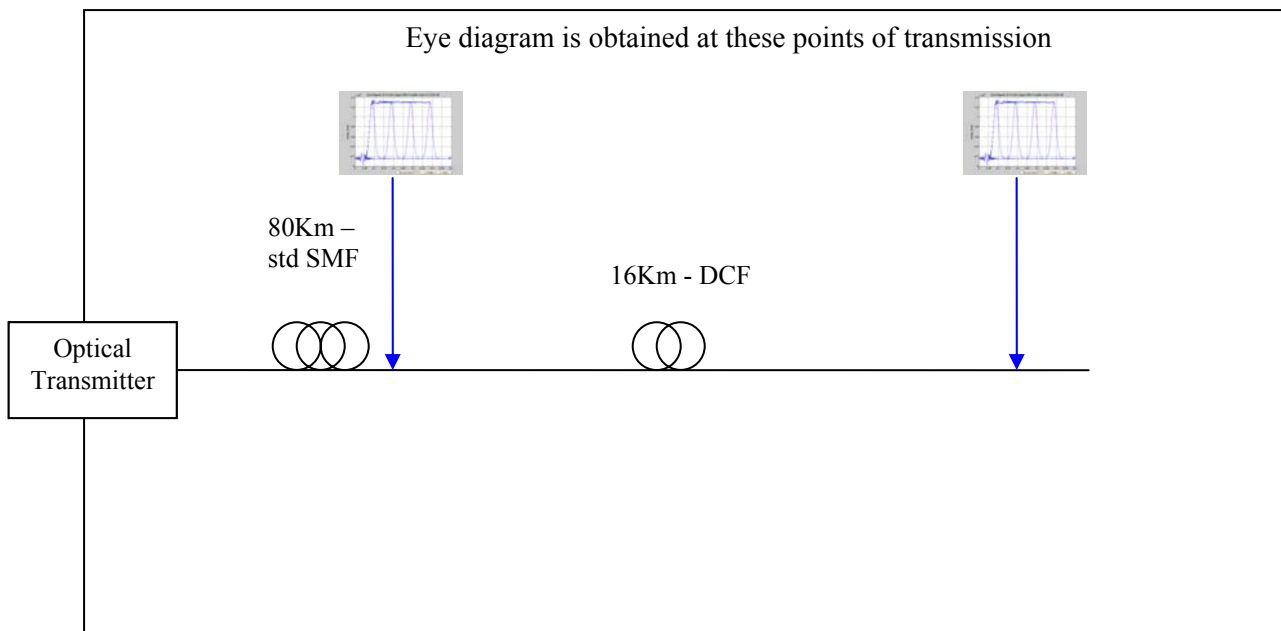


*Figure 73 – schematic diagram showing setup of the transmission system used for the simulations*

The standard SMF span is 80km, which is an ideal dispersion limited distance for 10 Gb/s with a required DCF span of 16km. this configuration is compared with the Simulink platform's results. *Figure 74* shows the system configuration Simulink block diagram consisting of a square pulse with NRZ modulation format, transmitted for 80km SSMF and a 16 kms DCF [5].

Non-Return to Zero (NRZ) Transmitter with Single Mode Fiber (SMF) and Dispersion Compensation Module (DCM)

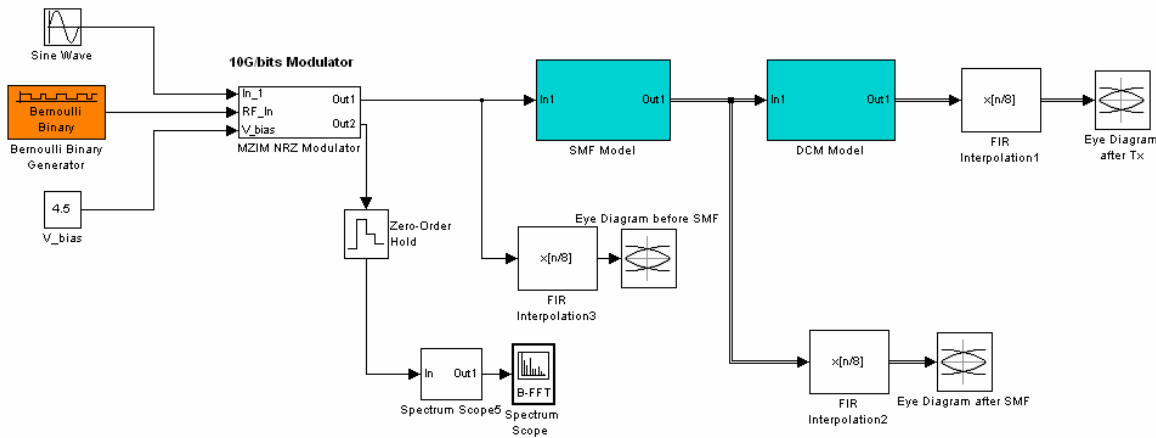
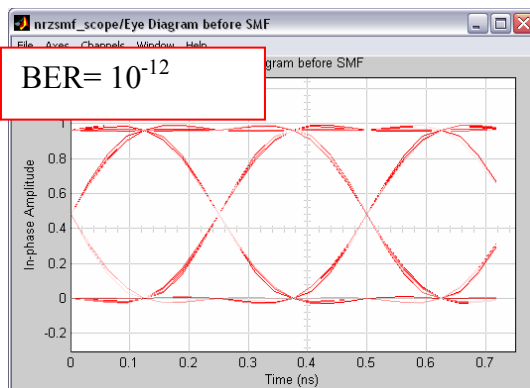
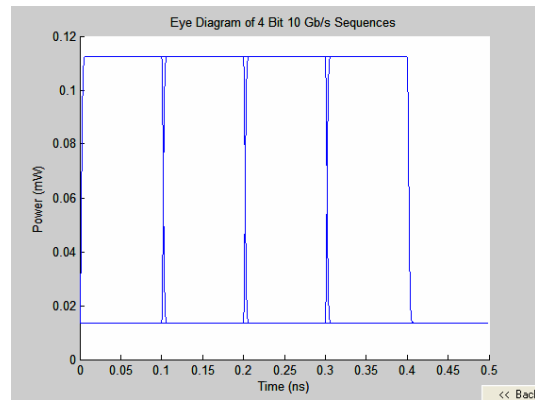


Figure 74 – NRZ Transmitter with a SMF(80km) and DCF (16km)

Shown below in Figure 75, Figure 76 and Figure 77 are the eye diagrams of 10 Gb/s Square pulse, NRZ modulation transmission system respectively for the Simulink systems as well as for the OC2004 simulation system. The figures on the left hand side are the Simulink[5] simulated eye diagrams together with the BER and the eye diagram on the right hand side are OC2004 simulated eye diagrams. Eye diagrams are obtained at 3 different points, at the end of the transmitter; end of the SMF and at the end of the DCF.

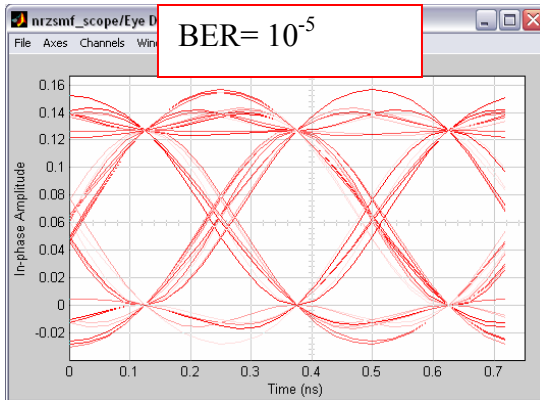


(a)

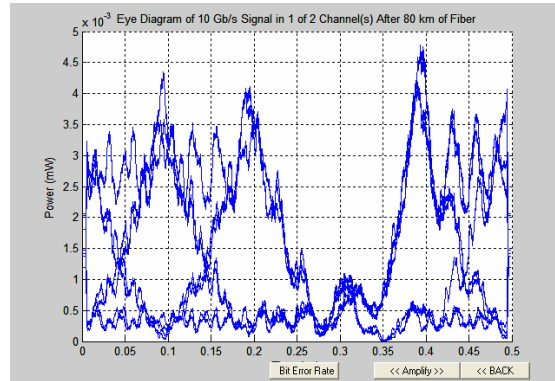


(b)

Figure 75 - Eye Diagram before the SMF fiber (a – Simulink and b – OC2004)

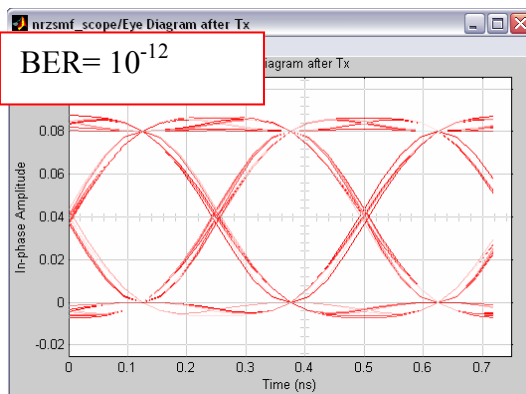


(a)

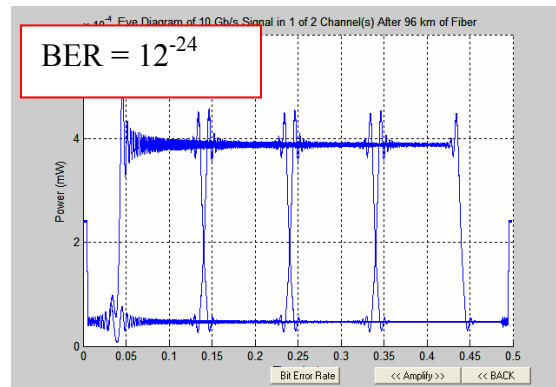


(b)

Figure 76 – Electrical and optical Eye Diagram after the SMF fiber (a)– Simulink and (b) OC2004.



(a)



(b)

Figure 77 - Eye Diagram after the SMF and DCM (a) Simulink and (b) OC2004.

It can be observed that the eye diagram at the end of the transmitter has a very low BER. Following the 80km SSMF span, the eye diagram obtained by Simulink gives a BER of  $10^{-5}$ . It is unable to produce a BER for the eye obtained in OC2004 due to the vast amount of dispersion together with the ‘ringing’ present in the eye diagram. But it can be seen that it also has a higher BER. At the end of DCF the eye diagram is recovered to have the same BER as at the transmitter end for the Simulink. The BER recover greatly for the OC2004 package as well. However the BER for OC2004 and Simulink can not be compared due to the fact that different number of bit pattern being used to generate the eye diagram. OC2004 uses  $2^4$  bit patterns, where the Simulink uses  $2^7 - 1$  PRBS. Thus OC2004 has lot less bit-pattern overlapping leading to a higher BER comparing to the Simulink BER.

## 8.2 Gaussian pulse, RZ modulation format - SMF 80 km and DCF 16km

The following figure shows the DQPSK system configuration Simulink block diagram simulated by Bernard. The set consists of a Gaussian pulse with NRZ modulation format, transmitted for 80kmSSMF and a DCF of 16 km.

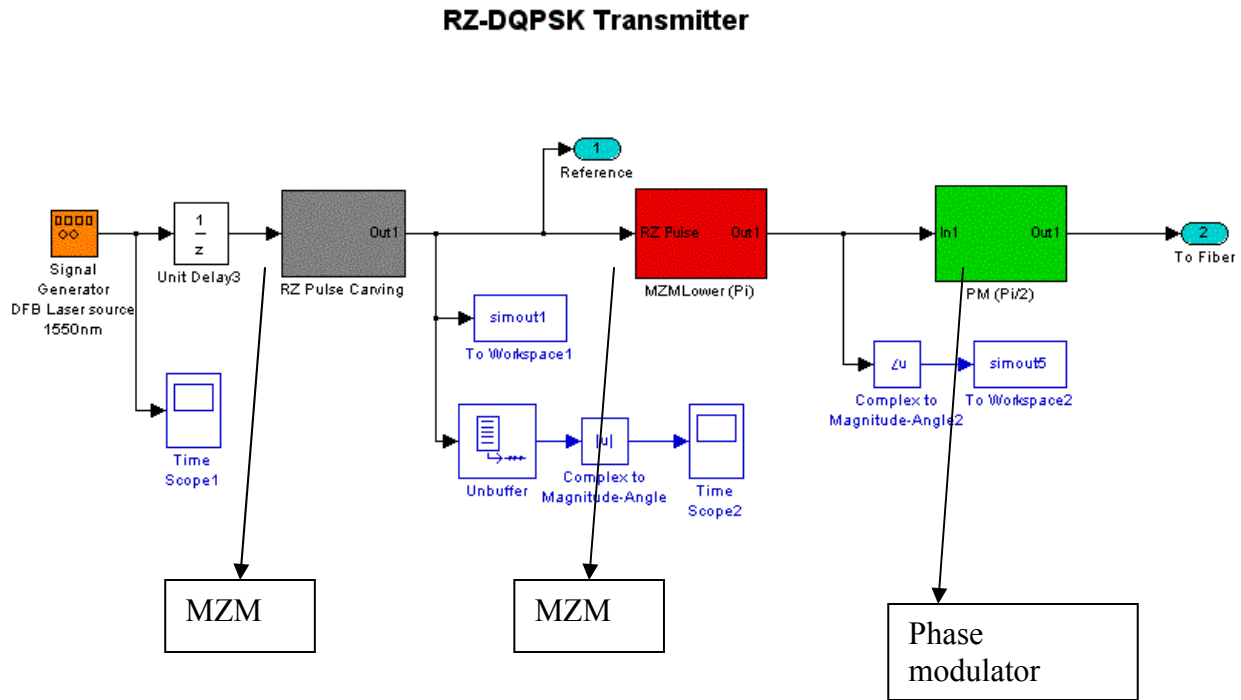
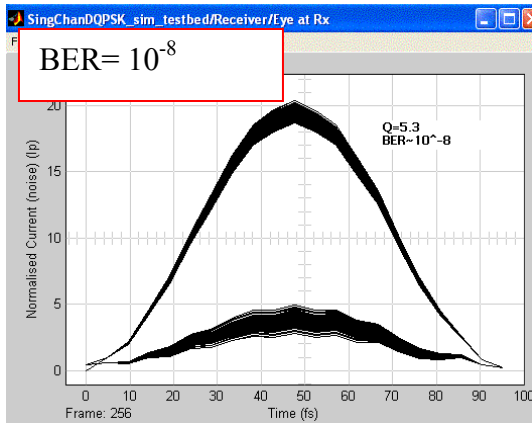
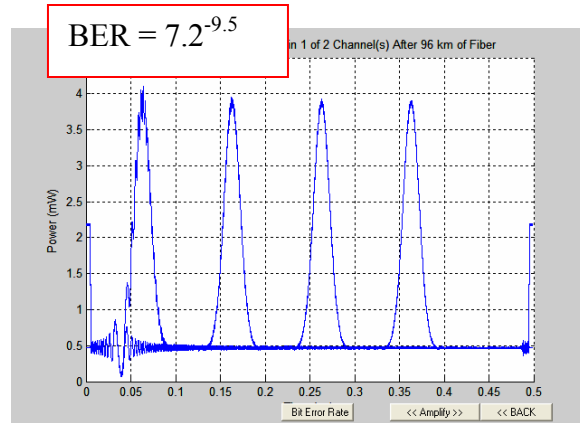


Figure 78 – RZ -DQPSK Transmitter with 80Kms SSMF and 16 Kms DCF.

Shown below in **Figure 79** are the eye diagrams at 10 Gb/s square pulse, RZ modulation transmission system for the Simulink simulator as well as for the OC2004 simulator. The figure on the left hand side is the Simulink simulated eye diagram together with the BER and the eye diagram on the right hand side are OC2004 simulated eye diagram. Eye diagrams are obtained at the end of the DCF. Eye diagram for DPQSK simulation is generated by single channel 10 Gb/s DQPSK transmission system. Where as the OC2004 is generated by 2 channels at 10Gb/s.



a)



b)

Figure 79 Eye Diagram after the SMF and DCM. (a) DPQSK[8] and (b) OC2004

From the BER generated above it can be seen that the results are significantly different. This is due to the fact that a DQPSK has half the bandwidth of the OC2004 system. Thus the BER is incomparable. Once again the Simulink model generates a 256 bit combination while OC2004 package only generates for a 16 bit configuration. Obviously, more number of bits leads to greater overlap and larger BER. Thus the results are not directly comparable due to the above reasons.

### 8.3 Square pulse, NRZ modulation format – NZ DSF 80 km

Figure 80 shows the system configuration Simulink block diagram. The set consists of a square pulse with NRZ modulation format, transmitted for 80 km using a NZ-DSF.

Non-Return to Zero (NRZ) Transmitter with 80Km of Dispersion Shifted Fiber (DSF)

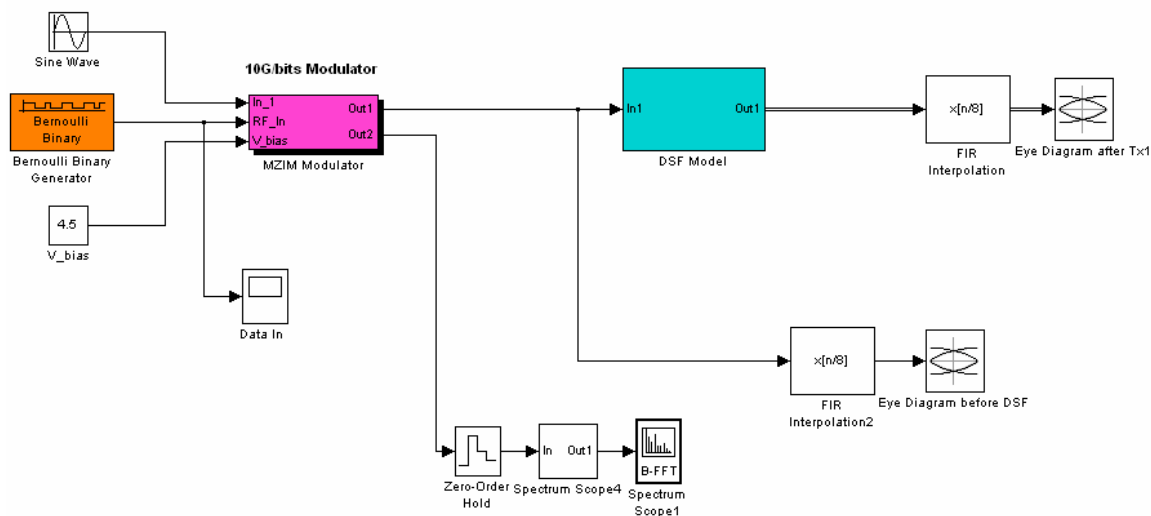


Figure 80 – Square pulse, NRZ format Transmitter with 80km DSF

Shown below are the eye diagrams at 10Gb/s Square pulse, NRZ modulation transmission system for the Simulink systems as well as for the OC2004 simulation system. The figures on the left hand side are the Simulink simulated eye diagrams together with the BER and the eye diagram on the right hand side are OC2004 simulated eye diagrams. Eye diagrams are obtained at 2 different points, at the end of the transmitter and at the end of the 80km NZ-DSF.

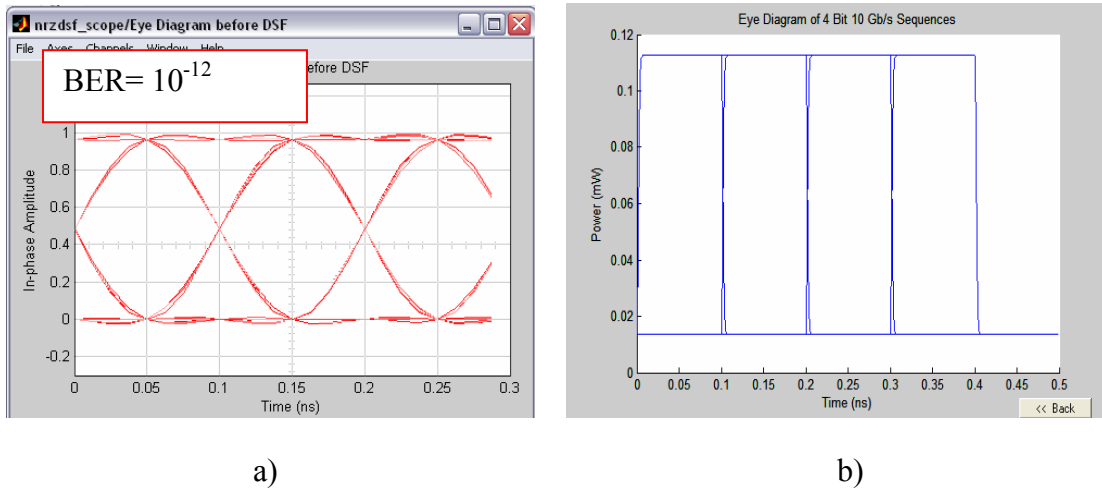


Figure 81 Eye Diagram at 10Gbps before the DSF (a) Simulink[4, 5] and (b) OC2004.

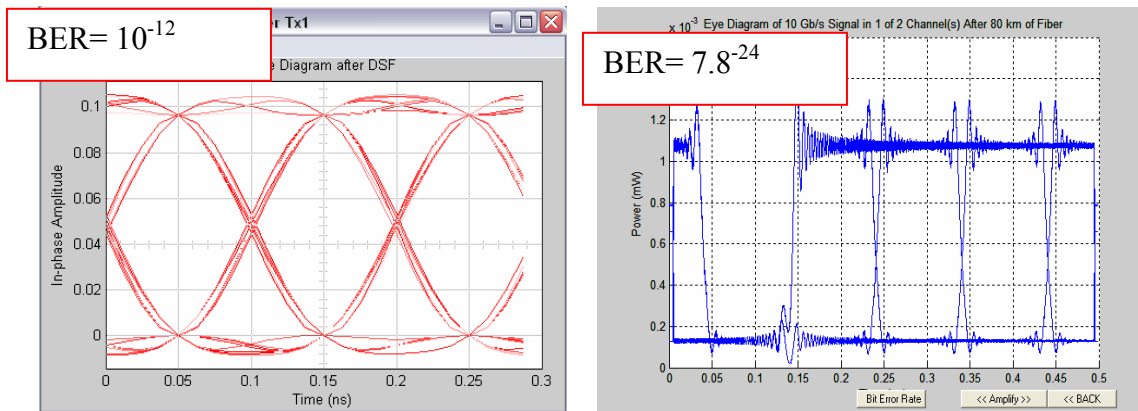


Figure 82- Eye Diagram at 10Gbps after the DSF (a) Simulink and (b) OC2004

Even though the BER cannot be directly compared due to number of bits being generated in both systems are different, the changes from initial to final eye diagram can be observed and commented on. It can be seen how the eye diagram has mostly been recovered however it still has some dispersion and non-linear effects present. It is appropriate to comment that a Gaussian pulse produces a better BER for the same configuration compared to a square pulse. This again verifies that the OC2004 package works better for a Gaussian pulse format.

## 8.4 Verification of Q-factor of the eye diagram

In order to verify that the Q factor and the BER implemented in OC2004 for the 80km SMF and 16km DCF configuration, a set of eye diagrams for Gaussian pulse and Square pulse for RZ and NRZ format operating at C-Band had Q factor worked out by hand. The following table summarizes the values obtained by both the OC2004 and manually calculated Q factor values.

Manual calculation of the Q-factor is estimated using:

$$Q = \frac{I_1 - I_0}{\sigma_1 + \sigma_0} \quad (35)$$

where  $\sigma_1$  and  $\sigma_0$  are measured by taking 68% of the variation as shown in the figure below, which corresponds the 2 standard deviation in a Gaussian distribution as shown by

$$\begin{aligned} \sigma_1 &= \delta_1 \\ \sigma_0 &= \delta_0 \end{aligned} \quad (36)$$

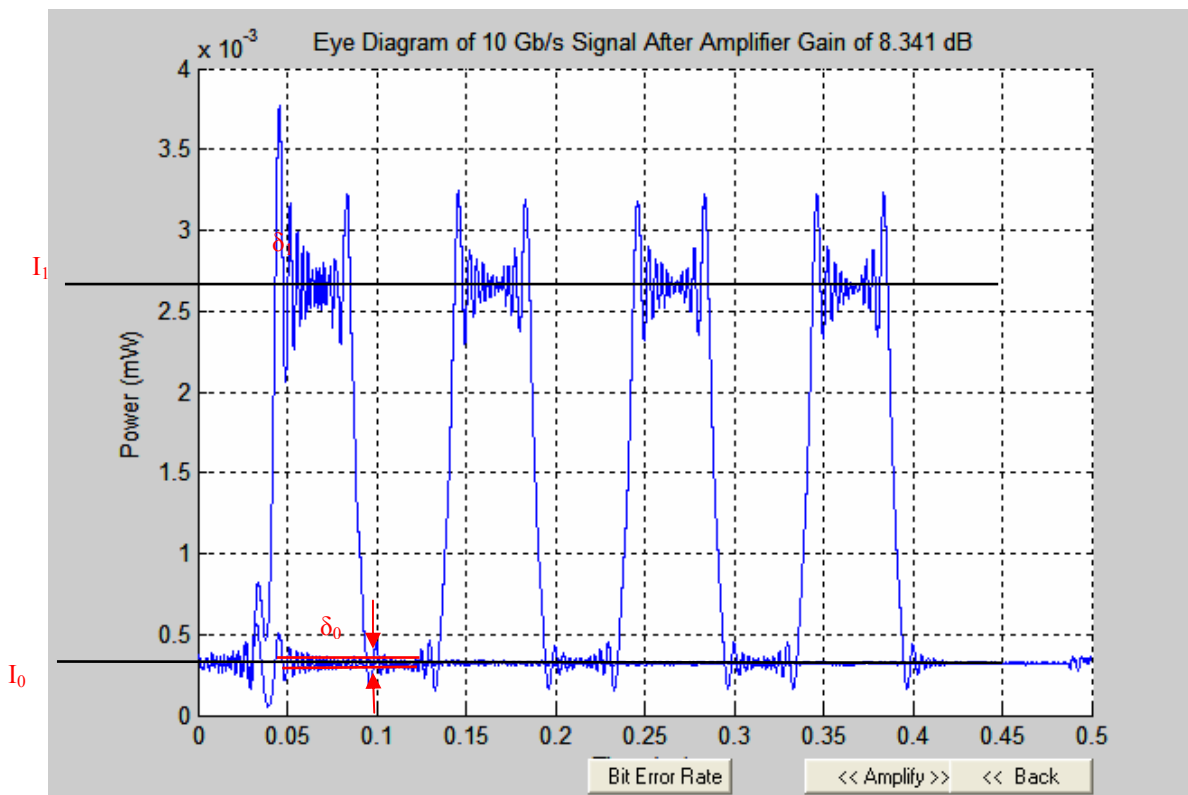


Figure 83 – Measurements for manually reading Q factor

The points caused by the ‘ringing’ effect are ignored in the manual calculations for better accuracy. The uncertainty of the Q-factor is calculated using

$$\frac{\Delta Q}{Q} = \frac{2\Delta I}{I_1 - I_0} + \left( \frac{2\Delta\delta}{\delta_1 + \delta_0} \right) \quad (37)$$

Since  $0.02 \times 10^{-3}$  is the smallest value that can be read in the scale thus  $\Delta\delta$  and  $\Delta I = 0.02 \times 10^{-3}$  cm. The following table shows the measurements obtained by manually measuring the eye diagrams. The eye diagrams and the excel files used for the manual Q-factor calculations.

Measurement	Gaussian		Square	
	RZ	NRZ	RZ	NRZ
$I_0$	0.000049	0.000045	0.0003	0.0002
$I_1$	0.00039	0.000385	0.0027	0.00355
$\delta_0$	0.000008	0.000008	0.00005	0.00005
$\delta_1$	0.000009	0.00001	0.0002	0.0004
Q calculations	20.06	18.89	9.60	12.6
$Q = \frac{I_1 - I_0}{\sigma_1 + \sigma_0}$				

Table 7 Q- factor measured for different pulse profiles

The following table summarizes and compares the Q-factor value obtained by Simulation (S) and manually (M).

System		$Q_S$	$Q_M$	$\Delta Q_M$	$\Delta Q_M$ (%)	$Q_M \pm \Delta Q_M$
Gaussian	RZ	20.63	20.06	4.7	23.4	$20.06 \pm 4.7$
	NRZ	18.50	18.89	4.2	22.2	$18.89 \pm 4.2$
Square	RZ	8.05	9.6	1.6	16.7	$9.6 \pm 1.6$
	NRZ	10.86	12.6	2.0	15.8	$12.6 \pm 2.0$

Table 8 Q factor value by Simulation (S) and manual calculation (M).

From the above table it can be seen that the simulation results for  $Q$  is within the acceptable range comparing to the manually obtained values. It can also be seen that the uncertainty values for Gaussian pulse system is larger than the square pulse system. This is due to the fact that the Gaussian pulse waveform has a very small distortion after the DCF and amplification compared to the square pulse waveform. Because of this even a slight variation in the measurements obtained from the eye diagrams can greatly affect the manually obtained Q-factor values.

It must be noted that the BER and Q-factor model in the OC2004 package is only configured to read for the 80km SSMF and 16km DCF with or without the OAs. This is due to the fact of setting the sampling range for reading the eye. Any other system configurations require adjustment in the sampling code in order to obtain

the correct estimations for the Q-factor from the eye diagrams. This is also due to the ‘ringing’ effect that is caused by the discontinuity in ‘FFT’ function used in the propagation model. This ‘ringing’ effect has been investigated in the previous section.

## 9 Concluding Remarks

The OC2004 simulation package has been developed to include laser sources, ITU Grid conforming MUX/DEMUX modules and optical amplifiers which provide for both C-Band and L-Band operation. Also included are various line coding and pulse formats such as NRZ and RZ modulation formats as well as square and Gaussian pulse waveforms. An efficient fiber propagation method for variable step-size selection, based on the split step Fourier method, has also been included to decrease time needed for simulations. Although an optical receiver is yet to be fully modeled in this simulation package, a module has been added to measure system performance using the Q-factor and BER.

The results obtained from simulations show that the best system configuration for an optical transmission system with the best performance incorporates a transmitter using the RZ modulation format and a Gaussian pulse waveform operating in the C-Band region. In the case where C-Band performance seems to always outperform the L-Band operation, this can be improved by implementing an EDFA where the lengths, pump power and pumping scheme can be optimized to obtain a flat gain spectrum over the L-Band.

It can also be observed that a Gaussian pulse waveform is more resilient in fiber propagation as well as to the oscillations due to the ‘ringing’ effect. This ‘ringing’ effect problem causes degraded Q-factor evaluation especially in system configurations that involve RZ line coding format using square pulse operating in the L-Band.

Simulated results have shown that the OC2004 program can accommodate for up to 50GHz channel spacing before signal waveforms are distorted such that ‘1’ and ‘0’ bits cannot be distinguished anymore. However, redesigning the MUX/DEMUX model to account for much closer channel spacing will allow for greater system capacity.

In the case where the Q-factor and BER estimation module is now limited to a fixed system configuration, future developments can improve on this aspect by accounting for various system configurations such as length of transmission and placement of components such as optical amplifiers and dispersion compensating fiber.

Readers of this document should note that the OC2004 package only simulates a 4-bit combination random pattern. The development of  $2^{31}-1$  PRBS will be reported in the next version. Further improvements that can be made to the OC2004 simulation package is to eliminate the ‘ringing’ effect, to extend the transmission rate to 40 Gb/s and above. Furthermore the model the optical receiver incorporating its physical limitations and receiver noises should be incorporated. More realistic performance evaluation could also be obtained by extending the eye diagram simulation up to at least 64-bit and 128-bit input PRBS sequences per eye. Finally, the eye diagrams can also be further improved by modeling each of the input channels interdependently to monitor the effect of channel crosstalk more effectively.

## 10 References

- [1] L. N. Binh, Lam,D., Chin, K.Y., "Monash Optical Communications Systems Simulator," ECSE Monash University, Melbourne Australia 1995.
- [2] I. Y. S. Gan, " "Undergraduate Work 2004 (Simulink SMF Model)", ." in *Department of Electrical and Computer Systems Engineering*: Monash University, 2004.
- [3] B. Laville, ""Honors thesis 2004 (Simulink DQ-PSK Model)",," in *Department of Electrical and Computer Systems Engineering*,: Monash University, 2004.
- [4] W. B. L. Tan, " "Honors thesis 2004 (Simulink NZ-DSF Model)",," in *Department of Electrical and Computer Systems Engineering*,: Monash University, 2004.
- [5] D. S. Wong, " "Honors thesis 2004 (Simulink Transmitter Model)",," in *Department of Electrical and Computer Systems Engineering*: Monash University, 2004.
- [6] M. Karasek, ""The design of L-Band EDFAs for multi-wavelength applications", J," *Journal of Optics A: Pure and Applied Optics*, 2000.
- [7] L. N. Binh, *ECE 4405 Lecture Notes on Optical Communications Systems*. Melbourne, Australia: MiTec, 2003.
- [8] J. Hetch, "*Understanding Fiber Optics*", 4th ed: Prentice Hall, 2002.
- [9] G. P. Agrawal *Fiber-optic Communication Systems*, 2nd ed. N.Y.: Academic Press, 2002.
- [10] Wiley, "*Wiley Encyclopedia of Telecommunications*";: John Wiley & Sons, 2003.
- [11] G. Alagaratnam, " "Honors thesis 2004 (OC2004)",," in *Department of Electrical and Computer Systems Engineering*.. Monash University, 2004.
- [12] T. Sakamoto, Kani, J., Jinno, M., Aisawa, S., Fukui, M., Yamada, M. & Oguchi, K., " ." *Electronic Letters*, pp. 392, 1998.
- [13] O. V. Sinkin, Holzlohner, R., Zweck, J. & Menyuk, C. R., ""Optimization of the Split-Step Fourier Method in Modeling Optical-Fiber Communications Systems", ." *IEEE J. Lightwave Technology*, 2003.
- [14] MATLAB, "MATLAB 6.5 Release 13 Help Files," 2002.
- [15] J. G. Proakis, and Salehi M., *Communication Systems Engineering 2nd Ed*, Prentice Hall. New Jersey, 1995.
- [16] J. Armstrong, ""Simulink Optical Simulator",," in *Electrical and Computer Systems Engineering*. Clayton, Australia: Monash, 2003, pp. 62.
- [17] L. N. Binh, "*Optical Receiver: Noise and Sensitivity considerations for OFCS and networks*". Melbourne Australia: MiTec, 2003.
- [18] H. J. R. Dutton, *Understanding optical communications, N.J.*. New Jersey,: Prentice Hall, 1998.

- [19] E. Kreyszig, *Advancement Engineering Mathematics*, 8th ed. New York,: John Wiley and Sons, 1999.
- [20] K. Fukuchi, Morie, M., Tezuka, H., Suzaki, T., Ono, T.,, " '20 Gb/s, 125km standard fiber repeater less transmission experiment using dispersion-compensating fiber',," presented at Optical Fiber Conference, OFC'95, 1995.

## **11 APPENDIX**

This section includes:

- **ITU Grid Wavelength Generation Files**
- **OC2004 PROGRAM FLOWCHARTS**
- **OC2004 Program MATLAB M-files**

### **11.1 ITU GRID EXCEL FILES**

<b>c=</b>	<b>299792458 m/s</b>	<b>spacing (Hz)</b>	27	1.948E+14	1.53898E-06	57	1.933E+14	1.55092E-06
			28	1.9475E+14	1.53937E-06	58	1.9325E+14	1.55132E-06
<b>C-band</b>		<b>50000000000</b>	29	1.947E+14	1.53977E-06	59	1.932E+14	1.55172E-06
50Ghz	frequency (Hz)	wavelength (nm)	30	1.9465E+14	1.54016E-06	60	1.9315E+14	1.55212E-06
1	1.961E+14	1.52877E-06	31	1.946E+14	1.54056E-06	61	1.931E+14	1.55252E-06
2	1.9605E+14	1.52916E-06	32	1.9455E+14	1.54095E-06	62	1.9305E+14	1.55293E-06
3	1.96E+14	1.52955E-06	33	1.945E+14	1.54135E-06	63	1.93E+14	1.55333E-06
4	1.9595E+14	1.52994E-06	34	1.9445E+14	1.54175E-06	64	1.9295E+14	1.55373E-06
5	1.959E+14	1.53033E-06	35	1.944E+14	1.54214E-06	65	1.929E+14	1.55413E-06
6	1.9585E+14	1.53072E-06	36	1.9435E+14	1.54254E-06	66	1.9285E+14	1.55454E-06
7	1.958E+14	1.53112E-06	37	1.943E+14	1.54294E-06	67	1.928E+14	1.55494E-06
8	1.9575E+14	1.53151E-06	38	1.9425E+14	1.54333E-06	68	1.9275E+14	1.55534E-06
9	1.957E+14	1.5319E-06	39	1.942E+14	1.54373E-06	69	1.927E+14	1.55575E-06
10	1.9565E+14	1.53229E-06	40	1.9415E+14	1.54413E-06	70	1.9265E+14	1.55615E-06
11	1.956E+14	1.53268E-06	41	1.941E+14	1.54453E-06	71	1.926E+14	1.55655E-06
12	1.9555E+14	1.53307E-06	42	1.9405E+14	1.54492E-06	72	1.9255E+14	1.55696E-06
13	1.955E+14	1.53347E-06	43	1.94E+14	1.54532E-06			
14	1.9545E+14	1.53386E-06	44	1.9395E+14	1.54572E-06			
15	1.954E+14	1.53425E-06	45	1.939E+14	1.54612E-06			
16	1.9535E+14	1.53464E-06	46	1.9385E+14	1.54652E-06			
17	1.953E+14	1.53504E-06	47	1.938E+14	1.54692E-06			
18	1.9525E+14	1.53543E-06	48	1.9375E+14	1.54732E-06			
19	1.952E+14	1.53582E-06	49	1.937E+14	1.54772E-06			
20	1.9515E+14	1.53622E-06	50	1.9365E+14	1.54811E-06			
21	1.951E+14	1.53661E-06	51	1.936E+14	1.54851E-06			
22	1.9505E+14	1.537E-06	52	1.9355E+14	1.54891E-06			
23	1.95E+14	1.5374E-06	53	1.935E+14	1.54932E-06			
24	1.9495E+14	1.53779E-06	54	1.9345E+14	1.54972E-06			
25	1.949E+14	1.53819E-06	55	1.934E+14	1.55012E-06			
26	1.9485E+14	1.53858E-06	56	1.9335E+14	1.55052E-06			
<b>c=</b>	<b>299792458</b>	<b>spacing (Hz)</b>	145	1.889E+14	1.58704E-06	191	1.866E+14	1.6066E-6
			146	1.8885E+14	1.58746E-06	192	1.8655E+14	1.60704E-6
			147	1.888E+14	1.58788E-06	193	1.865E+14	1.60747E-06
<b>L-band</b>		<b>50000000000</b>	148	1.8875E+14	1.5883E-06	194	1.8645E+14	1.6079E-06
50Ghz	frequency (Hz)	wavelength (nm)	149	1.887E+14	1.58873E-06	195	1.864E+14	1.60833E-06
104	1.9095E+14	1.57001E-06	150	1.8865E+14	1.58915E-06	196	1.8635E+14	1.60876E-06
105	1.909E+14	1.57042E-06	151	1.886E+14	1.58957E-06	197	1.863E+14	1.60919E-06
106	1.9085E+14	1.57083E-06	152	1.8855E+14	1.58999E-06	198	1.8625E+14	1.60962E-06
107	1.908E+14	1.57124E-06	153	1.885E+14	1.59041E-06	199	1.862E+14	1.61006E-06
108	1.9075E+14	1.57165E-06	154	1.8845E+14	1.59083E-06	200	1.8615E+14	1.61049E-06
109	1.907E+14	1.57206E-06	155	1.884E+14	1.59126E-06	201	1.861E+14	1.61092E-06
110	1.9065E+14	1.57248E-06	156	1.8835E+14	1.59168E-06	202	1.8605E+14	1.61135E-06
111	1.906E+14	1.57289E-06	157	1.883E+14	1.5921E-06	203	1.86E+14	1.61179E-06
112	1.9055E+14	1.5733E-06	158	1.8825E+14	1.59252E-06	204	1.8595E+14	1.61222E-06

113	1.905E+14	1.57371E-06	159	1.882E+14	1.59295E-06	205	1.859E+14	1.61265E-06
114	1.9045E+14	1.57413E-06	160	1.8815E+14	1.59337E-06	206	1.8585E+14	1.61309E-06
115	1.904E+14	1.57454E-06	161	1.881E+14	1.59379E-06	207	1.858E+14	1.61352E-06
116	1.9035E+14	1.57495E-06	162	1.8805E+14	1.59422E-06	208	1.8575E+14	1.61396E-06
117	1.903E+14	1.57537E-06	163	1.88E+14	1.59464E-06	209	1.857E+14	1.61439E-06
118	1.9025E+14	1.57578E-06	164	1.8795E+14	1.59506E-06	210	1.8565E+14	1.61483E-06
119	1.902E+14	1.5762E-06	165	1.879E+14	1.59549E-06	211	1.856E+14	1.61526E-06
120	1.9015E+14	1.57661E-06	166	1.8785E+14	1.59591E-06	212	1.8555E+14	1.6157E-06
121	1.901E+14	1.57703E-06	167	1.878E+14	1.59634E-06	213	1.855E+14	1.61613E-06
122	1.9005E+14	1.57744E-06	168	1.8775E+14	1.59676E-06	214	1.8545E+14	1.61657E-06
123	1.9E+14	1.57786E-06	169	1.877E+14	1.59719E-06	215	1.854E+14	1.617E-06
124	1.8995E+14	1.57827E-06	170	1.8765E+14	1.59762E-06	216	1.8535E+14	1.61744E-06
125	1.899E+14	1.57869E-06	171	1.876E+14	1.59804E-06	217	1.853E+14	1.61788E-06
126	1.8985E+14	1.5791E-06	172	1.8755E+14	1.59847E-06	218	1.8525E+14	1.61831E-06
127	1.898E+14	1.57952E-06	173	1.875E+14	1.59889E-06	219	1.852E+14	1.61875E-06
128	1.8975E+14	1.57993E-06	174	1.8745E+14	1.59932E-06	220	1.8515E+14	1.61919E-06
129	1.897E+14	1.58035E-06	175	1.874E+14	1.59975E-06	221	1.851E+14	1.61962E-06
130	1.8965E+14	1.58077E-06	176	1.8735E+14	1.60017E-06	222	1.8505E+14	1.62006E-06
131	1.896E+14	1.58118E-06	177	1.873E+14	1.6006E-06	223	1.85E+14	1.6205E-06
132	1.8955E+14	1.5816E-06	178	1.8725E+14	1.60103E-06			
133	1.895E+14	1.58202E-06	179	1.872E+14	1.60146E-06			
134	1.8945E+14	1.58244E-06	180	1.8715E+14	1.60188E-06			
135	1.894E+14	1.58285E-06	181	1.871E+14	1.60231E-06			
136	1.8935E+14	1.58327E-06	182	1.8705E+14	1.60274E-06			
137	1.893E+14	1.58369E-06	183	1.87E+14	1.60317E-06			
138	1.8925E+14	1.58411E-06	184	1.8695E+14	1.6036E-06			
139	1.892E+14	1.58453E-06	185	1.869E+14	1.60403E-06			
140	1.8915E+14	1.58495E-06	186	1.8685E+14	1.60446E-06			
141	1.891E+14	1.58536E-06	187	1.868E+14	1.60488E-06			
142	1.8905E+14	1.58578E-06	188	1.8675E+14	1.60531E-06			
143	1.89E+14	1.5862E-06	189	1.867E+14	1.60574E-06			
144	1.8895E+14	1.58662E-06	190	1.8665E+14	1.60617E-06			

c=	299792458	spacing (Hz)	37	1.925E+14	1.55736E-06
			38	1.924E+14	1.55817E-06
C-band		1E+11	39	1.923E+14	1.55898E-06
<b>100GHz spacing</b>	<b>frequency (Hz)</b>	<b>wavelength (nm)</b>	40	1.922E+14	1.55979E-06
1	1.961E+14	1.52877E-06	41	1.921E+14	1.56061E-06
2	1.96E+14	1.52955E-06	42	1.92E+14	1.56142E-06
3	1.959E+14	1.53033E-06	43	1.919E+14	1.56223E-06
4	1.958E+14	1.53112E-06	44	1.918E+14	1.56305E-06
5	1.957E+14	1.5319E-06	45	1.917E+14	1.56386E-06
6	1.956E+14	1.53268E-06	46	1.916E+14	1.56468E-06

7	1.955E+14	1.53347E-06	47	1.915E+14	1.5655E-06
8	1.954E+14	1.53425E-06	48	1.914E+14	1.56631E-06
9	1.953E+14	1.53504E-06	49	1.913E+14	1.56713E-06
10	1.952E+14	1.53582E-06	50	1.912E+14	1.56795E-06
11	1.951E+14	1.53661E-06	51	1.911E+14	1.56877E-06
12	1.95E+14	1.5374E-06	52	1.91E+14	1.56959E-06
13	1.949E+14	1.53819E-06			
14	1.948E+14	1.53898E-06			
15	1.947E+14	1.53977E-06			
16	1.946E+14	1.54056E-06			
17	1.945E+14	1.54135E-06			
18	1.944E+14	1.54214E-06			
19	1.943E+14	1.54294E-06			
20	1.942E+14	1.54373E-06			
21	1.941E+14	1.54453E-06			
22	1.94E+14	1.54532E-06			
23	1.939E+14	1.54612E-06			
24	1.938E+14	1.54692E-06			
25	1.937E+14	1.54772E-06			
26	1.936E+14	1.54851E-06			
27	1.935E+14	1.54932E-06			
28	1.934E+14	1.55012E-06			
29	1.933E+14	1.55092E-06			
30	1.932E+14	1.55172E-06			
31	1.931E+14	1.55252E-06			
32	1.93E+14	1.55333E-06			
33	1.929E+14	1.55413E-06			
34	1.928E+14	1.55494E-06			
35	1.927E+14	1.55575E-06			
36	1.926E+14	1.55655E-06			
			85	1.877E+14	1.59719E-06
c=	299792458	spacing (Hz)	86	1.876E+14	1.59804E-06
			87	1.875E+14	1.59889E-06
<b>L-band</b>		<b>1E+11</b>	88	1.874E+14	1.59975E-06
<b>100GHz spacing</b>	<b>frequency (Hz)</b>	<b>wavelength (nm)</b>	89	1.873E+14	1.6006E-06
53	1.909E+14	1.57042E-06	90	1.872E+14	1.60146E-06
54	1.908E+14	1.57124E-06	91	1.871E+14	1.60231E-06
55	1.907E+14	1.57206E-06	92	1.87E+14	1.60317E-06
56	1.906E+14	1.57289E-06	93	1.869E+14	1.60403E-06
57	1.905E+14	1.57371E-06	94	1.868E+14	1.60488E-06
58	1.904E+14	1.57454E-06	95	1.867E+14	1.60574E-06
59	1.903E+14	1.57537E-06	96	1.866E+14	1.6066E-06

60	1.902E+14	1.5762E-06	97	1.865E+14	1.60747E-06
61	1.901E+14	1.57703E-06	98	1.864E+14	1.60833E-06
62	1.9E+14	1.57786E-06	99	1.863E+14	1.60919E-06
63	1.899E+14	1.57869E-06	100	1.862E+14	1.61006E-06
64	1.898E+14	1.57952E-06	101	1.861E+14	1.61092E-06
65	1.897E+14	1.58035E-06	102	1.86E+14	1.61179E-06
66	1.896E+14	1.58118E-06	103	1.859E+14	1.61265E-06
67	1.895E+14	1.58202E-06	104	1.858E+14	1.61352E-06
68	1.894E+14	1.58285E-06	105	1.857E+14	1.61439E-06
69	1.893E+14	1.58369E-06	106	1.856E+14	1.61526E-06
70	1.892E+14	1.58453E-06	107	1.855E+14	1.61613E-06
71	1.891E+14	1.58536E-06	108	1.854E+14	1.617E-06
72	1.89E+14	1.5862E-06	109	1.853E+14	1.61788E-06
73	1.889E+14	1.58704E-06	110	1.852E+14	1.61875E-06
74	1.888E+14	1.58788E-06	111	1.851E+14	1.61962E-06
75	1.887E+14	1.58873E-06	112	1.85E+14	1.6205E-06
76	1.886E+14	1.58957E-06			
77	1.885E+14	1.59041E-06			
78	1.884E+14	1.59126E-06			
79	1.883E+14	1.5921E-06			
80	1.882E+14	1.59295E-06			
81	1.881E+14	1.59379E-06			
82	1.88E+14	1.59464E-06			
83	1.879E+14	1.59549E-06			
84	1.878E+14	1.59634E-06			
c=	299792458	spacing (Hz)			
C-band		2E+11			
<b>200GHz</b>					
<b>spacing</b>	<b>frequency (Hz)</b>	<b>wavelength (nm)</b>			
1	1.961E+14	1.52877E-06			
2	1.959E+14	1.53033E-06			
3	1.957E+14	1.5319E-06			
4	1.955E+14	1.53347E-06			
5	1.953E+14	1.53504E-06			
6	1.951E+14	1.53661E-06			
7	1.949E+14	1.53819E-06			
8	1.947E+14	1.53977E-06			

9	1.945E+14	1.54135E-06
10	1.943E+14	1.54294E-06
11	1.941E+14	1.54453E-06
12	1.939E+14	1.54612E-06
13	1.937E+14	1.54772E-06
14	1.935E+14	1.54932E-06
15	1.933E+14	1.55092E-06
16	1.931E+14	1.55252E-06
17	1.929E+14	1.55413E-06
18	1.927E+14	1.55575E-06
19	1.925E+14	1.55736E-06
20	1.923E+14	1.55898E-06
21	1.921E+14	1.56061E-06
22	1.919E+14	1.56223E-06
23	1.917E+14	1.56386E-06
24	1.915E+14	1.5655E-06
25	1.913E+14	1.56713E-06
26	1.911E+14	1.56877E-06

c= 299792458 spacing (Hz)

L-band 2E+11

200GHz spacing	frequency (Hz)	wavelength (nm)
27	1.909E+14	1.57042E-06
28	1.907E+14	1.57206E-06
29	1.905E+14	1.57371E-06
30	1.903E+14	1.57537E-06
31	1.901E+14	1.57703E-06
32	1.899E+14	1.57869E-06
33	1.897E+14	1.58035E-06
34	1.895E+14	1.58202E-06

35	1.893E+14	1.58369E-06
36	1.891E+14	1.58536E-06
37	1.889E+14	1.58704E-06
38	1.887E+14	1.58873E-06
39	1.885E+14	1.59041E-06
40	1.883E+14	1.5921E-06
41	1.881E+14	1.59379E-06
42	1.879E+14	1.59549E-06
43	1.877E+14	1.59719E-06
44	1.875E+14	1.59889E-06
45	1.873E+14	1.6006E-06
46	1.871E+14	1.60231E-06
47	1.869E+14	1.60403E-06
48	1.867E+14	1.60574E-06
49	1.865E+14	1.60747E-06
50	1.863E+14	1.60919E-06
51	1.861E+14	1.61092E-06
52	1.859E+14	1.61265E-06
53	1.857E+14	1.61439E-06
54	1.855E+14	1.61613E-06
55	1.853E+14	1.61788E-06
56	1.851E+14	1.61962E-06
57	1.849E+14	1.62138E-06

### 11.2 TABLES OF SUMMARY OF RESULTS FOR SIMULATIONS ON OC2004

SUMMARY OF RESULTS													
NRZ (square)													
C - BAND													
	Fixed Propagation							Variable Propagation					
	200	100	50	25	12.5	7		200	100	50	25	12.5	7
<b>80 km</b>													
Ave power loss	15.0074	15.0066	15.0065	15.0085	15.0115	15.0128		13.5925	13.5904	13.5884	13.5905	13.5932	13.5897
<b>OA1</b>													
Length	2.5	2.5	2.5	2.5	2.5	2.5		2.3	2.2	2.3	2.3	2.3	2.3
Ave power loss	0.0077777	0.06674	0.028286	0	0.073199	0.054863		0.018947	0.22559	0.016179	0.066364	0.019702	0.073262

Total amplified	14.9997	14.9399	14.9783	15.0361	14.9383	14.9579		13.5735	13.3648	13.5722	13.5241	13.5735	13.5164
<b>DCF</b>													
Ave power loss	8.942	8.9818	8.941	9.0415	9.0002	8.9724		9.7849	9.9906	9.789	9.7734	9.7374	9.7516
Q – MATLAB	10.4021	10.4022	10.4027	10.4036	10.3876	10.4044		10.405	10.4026	10.4102	10.4036	10.4047	10.4082
BER	1.2241e-25	1.2227e-25	1.2156e-25	1.204e-25	1.4245e-25	1.1942e-25		1.1875e-25	1.2138e-25	1.2352e-25	1.2047e-25	1.1907e-25	1.1275e-25
<b>OA2</b>													
Length	1.6	1.5	1.5	1.5	1.6	1.5		1.6	1.7	1.7	1.7	1.6	1.7
Amplified gain	9.5915	8.958	8.9547	8.9525	9.5906	8.9565		9.591	10.222	10.232	10.2318	9.5878	10.2259
Q – MATLAB	10.8561	10.8773	10.8551	10.8666	10.8495	10.8653		10.8665	10.8601	10.8658	10.8797	10.8515	10.8832
BER	9.4046e-28	7.4588e-28	9.5065e-28	8.3798e-28	1.01006e-27	8.5025e-25		8.3924e-28	9.0023e-28	8.453e-28	7.2636e-28	9.8884e-28	6.987e-28

NRZ (square)													
L - BAND													
	Fixed Propagation-500							Variable Propagation-500					
	200	100	50	25	12.5	7		200	100	50	25	12.5	7
<b>80 km</b>													
Ave power loss	13.2159	13.2168	13.2187	13.2217	13.2252	13.2279		14.8357	14.8357	14.8343	14.834	14.8354	14.8366
<b>OA1</b>													
Length	4	3.8	3.7	3.7	3.7	3.7		4.7	4.5	4.2	4.2	4.2	4.2
Ave power loss	0	0	0.03883 4	0.0072123	0.014521	0.024487		0	0	0.05660 1	0.04267	0.048502	0.061581
Total amplified	13.2159	13.7623	13.1799	13.2145	13.2107	13.2034		14.404	16.5644	14.7777	14.7914	14.7869	14.775
<b>DCF</b>													
Ave power loss	9.6612	9.4616	9.6849	9.6584	9.6473	9.6467		7.4757	7.4813	7.5323	7.5247	7.5294	7.5309
Q – MATLAB	7.297	7.2961	7.2971	7.2934	7.2964	7.2955		7.2961	7.2975	7.2954	7.3023	7.2972	7.2975
BER	1.4982e- 13	1.7055e- 13	1.4972e- 13	1.539e-13	1.5045e- 13	1.3147e- 13		1.5082e- 18	1.4922e- 13	1.5163e- 13	1.4404e- 13	1.4959e- 13	1.4928e- 13
<b>OA2</b>													
Length	3.3	2.8	3	3	2.9	2.8		2.5	2.4	2.3	2.3	2.3	2.3
Amplified gain	11.8495	9.8974	10.6728	10.6708	10.2821	9.9006		8.7588	8.3752	7.9984	8.0082	7.9957	8.0001
Q – MATLAB	7.4401	7.4315	7.4298	7.4303	7.4348	7.4259		7.4293	7.4317	7.4297	7.4321	7.4241	7.4298
BER	5.1194e- 14	5.4627e- 14	5.5345e- 14	5.513e-14	5.3263e- 14	5.7006e- 14		5.5532e- 14	5.4526e- 14	5.5387e- 14	5.4361e- 14	5.7762e- 14	5.5345e- 14

RZ (square)													
C - BAND													
	Fixed Propagation-500							Variable Propagation-500					
	200	100	50	25	12.5	7		200	100	50	25	12.5	7
<b>80 km</b>													
Ave power loss	16.1412	16.1409	16.1405	16.1412	16.1459	16.1448		15.8687	15.8694	15.8692	15.869	15.8686	15.8686
<b>OA1</b>													
Length	2.7	2.7	2.7	2.7	2.7	2.7		2.7	2.6	2.7	2.7	2.7	2.7
Ave power loss	0	0.0054211	0	0	0.057134	0.03893		0	0	0	0	0.015431	0
Total amplified	16.178	16.1355	16.174	16.174	16.0888	16.1058		15.8823	15.8737	15.8721	15.883	15.8532	15.8755
<b>DCF</b>													
Ave power loss	7.7597	7.7464	7.7487	7.7576	7.159	7.7464		7.5798	7.5663	7.5444	7.5587	7.5223	7.5283
Q – MATLAB	7.577	7.5774	7.5782	7.5776	7.5806	7.5776		7.577	7.5753	7.575	7.5748	7.5756	7.58
BER	1.7977e-14	1.7918e-14	1.7821e-14	1.789e-14	1.7489e-14	1.7902e-14		1.7982e-14	1.8215e-14	1.8265e-14	1.8286e-14	1.818e-14	1.747e-14
<b>OA2</b>													
Length	1.4	1.4	1.4	1.4	1.4	1.4		1.4	1.4	1.4	1.4	1.4	1.4
Amplified gain	8.341	8.3412	8.3456	8.3419	8.3437	8.3443		8.3436	8.3404	8.3479	8.3454	8.3451	8.3458
Q – MATLAB	8.0455	8.0594	8.0545	8.0394	8.063	8.0645		8.0622	8.0423	8.0673	8.0523	8.0487	8.063
BER	4.3605e-16	3.892e-16	4.0492e-16	4.5824e-16	3.7789e-16	3.7619e-16		3.6808e-16	4.4736e-16	3.646e-16	4.1221e-16	4.2459e-16	3.7797e-16

RZ (square)													
L - BAND													
	Fixed Propagation-500							Variable Propagation-500					
	200	100	50	25	12.5	7		200	100	50	25	12.5	7
<b>80 km</b>													
Ave power loss	15.2561	15.2564	15.2574	15.26	15.2618	15.2617		15.8398	15.8397	15.8391	15.8379	15.8401	15.84
<b>OA1</b>													
Length	4.7	4.6	4.2	4.2	4.2	4.2		4.7	4.5	4.3	4.4	4.4	4.3
Ave power loss	0.080108	0.06514	0.071791	0.07339	0.074092	0.061695		0.008191	0.0049676	0.014009	0.00049992	0.0075157	0.012786
Total amplified	15.1759	15.1913	15.1857	15.1866	15.1877	15.2		15.8317	15.8347	15.8251	15.8374	15.8326	15.8272
<b>DCF</b>													
Ave power loss	7.3728	7.3682	7.359	7.3587	7.366	7.3385		7.7448	7.7495	7.7605	7.7433	7.7389	7.753
Q – MATLAB	2.1649	2.1649	2.1646	2.1653	2.1645	2.1641		2.1647	2.1652	2.1654	2.1659	2.1652	2.1655
BER	0.017689	0.01769	0.017703	0.017672	0.01771	0.017727		0.0177	0.017676	0.017666	0.017645	0.017678	0.017665
<b>OA2</b>													
Length	2.5	2.4	2.3	2.1	2.3	2.3		2.6	2.4	2.3	2.3	2.3	2.3
Amplified gain	8.7648	8.3891	8.0139	7.269	8.0139	8.0095		9.1457	8.3869	8.0108	8.0169	8.0105	8.0123
Q – MATLAB	2.1246	2.1246	2.1236	2.1241	2.1235	2.1228		2.1242	2.1249	2.1236	2.1255	2.1237	2.1256
BER	0.0196	0.01965	0.019707	0.01967	0.019712	0.01974		0.019672	0.019639	0.019704	0.019066	0.019701	0.019603

	55	5		7		6							
--	----	---	--	---	--	---	--	--	--	--	--	--	--

<b>RZ(Gaussian)</b>													
<b>C - BAND</b>													
	<b>Fixed Propagation-500</b>							<b>Variable Propagation-500</b>					
	200	100	50	25	12.5	7		200	100	50	25	12.5	7
<b>80 km</b>													
Ave power loss	20.1239	20.1237	20.1261	20.1258	20.1276	20.131		20.1241	20.1236	20.1249	20.1249	20.125	20.1246
<b>OA1</b>													
Length	3.2	3.2	3.2	3.2	3.2	3.2		3.2	3.2	3.2	3.2	3.2	3.2
Ave power loss	0	0	0	0	0	0		0	0	0	0	0	0
Total amplified	20.1874	20.2	20.167	20.1754	20.1328	20.167		20.1867	20.1988	20.1668	20.1743	20.1388	20.172
<b>DCF</b>													
Ave power loss	4.5375	4.545	4.508	4.5012	4.472	4.5208		4.5395	4.5525	4.51	4.5043	4.4743	4.5328
Q – MATLAB	20.6303	20.6326	20.6336	20.6398	20.6364	20.6267		20.6303	20.6328	20.6319	20.6308	20.6362	20.6342
BER													
<b>OA2</b>													
Length	0.75	0.75	0.75	0.75	0.75	0.75		0.75	0.75	0.75	0.75	0.75	0.75
Amplified gain	4.3049	4.3039	4.3075	4.3058	4.302	4.3024		4.3042	4.3017	4.3038	4.3022	4.3071	4.3047
Q – MATLAB	25.619	25.3711	24.9387	25.4105	25.2239	25.1477		25.5235	25.2875	24.9263	25.1518	25.3362	25.2794
BER													

RZ(Gaussian)													
L - BAND													
	Fixed Propagation- 500							Variable Propagation -500					
	200	100	50	25	12.5	7		200	100	50	25	12.5	7
<b>80 km</b>													
Ave power loss	18.4984	18.4987	18.4993	18.4996	18.4987	18.4973		18.4999	18.4998	18.4993	18.4996	18.5011	18.5014
<b>OA1</b>													
Length	5	5	5	5	5	5		5	5	5	5	5	5
Ave power loss	0	0	0.0048	0.00555	0	0		0	0	0.0059	0.00825	0.00458	0
Total amplified	18.5061	18.5046	18.4944	18.4941	18.4986	18.4999		18.5059	18.5033	18.4934	18.4914	18.4965	18.5019
<b>DCF</b>													
Ave power loss	5.4805	5.4888	5.4845	5.473	5.4747	5.488		5.4816	5.4836	5.4848	5.4761	5.4846	5.4949
Q – MATLAB	10.7653	10.7651	10.7645	10.7632	10.768	10.7659		10.7633	10.7624	10.7639	10.7647	10.7652	10.764
BER													
<b>OA2</b>													
Length	1.6	1.6	1.6	1.6	1.6	1.6		1.6	1.6	1.6	1.6	1.6	1.6
Amplified gain	5.3907	5.387	5.3907	5.3866	5.3886	5.387		5.3883	5.3904	5.3876	5.3883	5.3859	5.3859
Q – MATLAB	12.6313	12.7201	12.6909	12.6527	12.6561	12.6527		12.6274	12.6056	12.6778	12.6502	12.7017	12.6624
BER													

NRZ(Gaussian)													
C - BAND													
	Fixed Propagation-500							Variable Propagation-500					
	200	100	50	25	12.5	7		200	100	50	25	12.5	7
<b>80 km</b>													
Ave power loss	19.2673	19.2676	19.2686	19.2711	19.271	19.272		19.2647	19.2678	19.2674	19.2678	19.2671	19.2667
<b>OA1</b>													
Length	3.1	3.07	3.1	3.2	3.1	3.1		3.1	3.1	3.1	3.1	3.1	3.1
Ave power loss	0	0	0	0	0	0		0	0.0018	0	0	0.03116	0
Total amplified	19.3275	19.336	19.3117	19.3213	19.2852	19.2809		19.327	19.2659	19.2708	19.2919	19.2359	19.2833
<b>DCF</b>													
Ave power loss	5.3421	5.2599	5.2614	5.2521	5.2487	5.2939		5.3405	5.2642	5.2574	5.214	5.2634	5.3016
Q – MATLAB	18.496	18.4906	18.4927	18.4994	18.4877	18.4926		18.499	18.4962	18.4991	16.4987	18.4991	18.4989
BER													
<b>OA2</b>													
Length	0.9	0.9	0.95	0.9	0.9	0.9		0.9	0.9	0.9	0.9	0.9	0.9
Amplified gain	5.2741	5.2711	5.5808	5.2737	5.2735	5.2728		5.2731	5.2733	5.2737	5.2791	5.2759	5.2744
Q – MATLAB	19.087	19.0703	19.1069	19.0755	19.0737	19.0767		19.1169	19.0801	19.0928	19.1132	19.1119	19.1267
BER													

NRZ(Gaussian)													
L - BAND													
	<i>Fixed Propagation -500</i>							<i>Variable Propagation -500</i>					
	200	100	50	25	12.5	7		200	100	50	25	12.5	7
<b>80 km</b>													
Ave power loss	17.3957	17.3959	17.3964	17.3964	17.3962	17.3963		17.3964	17.3958	17.3957	17.3961	17.3964	17.3962
<b>OA1</b>													
Length	5	5	4.8	4.7	4.7	4.7		5	5	4.8	4.7	4.7	4.7
Ave power loss	0.0085	0.0084	0.00811	0.017381	0.0151	0.0255		0.01	0.0092	0.0061	0.0001	0.0186	0.0239
Total amplified	17.3871	17.3871	17.3883	17.3968	17.381	17.3709		17.3864	17.3866	17.3896	17.396	17.3778	17.3722
<b>DCF</b>													
Ave power loss	6.2999	6.3106	6.3143	6.2929	6.2932	6.3076		6.3014	6.3128	6.316	6.2958	6.3018	6.3193
Q – MATLAB	11.763	11.7643	11.7643	11.7662	11.7631	11.7628		11.762	11.7605	11.7624	11.7629	11.7625	11.7601
BER													
<b>OA2</b>													
Length	2	2	2	2	2	2		2	2	2	2	2	2
Amplified gain	6.8812	6.8837	6.8841	6.8844	6.8822	6.8795		6.8837	6.8837	6.8816	6.8819	6.8812	6.8826
Q – MATLAB	12.4559	12.4552	12.4513	12.4605	12.4559	12.4543		12.4503	12.4459	12.4504	12.4515	12.4447	12.4585
BER													

**FLOWCHART FOR OC2004 PACKAGE (CHART 1)**  
**TRANSMITTER MODULE UP TO WDM TRANSMISSION AND MUX/DEMUX**

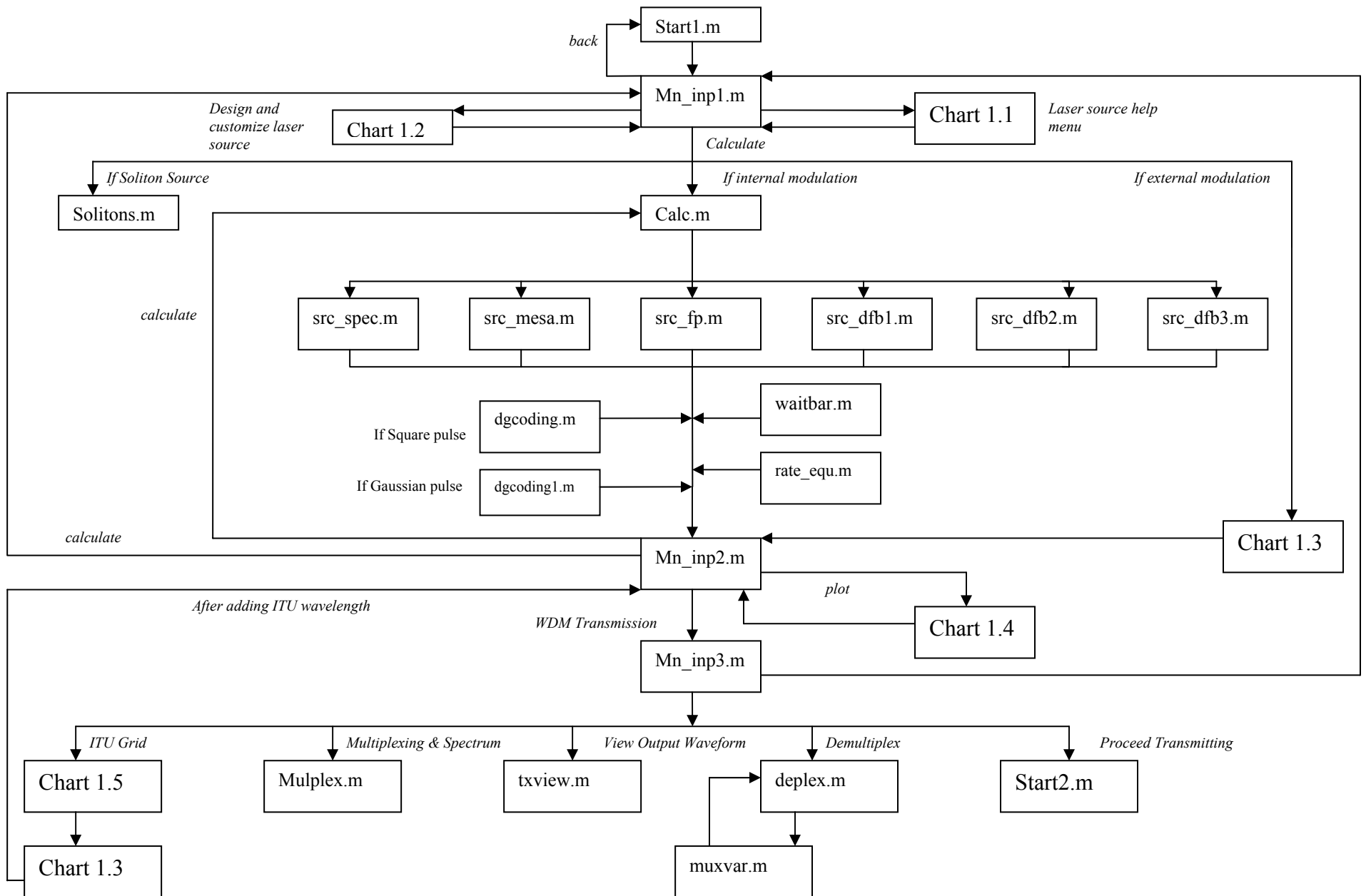


**CHART 1.1 – Laser Source Help Menu**

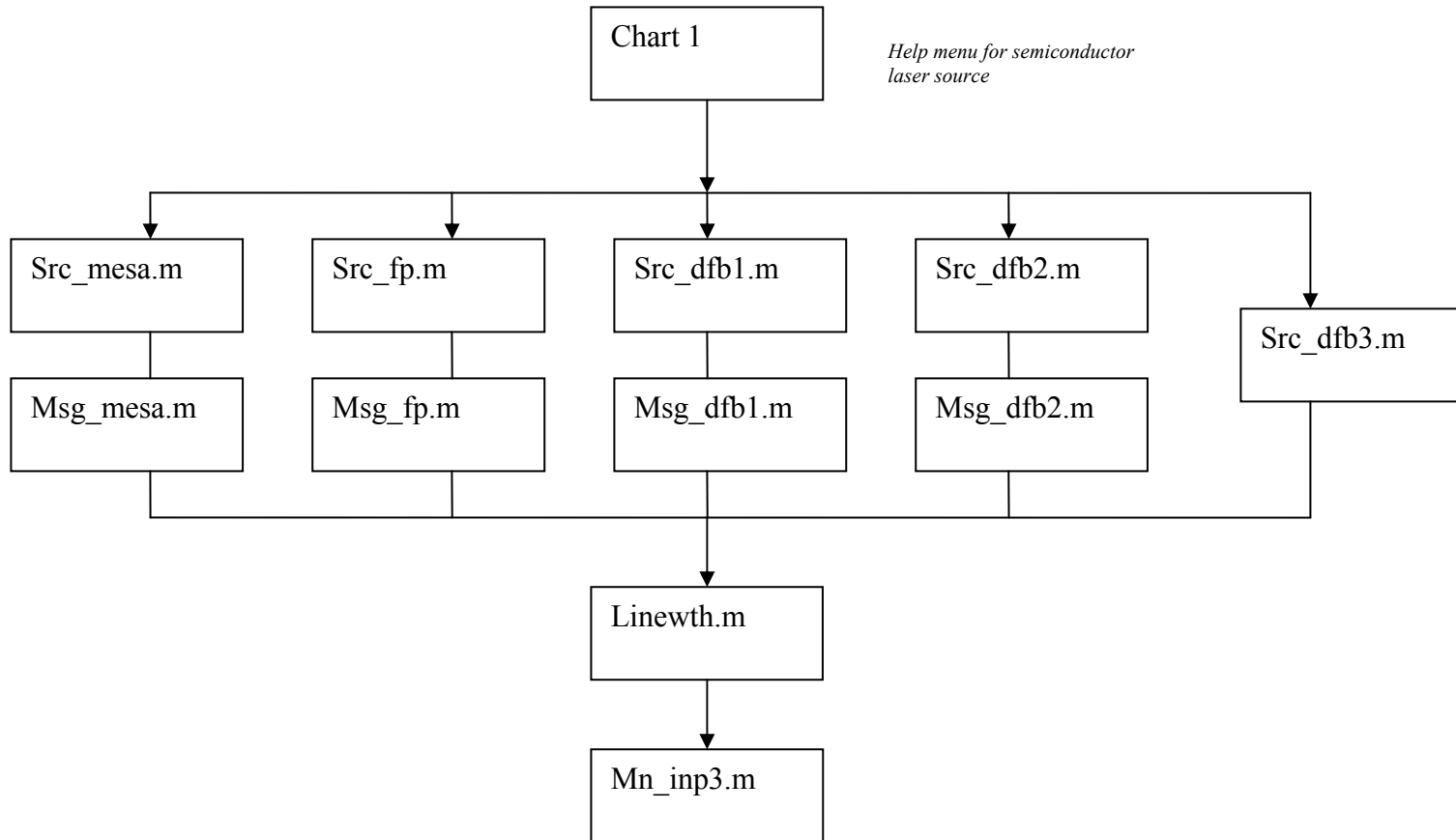


## CHART 1.2 – Design and Customize Laser

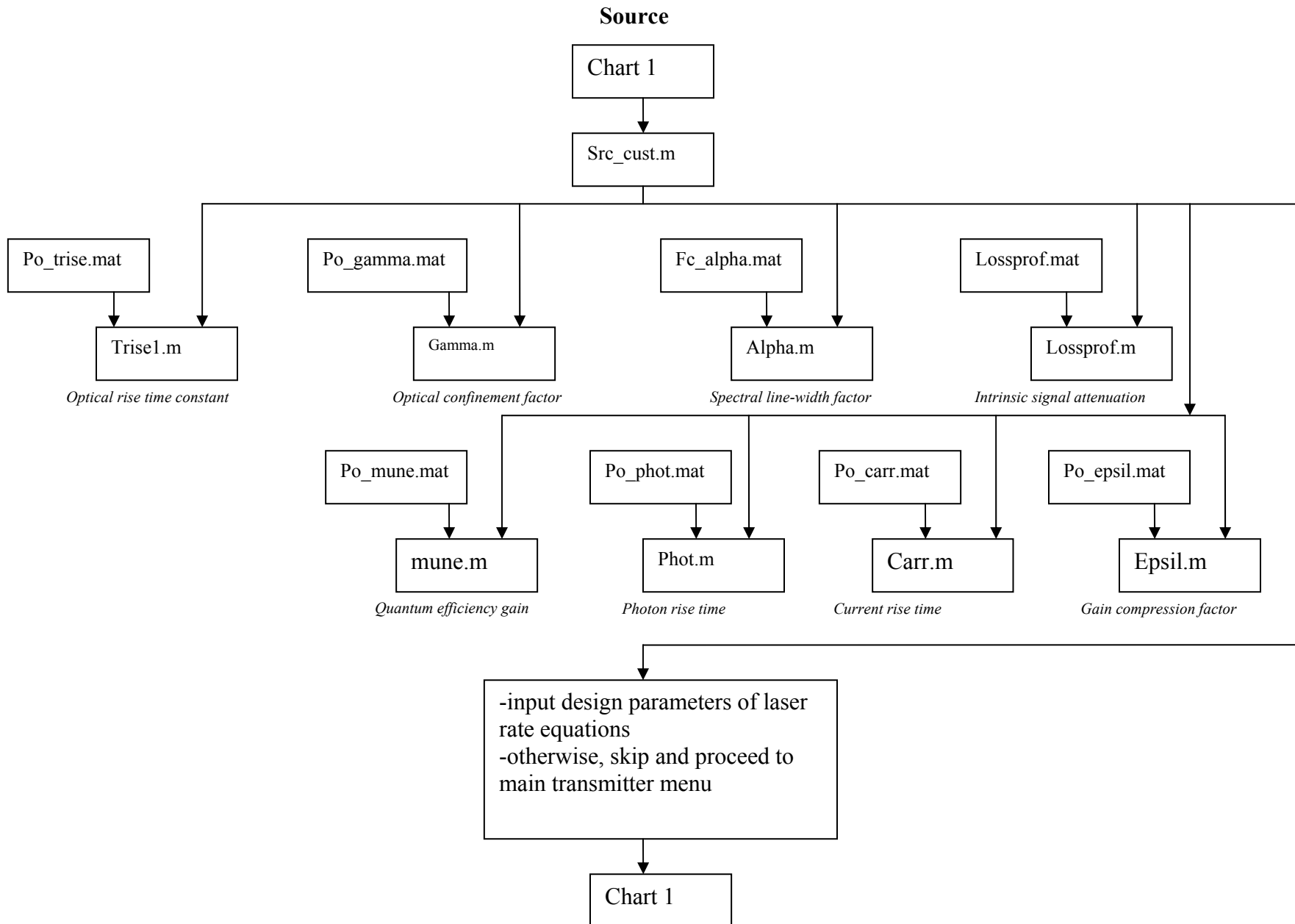


**CHART 1.3 – External Modulation**

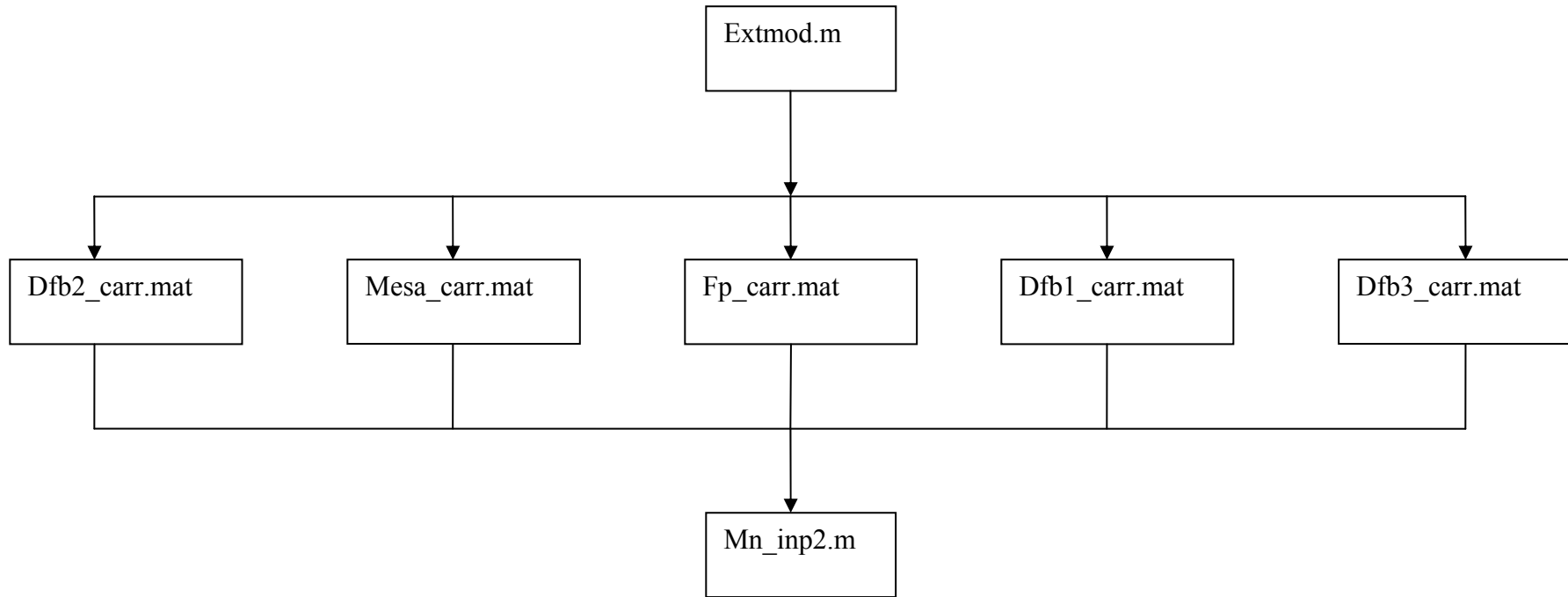


**CHART 1.4 – Plot Various Optical Output**

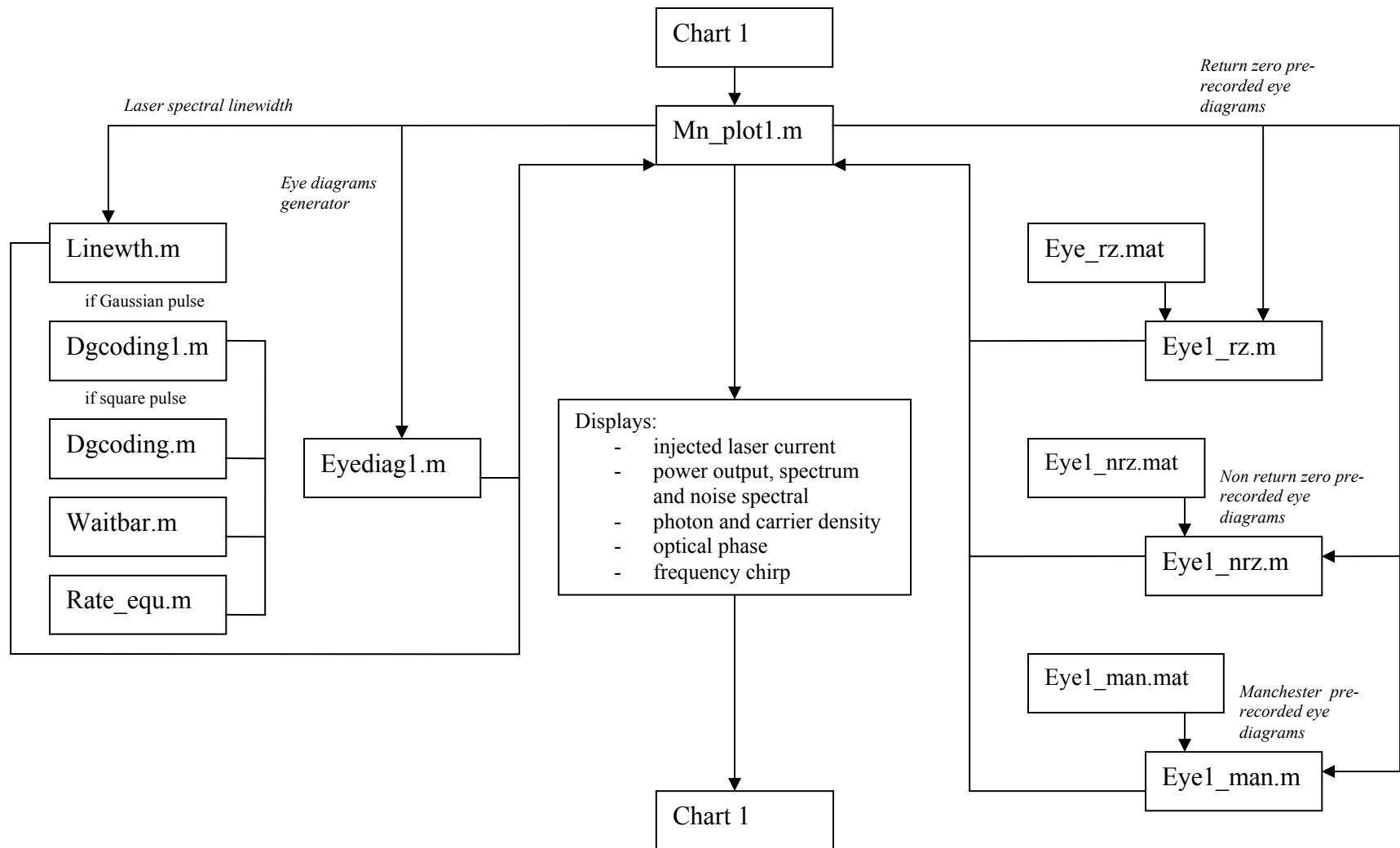
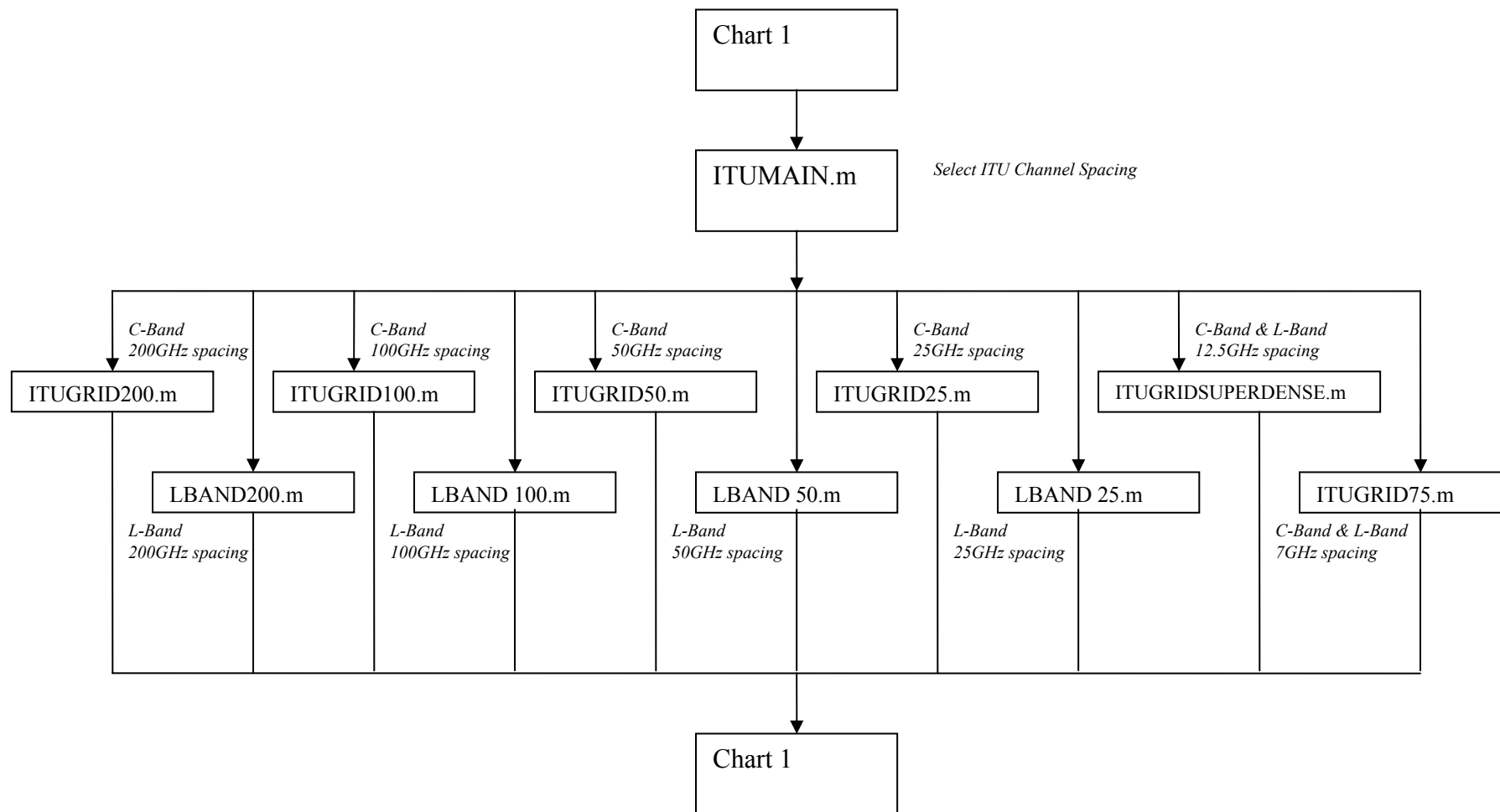
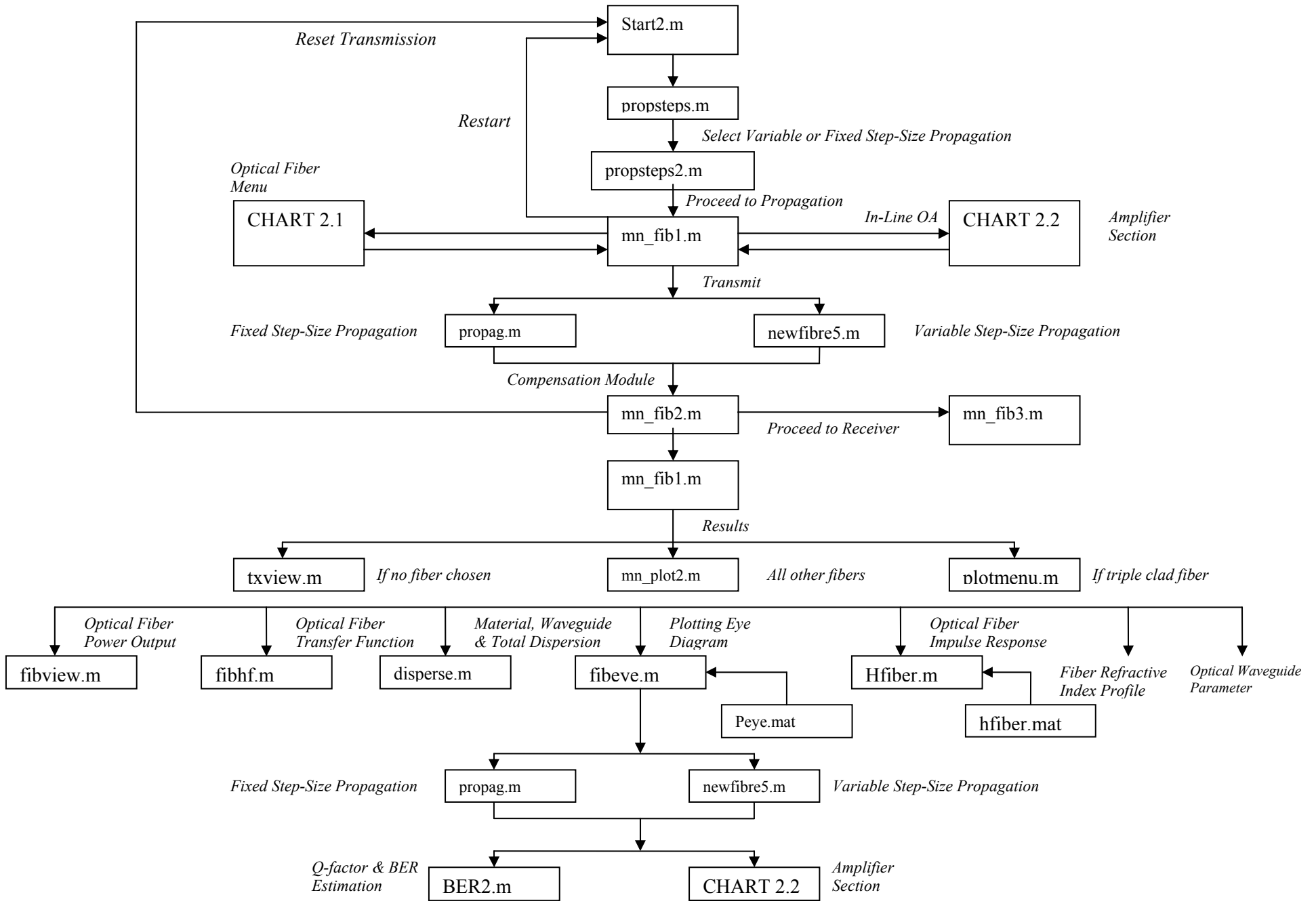


CHART 1.5 – ITU GRID



## FLOWCHART FOR OC2004 PACKAGE (CHART 2)

### FIBER TRANSMISSION MODULE



**CHART 2.1 – Optical Fiber Menu**

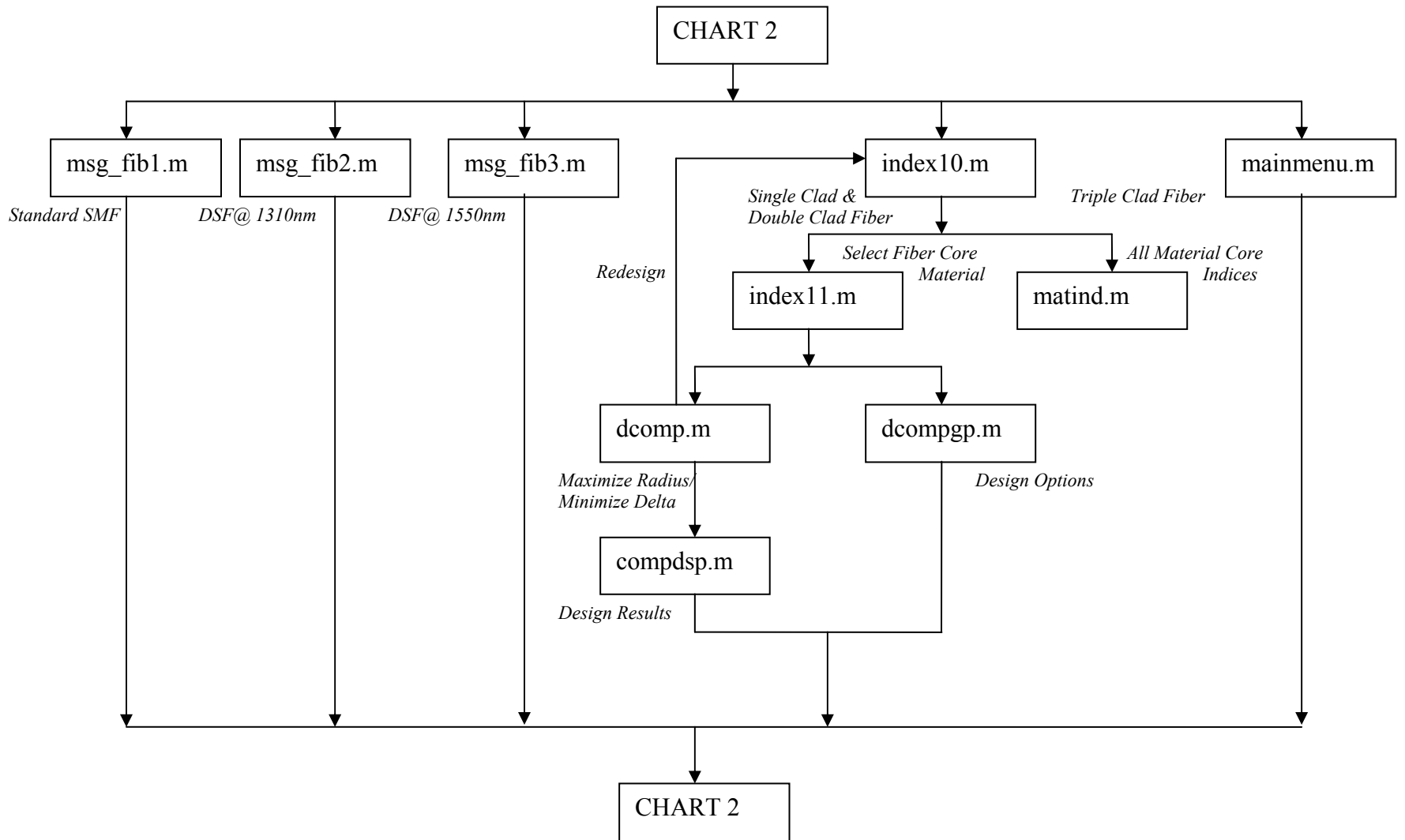


## CHART 2.2 – Optical Amplifier

